4

Atmospheric Chemistry and Greenhouse Gases

Co-ordinating Lead Authors
D. Ehhalt, M. Prather

Lead Authors
F. Dentener, R. Derwent, E. Dlugokencky, E. Holland, I. Isaksen, J. Katima, V. Kirchhoff, P. Matson, P. Midgley, M. Wang

Contributing Authors
T. Berntsen, I. Bey, G. Brasseur, L. Buja, W.J. Collins, J. Daniel, W.B. DeMore, N. Derek, R. Dickerson, D. Etheridge, J. Feichter, P. Fraser, R. Friedl, J. Fuglestvedt, M. Gauss, L. Grenfell, A. Grübler, N. Harris, D. Hauglustaine, L. Horowitz, C. Jackman, D. Jacob, L. Jaeglé, A. Jain, M. Kanakidou, S. Karlsdottir, M. Ko, M. Kurylo, M. Lawrence, J.A. Logan, M. Manning, D. Mauzerall, J. McConnell, L. Mickley, S. Montzka, J.F. Müller, J. Olivier, K. Pickering, G. Pitari, G.J. Roelofs, H. Rogers, B. Rognerud, S. Smith, S. Solomon, J. Staehelin, P. Steele, D. Stevenson, J. Sundet, A. Thompson, M. van Weele, R. von Kuhlmann, Y. Wang, D. Weisenstein, T. Wigley, O. Wild, D. Wuebbles, R. Yantosca

Review Editors
F. Joos, M. McFarland

Contents

Executive Summary

Two important new findings since the IPCC WGI Second Assessment Report (IPCC, 1996) (hereafter SAR) demonstrate the importance of atmospheric chemistry in controlling greenhouse gases:

Currently, tropospheric ozone (O_3) is the third most important greenhouse gas after carbon dioxide (CO_2) and methane (CH_4). It is a product of photochemistry, and its future abundance is controlled primarily by emissions of CH_4, carbon monoxide (CO), nitrogen oxides (NO_x), and volatile organic compounds (VOC). There is now greater confidence in the model assessment of the increase in tropospheric O_3 since the pre-industrial period, which amounts to 30% when globally averaged, as well as the response to future emissions. For scenarios in which the CH_4 abundance doubles and anthropogenic CO and NO_x emissions triple, the tropospheric O_3 abundance is predicted to increase by an additional 50% above today's abundance.

CO is identified as an important indirect greenhouse gas. An addition of CO to the atmosphere perturbs the OH-CH_4-O_3 chemistry. Model calculations indicate that the emission of 100 Mt of CO stimulates an atmospheric chemistry perturbation that is equivalent to direct emission of about 5 Mt of CH_4.

A major conclusion of this report is that atmospheric abundances of almost all greenhouse gases reached the highest values in their measurement records during the 1990s:

The atmospheric abundance of CH_4 continues to increase, from about 1,520 ppb in 1978 to 1,745 ppb in 1998. However, the observed annual increase in CH_4 has declined during the last two decades. This increase is highly variable; it was near zero in 1992 and as large as +13 ppb during 1998. There is no clear, quantitative explanation for this variability. Since the SAR, quantification of certain anthropogenic sources of CH_4, such as that from rice production, has improved.

The atmospheric burden of nitrous oxide (N_2O) continues to increase by about 0.25%/yr. New, higher estimates of emissions from agricultural sources improve our understanding of the global N_2O budget.

The atmospheric abundances of major greenhouse gases that deplete stratospheric ozone are decreasing (CFC-11, CFC-113, CH_3CCl_3, CCl_4), or increasing more slowly (CFC-12), in response to the phase-out in their production agreed to under the Montreal Protocol and its Amendments.

HFC-152a and HFC-134a are increasing in the atmosphere. This growth is consistent with the rise in their industrial use. HFC-23, an unintended by-product of HCFC-22 production, is also increasing.

Perfluorocarbon (PFC) e.g., CF_4 (perfluoromethane) appears to have a natural background; however, current anthropogenic emissions exceed natural ones by a factor of 1,000 or more and are responsible for the observed increase.

There is good agreement between the increase in atmospheric abundances of sulphur hexafluoride (SF_6) and emissions estimates based on revised sales and storage data.

There has been little increase in global tropospheric O_3 since the 1980s at the few remote locations where it is regularly measured. Only two of the fourteen stations, one in Japan and one in Europe, had statistically significant increases in tropospheric O_3 between 1980 and 1995. By contrast, the four Canadian stations, all at high latitudes, had significant decreases in tropospheric O_3 for the same time period. However, limited observations from the late 19th and early 20th centuries combined with models suggest that tropospheric O_3 has increased from a global mean value of 25 DU (where 1 DU = 2.7×10^{16} O_3 molecules/cm^2) in the pre-industrial era to 34 DU today. While the SAR estimated similar values, the new analysis provides more confidence in this increase of 9 DU.

Changes in atmospheric composition and chemistry over the past century have affected, and those projected into the future will affect, the lifetimes of many greenhouse gases and thus alter the climate forcing of anthropogenic emissions:

The atmospheric lifetime relates emissions of a component to its atmospheric burden. In some cases, for instance for methane, a change in emissions perturbs the chemistry and thus the corresponding lifetime. The CH_4 feedback effect amplifies the climate forcing of an addition of CH_4 to the current atmosphere by lengthening the perturbation lifetime relative to the global atmospheric lifetime of CH_4 by a factor of 1.4. This earlier finding is corroborated here by new model studies that also predict only small changes in this CH_4 feedback for the different scenarios projected to year 2100. Another feedback has been identified for the addition of N_2O to the atmosphere; it is associated with stratospheric O_3 chemistry and shortens the perturbation lifetime relative to the global atmospheric lifetime of N_2O by about 5%.

Several chemically reactive gases – CO, NO_x (=NO+NO_2), and VOC – control in part the abundance of O_3 and the oxidising capacity (OH) of the troposphere. These pollutants act as indirect greenhouse gases through their influence on atmospheric chemistry, e.g., formation of tropospheric O_3 or changing the lifetime of CH_4. The emissions of NO_x and CO are dominated by human activities. The abundance of CO in the Northern Hemisphere is about twice that in the Southern Hemisphere and has increased in the second half of the 20th century along with industrialisation and population. The urban and regional abundance of NO_x has generally increased with industrialisation, but the global abundance of this short-lived, highly variable pollutant cannot be derived from measurements. Increased NO_x abundances will in general increase tropospheric O_3 and decrease CH_4. Deposition of NO_x reaction products fertilises the biosphere, stimulates CO_2 uptake, but also provides an input of acidic precipitation.

The IPCC Special Report on Emission Scenarios (SRES) generated six marker/illustrative scenarios (labelled A1B, A1T, A1FI, A2, B1, B2) plus four preliminary marker scenarios (labelled here A1p, A2p, B1p, and B2p). These projected changes in anthropogenic emissions of trace gases from year 2000 to year 2100, making different assumptions on population development, energy use, and technology. Results from both sets of scenarios are discussed here since the preliminary marker scenarios (December 1998) were used in this report:

Model calculations of the abundances of the primary greenhouse gases by year 2100 vary considerably across the SRES scenarios: in general A1B, A1T, and B1 have the smallest increases of emissions and burdens; and A1FI and A2 the largest. CH_4 changes from 1998 to 2100 range from −10 to +115%; and N_2O increases from 13 to 47%. The HFCs – 134a, 143a, and 125 – reach abundances of a few hundred to nearly a thousand ppt from negligible levels today. The PFC CF_4 is projected to increase to between 200 and 400 ppt; and SF_6 to between 35 and 65 ppt.

SRES projected anthropogenic emissions of the indirect greenhouse gases (NO_x, CO and VOC) together with changes in CH_4 are expected to change the global mean abundance of tropospheric OH by −20 to +6% over the next century. Comparable, but opposite sign, changes occur in the atmospheric lifetimes of the greenhouse gases, CH_4 and HFCs. This impact depends in large part on the magnitude of, and the balance between, NO_x and CO emissions.

For the SRES scenarios, changes in tropospheric O_3 between years 2000 and 2100 range from −4 to +21 DU. The largest increase predicted for the 21st century (scenarios A1FI and A2) would be more than twice as large as that experienced since the pre-industrial era. These O_3 increases are attributable to the concurrent, large (almost factor of 3) increases in anthropogenic NO_x and CH_4 emissions.

The large growth in emissions of greenhouse gases and other pollutants as projected in some SRES scenarios for the 21st century will degrade the global environment in ways beyond climate change:

Changes projected in the SRES A2 and A1FI scenarios would degrade air quality over much of the globe by increasing background levels of O_3. In northern mid-latitudes during summer, the zonal average increases near the surface are about 30 ppb or more, raising background levels to nearly 80 ppb, threatening attainment of air quality standards over most metropolitan and even rural regions, and compromising crop and forest productivity. This problem reaches across continental boundaries since emissions of NO_x influence photochemistry on a hemispheric scale.

A more complete and accurate assessment of the human impact on greenhouse gases requires greater understanding of sources, processes, and coupling between different parts of the climate system:

The current assessment is notably incomplete in calculating the total impact of individual industrial / agricultural sectors on greenhouse gases and aerosols. The IPCC Special Report on Aviation demonstrates that the total impact of a sector is not represented by (nor scalable to) the direct emissions of primary greenhouse gases alone, but needs to consider a wide range of atmospheric changes.

The ability to hindcast the detailed changes in atmospheric composition over the past decade, particularly the variability of tropospheric O_3 and CO, is limited by the availability of measurements and their integration with models and emissions data. Nevertheless, since the SAR there have been substantial advances in measurement techniques, field campaigns, laboratory studies, global networks, satellite observations, and coupled models that have improved the level of scientific understanding of this assessment. Better simulation of the past two decades, and in due course the upcoming one, would reduce uncertainty ranges and improve the confidence level of our projections of greenhouse gases.

Feedbacks between atmospheric chemistry, climate, and the biosphere were not developed to the stage that they could be included in the projected numbers here. Failure to include such coupling is likely to lead to systematic errors and may substantially alter the projected increases in the major greenhouse gases.

4.1 Introduction

This chapter investigates greenhouse gases whose atmospheric burdens[1] and climate impacts generally depend on atmospheric chemistry. These greenhouse gases include those listed in the Kyoto Protocol – methane (CH_4), nitrous oxide (N_2O), hydrofluorocarbons (HFCs), perfluorocarbons (PFCs), sulphur hexafluoride (SF_6) – and those listed under the Montreal Protocol and its Amendments – the chlorofluorocarbons (CFCs), the hydrochlorofluorocarbons (HCFCs), and the halons. A major focus of this assessment is the change in tropospheric ozone (O_3). Stratospheric water vapour (H_2O) is also treated here, but tropospheric H_2O, which is part of the hydrological cycle and calculated within climate models, is not discussed. This chapter also treats the reactive gases carbon monoxide (CO), volatile organic compounds (VOC), and nitrogen oxides (NO_x = $NO+NO_2$), termed indirect greenhouse gases. These pollutants are not significant direct greenhouse gases, but through atmospheric chemistry they control the abundances[1] of direct greenhouse gases. This chapter reviews the factors controlling the current atmospheric abundances of direct and indirect greenhouse gases; it looks at the changes since the pre-industrial era and their attribution to anthropogenic activities; and it calculates atmospheric abundances to the year 2100 based on projected emissions of greenhouse gases and pollutants. Carbon dioxide (CO_2) is treated in Chapter 3; and aerosols in Chapter 5. The atmospheric abundances of greenhouse gases and aerosols from all chapters are combined in Chapter 6 to calculate current and future radiative forcing. This chapter is an update of the IPCC WGI Second Assessment Report (IPCC, 1996) (hereafter SAR). For a review of the chemical processes controlling the abundance of greenhouse gases see the SAR (Prather *et al.*, 1995) or Ehhalt (1999). More recent assessments of changing atmospheric chemistry and composition include the IPCC Special Report on Aviation and the Global Atmosphere (Penner *et al.*, 1999) and the World Meteorological Organization / United Nations Environmental Programme (WMO/UNEP) Scientific Assessment of Ozone Depletion (WMO, 1999).

4.1.1 Sources of Greenhouse Gases

Substantial, pre-industrial abundances for CH_4 and N_2O are found in the tiny bubbles of ancient air trapped in ice cores. Both gases have large, natural emission rates, which have varied over past climatic changes but have sustained a stable atmospheric abundance for the centuries prior to the Industrial Revolution (see Figures 4.1 and 4.2). Emissions of CH_4 and N_2O due to human activities are also substantial and have caused large relative increases in their respective burdens over the last century. The atmospheric burdens of CH_4 and N_2O over the next century will likely be driven by changes in both anthropogenic and natural sources. A second class of greenhouse gases – the synthetic HFCs, PFCs, SF_6, CFCs, and halons – did not exist in the atmosphere before the 20th century (Butler *et al.*, 1999). CF_4, a PFC, is detected in ice cores and appears to have an extremely small natural source (Harnisch and Eisenhauer, 1998). The current burdens of these latter gases are derived from atmospheric observations and represent accumulations of past anthropogenic releases; their future burdens depend almost solely on industrial production and release to the atmosphere. Stratospheric H_2O could increase, driven by *in situ* sources, such as the oxidation of CH_4 and exhaust from aviation, or by a changing climate.

Tropospheric O_3 is both generated and destroyed by photochemistry within the atmosphere. Its *in situ* sources are expected to have grown with the increasing industrial emissions of its precursors: CH_4, NO_x, CO and VOC. In addition, there is substantial transport of ozone from the stratosphere to the troposphere (see also Section 4.2.4). The effects of stratospheric O_3 depletion over the past three decades and the projections of its recovery, following cessation of emissions of the Montreal Protocol gases, was recently assessed (WMO, 1999).

The current global emissions, mean abundances, and trends of the gases mentioned above are summarised in Table 4.1a. Table 4.1b lists additional synthetic greenhouse gases without established atmospheric abundances. For the Montreal Protocol gases, political regulation has led to a phase-out of emissions that has slowed their atmospheric increases, or turned them into decreases, such as for CFC-11. For other greenhouse gases, the anthropogenic emissions are projected to increase or remain high in the absence of climate-policy regulations. Projections of future emissions for this assessment, i.e., the IPCC Special Report on Emission Scenarios (SRES) (Nakićenović *et al.*, 2000) anticipate future development of industries and agriculture that represent major sources of greenhouse gases in the absence of climate-policy regulations. The first draft of this chapter and many of the climate studies in this report used the greenhouse gas concentrations derived from the SRES preliminary marker scenarios (i.e., the SRES database as of January 1999 and labelled 'p' here). The scenario IS92a has been carried along in many tables to provide a reference of the changes since the SAR. The projections of greenhouse gases and aerosols for the six new SRES marker/illustrative scenarios are discussed here and tabulated in Appendix II.

An important policy issue is the complete impact of different industrial or agricultural sectors on climate. This requires aggregation of the SRES scenarios by sector (e.g., transportation) or sub-sector (e.g., aviation; Penner *et al.*, 1999), including not only emissions but also changes in land use or natural ecosystems. Due to chemical coupling, correlated emissions can have synergistic effects; for instance NO_x and CO from transportation produce regional O_3 increases. Thus a given sector may act through several channels on the future trends of greenhouse gases. In this chapter we will evaluate the data available on this subject in the current literature and in the SRES scenarios.

[1] Atmospheric *abundances* for trace gases are reported here as the mole fraction (molar mixing ratio) of the gas relative to dry air (ppm = 10^{-6}, ppb = 10^{-9}, ppt = 10^{-12}); whereas the *burden* is reported as the total mass of that gas in the atmosphere (e.g., Mt = Tg = 10^{12} g). For most trace gases in this chapter, the burden is based on the total weight of the molecule; for the N-containing gases, it includes only the mass of the N; and for some VOC budgets where noted, it includes only the mass of the C.

Table 4.1(a): *Chemically reactive greenhouse gases and their precursors: abundances, trends, budgets, lifetimes, and GWPs.*

Chemical species	**Formula**	**Abundance**[a] **ppt** 1998	1750	**Trend ppt/yr**[a] 1990s	**Annual emission** late 90s	**Life-time** (yr)	**100-yr GWP**[b]
Methane	CH_4(ppb)	1745	700	7.0	600 Tg	8.4/12[c]	23
Nitrous oxide	N_2O (ppb)	314	270	0.8	16.4 TgN	120/114[c]	296
Perfluoromethane	CF_4	80	40	1.0	~15 Gg	>50000	5700
Perfluoroethane	C_2F_6	3.0	0	0.08	~2 Gg	10000	11900
Sulphur hexafluoride	SF_6	4.2	0	0.24	~6 Gg	3200	22200
HFC-23	CHF_3	14	0	0.55	~7 Gg	260	12000
HFC-134a	CF_3CH_2F	7.5	0	2.0	~25 Gg	13.8	1300
HFC-152a	CH_3CHF_2	0.5	0	0.1	~4 Gg	1.40	120
Important greenhouse halocarbons under Montreal Protocol and its Amendments							
CFC-11	$CFCl_3$	268	0	–1.4		45	4600
CFC-12	CF_2Cl_2	533	0	4.4		100	10600
CFC-13	CF_3Cl	4	0	0.1		640	14000
CFC-113	$CF_2ClCFCl_2$	84	0	0.0		85	6000
CFC-114	CF_2ClCF_2Cl	15	0	<0.5		300	9800
CFC-115	CF_3CF_2Cl	7	0	0.4		1700	7200
Carbon tetrachloride	CCl_4	102	0	–1.0		35	1800
Methyl chloroform	CH_3CCl_3	69	0	–14		4.8	140
HCFC-22	CHF_2Cl	132	0	5		11.9	1700
HCFC-141b	CH_3CFCl_2	10	0	2		9.3	700
HCFC-142b	CH_3CF_2Cl	11	0	1		19	2400
Halon-1211	CF_2ClBr	3.8	0	0.2		11	1300
Halon-1301	CF_3Br	2.5	0	0.1		65	6900
Halon-2402	CF_2BrCF_2Br	0.45	0	~ 0		<20	
Other chemically active gases dirctly or indirectly affecting radiative forcing							
Tropospheric ozone	O_3 (DU)	34	25	?	see text	0.01-0.05	–
Tropospheric NO_x	NO + NO_2	5-999	?	?	~52 TgN	<0.01-0.03	–
Carbon monoxide	CO (ppb)[d]	80	?	6	~2800 Tg	0.08 - 0.25	[d]
Stratospheric water	H_2O (ppm)	3-6	3-5	?	see text	1-6	–

[a] All abundances are tropospheric molar mixing ratios in ppt (10^{-12})and trends are in ppt/yr unless superseded by units on line (ppb = 10^{-9}, ppm = 10^{-6}). Where possible, the 1998 values are global, annual averages and the trends are calculated for 1996 to 1998.

[b] GWPs are from Chapter 6 of this report and refer to the 100-year horizon values.

[c] Species with chemical feedbacks that change the duration of the atmospheric response; global mean atmospheric lifetime (LT) is given first followed by perturbation lifetime (PT). Values are taken from the SAR (Prather *et al.*, 1995; Schimel *et al.*, 1996) updated with WMO98 (Kurylo and Rodriguez, 1999; Prinn and Zander, 1999) and new OH-scaling, see text. Uncertainties in lifetimes have not changed substantially since the SAR.

[d] CO trend is very sensitive to the time period chosen. The value listed for 1996 to 1998, +6 ppb/yr, is driven by a large increase during 1998. For the period 1991 to 1999, the CO trend was –0.6 ppb/yr. CO is an indirect greenhouse gas: for comparison with CH_4 see this chapter; for GWP, see Chapter 6.

Table 4.1(b): *Additional synthetic greenhouse gases.*

Chemical species	**Formula**	**Lifetime** (yr)	**GWP** [b]
Perfluoropropane	C_3F_8	2600	8600
Perfluorobutane	C_4F_{10}	2600	8600
Perfluorocyclobutane	C_4F_8	3200	10000
Perfluoropentane	C_5F_{12}	4100	8900
Perfluorohexane	C_6F_{14}	3200	9000
Trifluoromethyl-sulphur pentafluoride	SF_5CF_3	1000	17500
Nitrogen trifluoride	NF_3	>500	10800
Trifluoroiodomethane	CF_3I	<0.005	1
HFC-32	CH_2F_2	5.0	550
HFC-41	CH_3F	2.6	97
HFC-125	CHF_2CF_3	29	3400
HFC-134	CHF_2CHF_2	9.6	1100
HFC-143	CH_2FCHF_2	3.4	330
HFC-143a	CH_3CF_3	52	4300
HFC-152	CH_2FCH_2F	0.5	43
HFC-161	CH_3CH_2F	0.3	12
HFC-227ea	CF_3CHFCF_3	33	3500
HFC-236cb	$CF_3CF_2CH_2F$	13.2	1300
HFC-236ea	$CF_3CHFCHF_2$	10.0	1200
HFC-236fa	$CF_3CH_2CF_3$	220	9400
HFC-245ca	$CH_2FCF_2CHF_2$	5.9	640
HFC-245ea	$CHF_2CHFCHF_2$	4.0	
HFC-245eb	CF_3CHFCH_2F	4.2	
HFC-245fa	$CHF_2CH_2CF_3$	7.2	950
HFC-263fb	$CF_3CH_2CH_3$	1.6	
HFC-338pcc	$CHF_2CF_2CF_2CF_2H$	11.4	
HFC-356mcf	$CF_3CF_2CH_2CH_2F$	1.2	
HFC-356mff	$CF_3CH_2CH_2CF_3$	7.9	
HFC-365mfc	$CF_3CH_2CF_2CH_3$	9.9	890
HFC-43-10mee	$CF_3CHFCHFCF_2CF_3$	15	1500
HFC-458mfcf	$CF_3CH_2CF_2CH_2CF_3$	22	
HFC-55-10mcff	$CF_3CF_2CH_2CH_2CF_2CF_3$	7.7	
HFE-125	CF_3OCHF_2	150	14900
HFE-134	CF_2HOCF_2H	26	2400
HFE-143a	CF_3OCH_3	4.4	750
HFE-152a	CH_3OCHF_2	1.5	
HFE-245fa2	$CHF_2OCH_2CF_3$	4.6	570
HFE-356mff2	$CF_3CH_2OCH_2CF_3$	0.4	

4.1.2 Atmospheric Chemistry and Feedbacks

All greenhouse gases except CO_2 and H_2O are removed from the atmosphere primarily by chemical processes within the atmosphere. Greenhouse gases containing one or more H atoms (e.g., CH_4, HFCs and HCFCs), as well as other pollutants, are removed primarily by the reaction with hydroxyl radicals (OH). This removal takes place in the troposphere, the lowermost part of the atmosphere, ranging from the surface up to 7 to 16 km depending on latitude and season and containing 80% of the mass of the atmosphere. The greenhouse gases N_2O, PFCs, SF_6, CFCs and halons do not react with OH in the troposphere. These gases are destroyed in the stratosphere or above, mainly by solar ultraviolet radiation (UV) at short wavelengths (<240 nm), and are long-lived. Because of the time required to transport these gases to the region of chemical loss, they have a minimum lifetime of about 20 years. CO_2 is practically inert in the atmosphere and does not directly influence the chemistry, but it has a small *in situ* source from the oxidation of CH_4, CO and VOC.

Tropospheric OH abundances depend on abundances of NO_x, CH_4, CO, VOC, O_3 and H_2O plus the amount of solar UV (>300 nm) that reaches the troposphere. As a consequence, OH varies widely with geographical location, time of day, and season. Likewise the local loss rates of all those gases reacting with OH also vary. Because of its dependence on CH_4 and other pollutants, tropospheric OH is expected to have changed since the pre-industrial era and to change again for future emission scenarios. For some of these gases other removal processes, such as photolysis or surface uptake, are also important; and the total sink of the gas is obtained by integrating over all such processes. The chemistry of tropospheric O_3 is closely tied to that of OH, and its abundance also varies with changing precursor emissions. The chemistry of the troposphere is also directly influenced by the stratospheric burden of O_3, climatic changes in temperature (T) and humidity (H_2O), as well as by interactions between tropospheric aerosols and trace gases. Such couplings provide a "feedback" between the climate change induced by increasing greenhouse gases and the concentration of these gases. Another feedback, internal to the chemistry, is the impact of CH_4 on OH and hence its own loss. These feedbacks are expected to be important for tropospheric O_3 and OH. Such chemistry-chemistry or climate-chemistry coupling has been listed under "indirect effects" in the SAR (Prather *et al*., 1995; Schimel *et al.*, 1996).

This chapter uses 3-D chemistry-transport models (CTMs) to integrate the varying chemical processes over global conditions, to estimate their significance, and to translate the emission scenarios into abundance changes in the greenhouse gases CH_4, HFCs, and O_3. An extensive modelling exercise called OxComp (tropospheric oxidant model comparison) – involving model comparisons, sensitivity studies, and investigation of the IPCC SRES scenarios – was organised to support this report.

Stratospheric circulation and distribution of O_3 control the transport of the long-lived greenhouse gases to regions of photochemical loss as well as the penetration of solar UV into the atmosphere. At the same time, many of these gases (e.g., N_2O and CFCs) supply ozone-depleting radicals (e.g., nitric oxide (NO) and Cl) to the stratosphere, providing a feedback between the gas and its loss rate. Another consequence of the observed stratospheric ozone depletion is that tropospheric photochemical activity is expected to have increased, altering tropospheric OH and O_3. Climate change in the 21st century, including the radiative cooling of the stratosphere by increased levels of CO_2, is expected to alter stratospheric circulation and O_3, and, hence, the global mean loss rates of the long-lived gases. Some of these effects are discussed in WMO (1999) and are briefly considered here.

The biosphere's response to global change will impact the atmospheric composition of the 21st century. The anticipated changes in climate (e.g., temperature, precipitation) and in chemistry will alter ecosystems and thus the "natural", background emissions of trace gases. There is accumulating evidence that increased N deposition (the result of NO_x and ammonia (NH_3) emissions) and elevated surface O_3 abundances have opposite influences on plant CO_2 uptake: O_3 (>40 ppb) inhibits CO_2 uptake; while N deposition enhances it up to a threshold, above which the effects are detrimental. In addition, the increased N availability from atmospheric deposition and direct fertilisation accelerates the emission of N-containing trace gases (NO, N_2O and NH_3) and CH_4, as well as altering species diversity and biospheric functioning. These complex interactions represent a chemistry-biosphere feedback that may alter greenhouse forcing.

4.1.3 Trace Gas Budgets and Trends

The "budget" of a trace gas consists of three quantities: its global source, global sink and atmospheric burden. The burden is defined as the total mass of the gas integrated over the atmosphere and related reservoirs, which usually include just the troposphere and stratosphere. The global burden (in Tg) and its trend (i.e., the difference between sources and sinks, in Tg/yr) can be determined from atmospheric measurements and, for the long-lived gases, are usually the best-known quantities in the budgets. For short-lived, highly variable gases such as tropospheric O_3 and NO_x, the atmospheric burden cannot be measured with great accuracy. The global source strength is the sum of all sources, including emissions and *in situ* chemical production. Likewise, the sink strength (or global loss rate) can have several independent components.

The source strength (Tg/yr) for most greenhouse gases is comprised of surface emissions. For synthetic gases where industrial production and emissions are well documented, the source strengths may be accurately known. For CH_4 and N_2O, however, there are large, not well-quantified, natural emissions. Further, the anthropogenic emissions of these gases are primarily associated with agricultural sources that are difficult to quantify accurately. Considerable research has gone into identifying and quantifying the emissions from individual sources for CH_4 and N_2O, as discussed below. Such uncertainty in source strength also holds for synthetic gases with undocumented emissions. The source strength for tropospheric O_3 includes both a stratospheric influx and *in situ* production and is thus derived primarily from global chemical models.

The sink strength (Tg/yr) of long-lived greenhouse gases can be derived from a combination of atmospheric observations, laboratory experiments, and models. The atmospheric chemistry models are based on physical principles and laboratory data, and include as constraints the observed chemistry of the atmosphere over the past two decades. For example, stratospheric loss rates are derived from models either by combining observed trace gas distributions with theoretically calculated loss frequencies or from the measured correlation of the respective gas with a trace gas of known vertical flux. In such analyses there are a wide range of self-consistency checks. Mean global loss rates based on *a priori* modelling (e.g., the CH_4-lifetime studies from OxComp described later) can be compared with empirically-based loss rates that are scaled from a gas with similar loss processes that has well-known emissions and atmospheric burden (e.g., the AGAGE (Advanced Global Atmospheric Gases Experiment) calibration of mean tropo-

spheric OH using methyl chloroform (CH_3CCl_3); Prinn *et al.*, 1995). Our knowledge of the current budget of a greenhouse gas provides a key constraint in modelling its future abundance. For example, in both the IS92a and SRES projected emissions of CH_4 and N_2O, we apply a constant offset to each set of emissions so that our calculated burden is consistent with the observed budget and trend during the 1990s.

4.1.4 Atmospheric Lifetimes and Time-Scales

The global atmospheric lifetime (yr) characterises the time required to turn over the global atmospheric burden. It is defined as the burden (Tg) divided by the mean global sink (Tg/yr) for a gas in steady state (i.e., with unchanging burden). This quantity was defined as both "lifetime" and "turnover time" in the SAR (see also Bolin and Rodhe, 1973). Lifetimes calculated in this manner are listed in Table 4.1. A corollary of this definition is that, when in steady state (i.e., source strength = sink strength), the atmospheric burden of a gas equals the product of its lifetime and its emissions. A further corollary is that the integrated atmospheric abundance following a single emission is equal to the product of its steady-state lifetime for that emission pattern and the amount emitted (Prather, 1996). This latter, new result since the SAR supports the market-basket approach of aggregating the direct emissions of different greenhouse gases with a GWP (Global Warming Potential) weighting.

The atmospheric lifetime is basically a scale factor relating (i) constant emissions (Tg/yr) to a steady-state burden (Tg), or (ii) an emission pulse (Tg) to the time-integrated burden of that pulse (Tg/yr). The lifetime is often additionally assumed to be a constant, independent of the sources; and it is also taken to represent the decay time (e-fold) of a perturbation. These latter assumptions apply rigorously only for a gas whose local chemical lifetime is constant in space and time, such as for the noble gas radon, whose lifetime is fixed by the rate of its radioactive decay. In such a case the mean atmospheric lifetime equals the local lifetime: the lifetime that relates source strength to global burden is exactly the decay time of a perturbation.

This general applicability of the atmospheric lifetime breaks down for those greenhouse gases and pollutants whose chemical losses vary in space and time. NO_x, for instance, has a local lifetime of <1 day in the lower troposphere, but >5 days in the upper troposphere; and both times are less than the time required for vertical mixing of the troposphere. In this case emission of NO_x into the upper troposphere will produce a larger atmospheric burden than the same emission into the lower troposphere. Consequently, the definition of the atmospheric lifetime of NO_x is not unique and depends on the location (and season) of its emissions. The same is true for any gas whose local lifetime is variable and on average shorter than about 0.5 year, i.e., the decay time of a north-south difference between hemispheres representing one of the longer time-scales for tropospheric mixing. The majority of greenhouse gases considered here have atmospheric lifetimes greater than 2 years, much longer than tropospheric mixing times; and hence their lifetimes are not significantly altered by the location of sources within the troposphere. When lifetimes are reported for gases in Table 4.1, it is assumed that the gases are uniformly mixed throughout the troposphere. This assumption is unlikely for gases with lifetimes <1 year, and reported values must be viewed only as approximations.

Some gases have chemical feedbacks that change their lifetimes. For example, the increasing CH_4 abundance leads to a longer lifetime for CH_4 (Prather *et al.*, 1995; Schimel *et al.*, 1996). A chemical feedback with opposite effect has been identified for N_2O where a greater N_2O burden leads to increases in stratospheric NO_x which in turn depletes mid-stratospheric ozone. This ozone loss enhances the UV, and as a consequence N_2O is photolysed more rapidly (Prather, 1998). Such feedbacks cause the time-scale of a perturbation, henceforth called perturbation lifetime (*PT*), to differ from the global atmospheric lifetime (*LT*). In the limit of small perturbations, the relation between the perturbation lifetime of a gas and its global atmospheric lifetime can be derived from a simple budget relationship as $PT = LT / (1 - s)$, where the sensitivity coefficient $s = \partial ln(LT) / \partial ln(B)$ and B = burden. Without a feedback on lifetime, $s = 0$, and *PT* is identical to *LT*. The product, *PT* times a sustained change in emission, gives the resulting change in the burden. The ratio of *PT/LT* adopted here for CH_4, 1.4, is based on recent model studies (see Section 4.4) and is consistent with the SAR results.

To evaluate the total greenhouse effect of a given gas molecule, one needs to know, first, how long it remains in the atmosphere and, second, how it interacts chemically with other molecules. This effect is calculated by injecting a pulse of that gas (e.g., 1 Tg) into the atmosphere and watching the added abundance decay as simulated in a CTM. This decay is represented by a sum of exponential functions, each with its own decay time. These exponential functions are the chemical modes of the linearised chemistry-transport equations of the CTM (Prather, 1996). In the case of a CH_4 addition, the longest-lived mode has an e-fold time of 12 years, close to the perturbation lifetime (*PT*) of CH_4, and carries most of the added burden. (This e-fold time was called the adjustment time in the SAR.) In the case of a CO addition, this same mode is also excited, but at a reduced amplitude (Prather, 1996; Daniel and Solomon, 1998). The pulse of added CO, by causing the concentration of OH to decrease and thus the lifetime of CH_4 to increase temporarily, causes a build-up of CH_4 while the added burden of CO persists. After the initial period of a few months defined by the CO photochemical lifetime, this built-up CH_4 then decays in the same manner as would a direct pulse of CH_4. Similarly, an addition of NO_x (e.g., from aviation; see Isaksen and Jackman, 1999) will excite this mode, but with a negative amplitude. Thus, changes in the emissions of short-lived gases can generate long-lived perturbations as shown in 3-D CTMs (Wild and Prather, 2000; Derwent *et al.*, 2001). Changes in tropospheric O_3 accompany the CH_4 decay on a 12 year time-scale as an inherent component of this mode, a key example of chemical coupling in the troposphere. Thus, any chemically reactive gas, whether a greenhouse gas or not, will produce some level of indirect greenhouse effect through its impact on atmospheric chemistry.

4.2 Trace Gases: Current Observations, Trends, and Budgets

4.2.1 Non-CO_2 Kyoto Gases

4.2.1.1 Methane (CH_4)

Methane's globally averaged atmospheric surface abundance in 1998 was 1,745 ppb (see Figure 4.1), corresponding to a total burden of about 4,850 Tg(CH_4). The uncertainty in the burden is small (±5%) because the spatial and temporal distributions of tropospheric and stratospheric CH_4 have been determined by extensive high-precision measurements and the tropospheric variability is relatively small. For example, the Northern Hemisphere CH_4 abundances average about 5% higher than those in the Southern Hemisphere. Seasonal variations, with a minimum in late summer, are observed with peak-to-peak amplitudes of about 2% at mid-latitudes. The average vertical gradient in the troposphere is negligible, but CH_4 abundances in the stratosphere decrease rapidly with altitude, e.g., to 1,400 ppb at 30 km altitude in the tropics and to 500 ppb at 30 km in high latitude northern winter.

The most important known sources of atmospheric methane are listed in Table 4.2. Although the major source terms of atmospheric CH_4 have probably been identified, many of the source strengths are still uncertain due to the difficulty in assessing the global emission rates of the biospheric sources, whose strengths are highly variable in space and time: e.g., local emissions from most types of natural wetland can vary by a few orders of magnitude over a few metres. Nevertheless, new approaches have led to improved estimates of the global emissions rates from some source types. For instance, intensive studies on emissions from rice agriculture have substantially improved these emissions estimates (Ding and Wang, 1996; Wang and Shangguan, 1996). Further, integration of emissions over a whole growth period (rather than looking at the emissions on individual days with different ambient temperatures) has lowered the estimates of CH_4 emissions from rice agriculture from about 80 Tg/yr to about 40 Tg/yr (Neue and Sass, 1998; Sass *et al.*, 1999). There have also been attempts to deduce emission rates from observed spatial and temporal distributions of atmospheric CH_4 through inverse modelling (e.g., Hein *et al.*, 1997; Houweling *et al.*, 1999). The emissions so derived depend on the precise knowledge of the mean global loss rate and represent a relative attribution into aggregated sources of similar properties. The results of some of these studies have been included in Table 4.2. The global CH_4 budget can also be constrained by measurements of stable isotopes ($\delta^{13}C$ and δD) and radiocarbon ($^{14}CH_4$) in atmospheric CH_4 and in CH_4 from the major sources (e.g., Stevens and Engelkemeir, 1988; Wahlen *et al.*, 1989; Quay *et al.*, 1991, 1999; Lassey *et al.*, 1993; Lowe *et al.*, 1994). So far the measurements of isotopic composition of CH_4 have served mainly to constrain the contribution from fossil fuel related sources. The emissions from the various sources sum up to a global total of about 600 Tg/yr, of which about 60% are related to human activities such as agriculture, fossil fuel use and waste disposal. This is consistent with the SRES estimate of 347 Tg/yr for anthropogenic CH_4 emissions in the year 2000.

The current emissions from CH_4 hydrate deposits appear small, about 10 Tg/yr. However, these deposits are enormous, about 10^7 TgC (Suess *et al.*, 1999), and there is an indication of a catastrophic release of a gaseous carbon compound about 55 million years ago, which has been attributed to a large-scale perturbation of CH_4 hydrate deposits (Dickens, 1999; Norris and Röhl, 1999). Recent research points to regional releases of CH_4 from clathrates in ocean sediments during the last 60,000 years (Kennett *et al.*, 2000), but much of this CH_4 is likely to be oxidised by bacteria before reaching the atmosphere (Dickens, 2001). This evidence adds to the concern that the expected global warming may lead to an increase in these emissions and thus to another positive feedback in the climate system. So far, the size of that feedback has not been quantified. On the other hand, the historic record of atmospheric CH_4 derived from ice cores (Petit *et al.*, 1999), which spans several large temperature swings plus glaciations, constrains the possible past releases from methane hydrates to the atmosphere. Indeed, Brook *et al.* (2000) find little evidence for rapid, massive CH_4 excursions that might be associated with large-scale decomposition of methane hydrates in sediments during the past 50,000 years.

The mean global loss rate of atmospheric CH_4 is dominated by its reaction with OH in the troposphere.

$$OH + CH_4 \rightarrow CH_3 + H_2O$$

This loss term can be quantified with relatively good accuracy based on the mean global OH concentration derived from the methyl chloroform (CH_3CCL_3) budget described in Section 4.2.6 on OH. In that way we obtain a mean global loss rate of 507 Tg(CH_4)/yr for the current tropospheric removal of CH_4 by OH. In addition there are other minor removal processes for atmospheric CH_4. Reaction with Cl atoms in the marine boundary layer probably constitutes less than 2% of the total sink (Singh *et al.*, 1996). A recent process model study (Ridgwell *et al.*, 1999) suggested a soil sink of 38 Tg/yr, and this can be compared to SAR estimates of 30 Tg/yr. Minor amounts of CH_4 are also destroyed in the stratosphere by reactions with OH, Cl, and $O(^1D)$, resulting in a combined loss rate of 40 Tg/yr. Summing these, our best estimate of the current global loss rate of atmospheric CH_4 totals 576 Tg/yr (see Table 4.2), which agrees reasonably with the total sources derived from process models. The atmospheric lifetime of CH_4 derived from this loss rate and the global burden is 8.4 years. Attributing individual lifetimes to the different components of CH_4 loss results in 9.6 years for loss due to tropospheric OH, 120 years for stratospheric loss, and 160 years for the soil sink (i.e., 1/8.4 yr = 1/9.6 yr + 1/120 yr + 1/160 yr).

The atmospheric abundance of CH_4 has increased by about a factor of 2.5 since the pre-industrial era (see Figure 4.1a) as evidenced by measurements of CH_4 in air extracted from ice cores and firn (Etheridge *et al.*, 1998). This increase still continues, albeit at a declining rate (see Figure 4.1b). The global tropospheric CH_4 growth rate averaged over the period 1992 through 1998 is about 4.9 ppb/yr, corresponding to an average annual increase in atmospheric burden of 14 Tg. Superimposed on this long-term decline in growth rate are interannual variations in the trend (Figure 4.1c). There are no clear quantitative explanations for this variability, but understanding these variations in

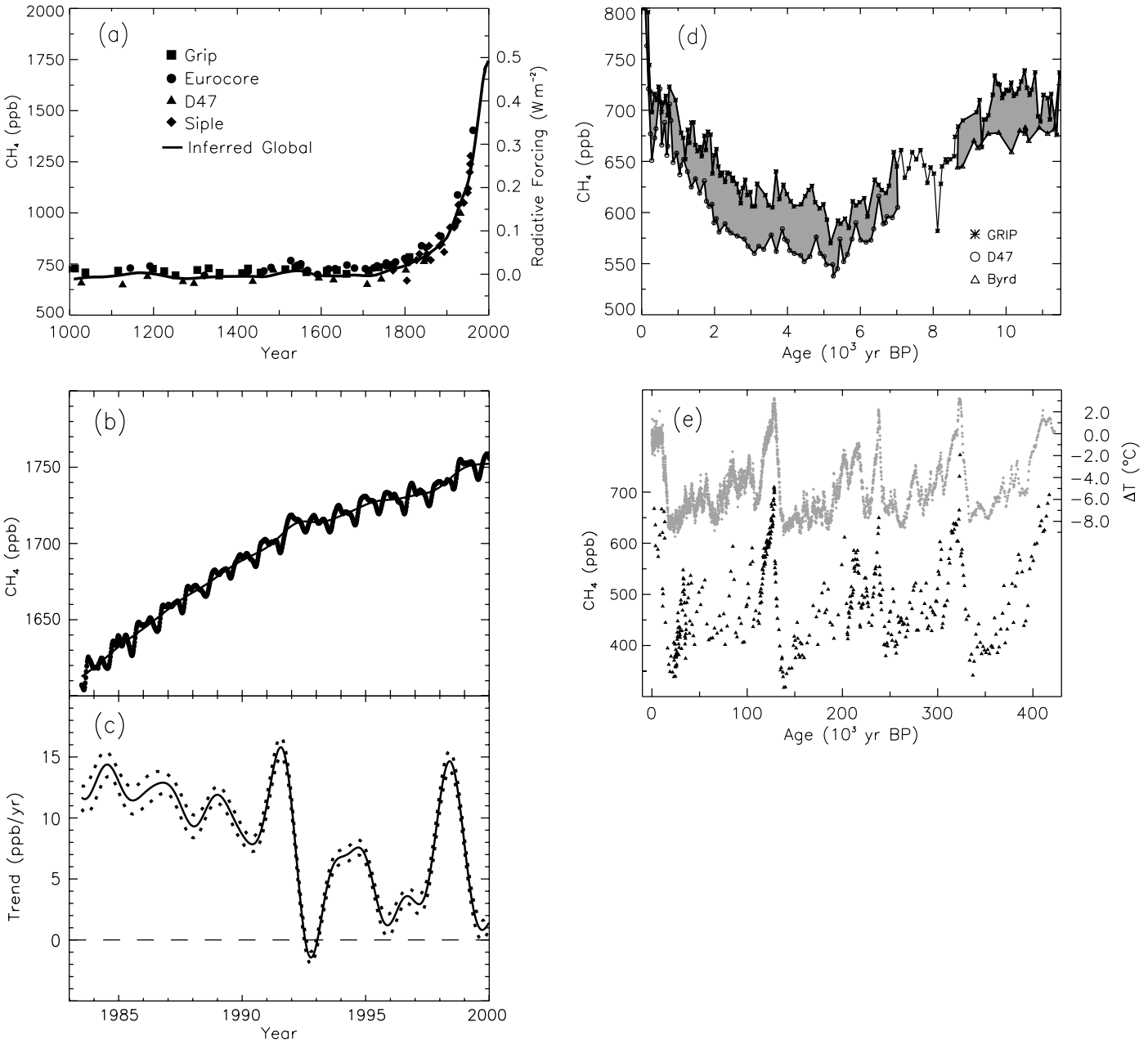

Figure 4.1: (a) Change in CH_4 abundance (mole fraction, in ppb = 10^{-9}) determined from ice cores, firn, and whole air samples plotted for the last 1,000 years. Data sets are as follows: Grip, Blunier *et al.* (1995) and Chappellaz *et al.* (1997); Eurocore, Blunier *et al.* (1993); D47, Chappellaz *et al.* (1997); Siple, Stauffer *et al.* (1985); Global (inferred from Antarctic and Greenland ice cores, firn air, and modern measurements), Etheridge *et al.* (1998) and Dlugokencky *et al.* (1998). Radiative forcing, approximated by a linear scale since the pre-industrial era, is plotted on the right axis. (b) Globally averaged CH_4 (monthly varying) and deseasonalised CH_4 (smooth line) abundance plotted for 1983 to 1999 (Dlugokencky *et al.*, 1998). (c) Instantaneous annual growth rate (ppb/yr) in global atmospheric CH_4 abundance from 1983 through 1999 calculated as the derivative of the deseasonalised trend curve above (Dlugokencky *et al.*, 1998). Uncertainties (dotted lines) are ±1 standard deviation. (d) Comparison of Greenland (GRIP) and Antarctic (D47 and Byrd) CH_4 abundances for the past 11.5 kyr (Chappellaz *et al.*, 1997). The shaded area is the pole-to-pole difference where Antarctic data exist. (e) Atmospheric CH_4 abundances (black triangles) and temperature anomalies with respect to mean recent temperature (grey diamonds) determined for the past 420 kyr from an ice core drilled at Vostok Station in East Antarctica (Petit *et al.*, 1999).

trend will ultimately help constrain specific budget terms. After the eruption of Mt. Pinatubo, a large positive anomaly in growth rate was observed at tropical latitudes. It has been attributed to short-term decreases in solar UV in the tropics immediately following the eruption that decreased OH formation rates in the troposphere (Dlugokencky *et al.*, 1996). A large decrease in growth was observed, particularly in high northern latitudes, in 1992. This feature has been attributed in part to decreased northern wetland emission rates resulting from anomalously low surface temperatures (Hogan and Harriss, 1994) and in part to

Table 4.2: *Estimates of the global methane budget (in Tg(CH_4/yr) from different sources compared with the values adopted for this report (TAR).*

Reference:	Fung *et al.* (1991)	Hein *et al.* (1997)	Lelieveld *et al.* (1998)	Houweling *et al.* (1999)	Mosier *et al.* (1998a)	Olivier *et al.* (1999)	Cao *et al.* (1998)	SAR	TAR[a]
Base year:	1980s	–	1992	–	1994	1990	–	1980s	1998
Natural sources									
Wetlands	115	237	225[c]	145			92		
Termites	20	–	20	20					
Ocean	10	–	15	15					
Hydrates	5	–	10	–					
Anthropogenic sources									
Energy	75	97	110	89		109			
Landfills	40	35	40	73		36			
Ruminants	80	90[b]	115	93	80	93[b]			
Waste treatment	–	[b]	25	–	14	[b]			
Rice agriculture	100	88	[c]	–	25-54	60	53		
Biomass burning	55	40	40	40	34	23			
Other	–	–	–	20	15				
Total source	**500**	**587**	**600**					**597**	**598**
Imbalance (trend)								+37	+22
Sinks									
Soils	10	–	30	30	44			30	30
Tropospheric OH	450	489	510					490	506
Stratospheric loss	–	46	40					40	40
Total sink	**460**	**535**	**580**					**560**	**576**

[a] TAR budget based on 1,745 ppb, 2.78 Tg/ppb, lifetime of 8.4 yr, and an imbalance of +8 ppb/yr.
[b] Waste treatment included under ruminants.
[c] Rice included under wetlands.

stratospheric ozone depletion that increased tropospheric OH (Bekki *et al.*, 1994; Fuglestvedt *et al.*, 1994). Records of changes in the $^{13}C/^{12}C$ ratios in atmospheric CH_4 during this period suggest the existence of an anomaly in the sources or sinks involving more than one causal factor (Lowe *et al.*, 1997; Mak *et al.*, 2000).

There is no consensus on the causes of the long-term decline in the annual growth rate. Assuming a constant mean atmospheric lifetime of CH_4 of 8.9 years as derived by Prinn *et al.* (1995), Dlugokencky *et al.* (1998) suggest that during the period 1984 to 1997 global emissions were essentially constant and that the decline in annual growth rate was caused by an approach to steady state between global emissions and atmospheric loss rate. Their estimated average source strength was about 550 Tg/yr. (Inclusion of a soil sink term of 30 Tg/yr would decrease the lifetime to 8.6 years and suggest an average source strength of about 570 Tg/yr.) Francey *et al.* (1999), using measurements of $^{13}CH_4$ from Antarctic firn air samples and archived air from Cape Grim, Tasmania, also concluded that the decreased CH_4 growth rate was consistent with constant OH and constant or very slowly increasing CH_4 sources after 1982. However, other analyses of the global methyl chloroform (CH_3CCl_3) budget (Krol *et al.*, 1998) and the changing chemistry of the atmosphere (Karlsdottir and Isaksen, 2000) argue for an increase in globally averaged OH of +0.5%/yr over the last two decades (see Section 4.2.6 below) and hence a parallel increase in global CH_4 emissions by +0.5%/yr.

The historic record of atmospheric CH_4 obtained from ice cores has been extended to 420,000 years before present (BP) (Petit *et al.*, 1999). As Figure 4.1e demonstrates, at no time during this record have atmospheric CH_4 mixing ratios approached today's values. CH_4 varies with climate as does CO_2. High values are observed during interglacial periods, but these maxima barely exceed the immediate pre-industrial CH_4 mixing ratio of 700 ppb. At the same time, ice core measurements from Greenland and Antarctica indicate that during the Holocene CH_4 had a pole-to-pole difference of about 44 ± 7 ppb with higher values in the Arctic as today, but long before humans influenced atmospheric methane concentrations (Chappelaz *et al.*, 1997; Figure 4.1d). Finally, study of CH_4 ice-core records at high time resolution reveals no evidence for rapid, massive CH_4 excursions that might be associated with large-scale decomposition of methane hydrates in sediments (Brook *et al.*, 2000).

The feedback of CH_4 on tropospheric OH and its own lifetime is re-evaluated with contemporary CTMs as part of OxComp, and results are summarised in Table 4.3. The calculated OH feedback, $\partial\ln(OH) / \partial\ln(CH_4)$, is consistent between the models, indicating that tropospheric OH abundances decline by 0.32% for every 1% increase in CH_4. The TAR value for the sensitivity coefficient $s = \partial\ln(LT) / \partial\ln(CH_4)$ is then 0.28 and the ratio PT/LT is 1.4. This 40% increase in the integrated effect of a CH_4 perturbation does not appear as a 40% larger amplitude in the perturbation but rather as a lengthening of the duration of the perturbation to 12 years. This feedback is difficult

Table 4.3: *Methane lifetime and feedback on tropospheric OH[a] for the 1990s.*

CTM	lifetime vs. OH(yr)[b]	$\delta\ln(OH)/\delta\ln(CH_4)$	$s=\delta\ln(LT)/\delta\ln(CH_4)$	PT/LT
IASB	8.1	–0.31	+0.27	1.37
KNMI	9.8	–0.35	+0.31	1.45
MPIC	8.5	–0.29	+0.25	1.33
UCI	9.0	–0.34 (–0.38)[c]	+0.30	1.43
UIO1	6.5	–0.33	+0.29	1.41
UKMO	8.3	–0.31 (–0.34)[c]	+0.27	1.37
ULAQ	13.8	–0.29	+0.25	1.33
TAR value[d]	9.6	–0.32		1.4

[a] Global mean tropospheric OH is weighted by the CH_4 loss rate.

[b] Lifetime against tropospheric OH loss at 1,745 ppb.

[c] Evaluated at 4,300 ppb CH_4 plus emissions for Y2100/draft-A2 scenario.

[d] TAR recommended OH lifetime for CH_4, 9.6 yr, is scaled from a CH_3CCl_3 OH lifetime of 5.7 yr (WMO, 1999; based on Prinn *et al.*, 1995) using a temperature of 272K (Spivakovsky *et al*., 2000). Stratospheric (120 yr) and soil-loss (160 yr) lifetimes are added (inversely) to give mean atmospheric lifetime of 8.4 yr. Only the OH lifetime is diagnosed and is subject to chemical feedback factor, and thus the total atmospheric lifetime for a CH_4 perturbation is 12 yr. In the SAR, the feedback factor referred only to the increase in the lifetime against tropospheric OH, and hence was larger. For Chemistry Transport Model (CTM) code see Table 4.10.

to observe, since it would require knowledge of the *increase* in CH_4 sources plus other factors affecting OH over the past two decades. Unlike for the global mean tropospheric OH abundance, there is also no synthetic compound that can calibrate this feedback; but it is possible that an analysis of the budgets of $^{13}CH_4$ and $^{12}CH_4$ separately may lead to an observational constraint (Manning, 1999).

4.2.1.2 Nitrous oxide (N_2O)

The globally averaged surface abundance of N_2O was 314 ppb in 1998, corresponding to a global burden of 1510 TgN. N_2O abundances are about 0.8 ppb greater in the Northern Hemisphere than in the Southern Hemisphere, consistent with about 60% of emissions occurring in the Northern Hemisphere. Almost no vertical gradient is observed in the troposphere, but N_2O abundances decrease in the stratosphere, for example, falling to about 120 ppb by 30 km at mid-latitudes.

The known sources of N_2O are listed in Table 4.4 with estimates of their emission rates and ranges. As with methane, it remains difficult to assess global emission rates from individual sources that vary greatly over small spatial and temporal scales. Total N_2O emissions of 16.4 TgN/yr can be inferred from the N_2O global sink strength (burden/lifetime) plus the rate of increase in the burden. In the SAR the sum of N_2O emissions from specific sources was notably less than that inferred from the loss rate. The recent estimates of global N_2O emissions from Mosier *et al.* (1998b) and Kroeze *et al.* (1999) match the global loss rate and underline the progress that has been made on quantification of natural and agricultural sources. The former study calculated new values for N_2O agricultural emissions that include the full impact of agriculture on the global nitrogen cycle and show that N_2O emissions from soils are the largest term in the budget (Table 4.4). The latter study combined these with emissions from other anthropogenic and natural sources to calculate a total emission of 17.7 TgN/yr for 1994.

The enhanced N_2O emissions from agricultural and natural ecosystems are believed to be caused by increasing soil N availability driven by increased fertilizer use, agricultural nitrogen (N_2) fixation, and N deposition; and this model can explain the increase in atmospheric N_2O abundances over the last 150 years (Nevison and Holland, 1997). Recent discovery of a faster-than-linear feedback in the emission of N_2O and NO from soils in response to external N inputs is important, given the projected increases of N fertilisation and deposition increases in tropical countries (Matson *et al.*, 1999). Tropical ecosystems, currently an important source of N_2O (and NO) are often phosphorus-limited rather than being N-limited like the Northern Hemispheric terrestrial ecosystems. Nitrogen fertiliser inputs into these phosphorus-limited ecosystems generate NO and N_2O fluxes that are 10 to 100 times greater than the same fertiliser addition to nearby N-limited ecosystems (Hall and Matson, 1999). In addition to N availability, soil N_2O emissions are regulated by temperature and soil moisture and so are likely to respond to climate changes (Frolking *et al.*, 1998; Parton *et al.*, 1998). The magnitude of this response will be affected by feedbacks operating through the biospheric carbon cycle (Li *et al.*, 1992, 1996).

The industrial sources of N_2O include nylon production, nitric acid production, fossil fuel fired power plants, and vehicular emissions. It was once thought that emission from

Table 4.4: *Estimates of the global nitrous oxide budget (in TgN/yr) from different sources compared with the values adopted for this report (TAR).*

Reference:	Mosier *et al.* (1998b) Kroeze *et al.* (1999)		Olivier *et al.* (1998)		SAR	TAR
Base year:	1994	range	1990	range	1980s	1990s
Sources						
Ocean	3.0	1 – 5	3.6	2.8 – 5.7	3	
Atmosphere (NH_3 oxidation)	0.6	0.3 – 1.2	0.6	0.3 – 1.2		
Tropical soils						
Wet forest	3.0	2.2 – 3.7			3	
Dry savannas	1.0	0.5 – 2.0			1	
Temperate soils						
Forests	1.0	0.1 – 2.0			1	
Grasslands	1.0	0.5 – 2.0			1	
All soils			6.6	3.3 – 9.9		
Natural sub-total	9.6	4.6 – 15.9	10.8	6.4 – 16.8	9	
Agricultural soils	4.2	0.6 – 14.8	1.9	0.7 – 4.3	3.5	
Biomass burning	0.5	0.2 – 1.0	0.5	0.2 – 0.8	0.5	
Industrial sources	1.3	0.7 – 1.8	0.7	0.2 – 1.1	1.3	
Cattle and feedlots	2.1	0.6 – 3.1	1.0	0.2 – 2.0	0.4	
Anthropogenic Sub-total	8.1	2.1 – 20.7	4.1	1.3 – 7.7	5.7	6.9 [a]
Total sources	**17.7**	**6.7 – 36.6**	**14.9**	**7.7 – 24.5**	**14.7** [b]	
Imbalance (trend)	3.9	3.1 – 4.7			3.9	3.8
Total sinks (stratospheric)	**12.3**	**9 – 16**			**12.3**	**12.6**
Implied total source	16.2				16.2	16.4

[a] SRES 2000 anthropogenic N_2O emissions.
[b] N.B. total sources do not equal sink + imbalance.

automobile catalytic converters were a potential source of N_2O, but extrapolating measurements of N_2O emissions from automobiles in roadway tunnels in Stockholm and Hamburg during 1992 to the global fleet gives a source of only 0.24 ± 0.14 TgN/yr (Berges *et al.*, 1993). More recent measurements suggest even smaller global emissions from automobiles, 0.11 ± 0.04 TgN/yr (Becker *et al.*, 1999; Jiménez *et al.*, 2000).

The identified sinks for N_2O are photodissociation (90%) and reaction with electronically excited oxygen atoms ($O(^1D)$); they occur in the stratosphere and lead to an atmospheric lifetime of 120 years (SAR; Volk *et al.*, 1997; Prinn and Zander, 1999). The small uptake of N_2O by soils is not included in this lifetime, but is rather incorporated into the net emission of N_2O from soils because it is coupled to the overall N-partitioning.

Isotopic ($\delta^{15}N$ and $\delta^{18}O$) N_2O measurements are also used to constrain the N_2O budget. The isotopic composition of tropospheric N_2O derives from the flux-weighted isotopic composition of sources corrected for fractionation during destruction in the stratosphere. Typical observed values are $\delta^{15}N = 7$ ‰ and $\delta^{18}O = 20.7$ ‰ relative to atmospheric N_2 and oxygen (O_2) (Kim and Craig, 1990). Most surface sources are depleted in ^{15}N and ^{18}O relative to tropospheric N_2O (e.g., Kim and Craig, 1993), and so other processes (sources or sinks) must lead to isotopic enrichment. Rahn and Wahlen (1997) use stratospheric air samples to show that the tropospheric isotope signature of N_2O can be explained by a return flux of isotopically enriched N_2O from the stratosphere, and no exotic sources of N_2O are needed. Yung and Miller (1997) point out that large isotopic fractionation can occur in the stratosphere during photolysis due to small differences in the zero point energies of the different isotopic species, and Rahn *et al.* (1998) have verified this latter effect with laboratory measurements. Wingen and Finlayson-Pitts (1998) failed to find evidence that reaction of CO_3 with N_2 (McElroy and Jones, 1996) is an atmospheric source of N_2O. The use of isotopes has not yet conclusively identified new sources nor constrained the N_2O budget better than other approaches, but the emerging data set of isotopic measurements, including measurements of the intramolecular position of ^{15}N in N_2O isotopomers (Yoshida and Toyoda, 2000) will provide better constraints in the future.

Tropospheric N_2O abundances have increased from pre-industrial values of about 270 ppb (Machida *et al.*, 1995; Battle *et al.*, 1996; Flückiger *et al.*, 1999) to a globally averaged value of 314 ppb in 1998 (Prinn *et al.*, 1990, 1998; Elkins *et al.*, 1998) as shown in Figure 4.2. The pre-industrial source is estimated to

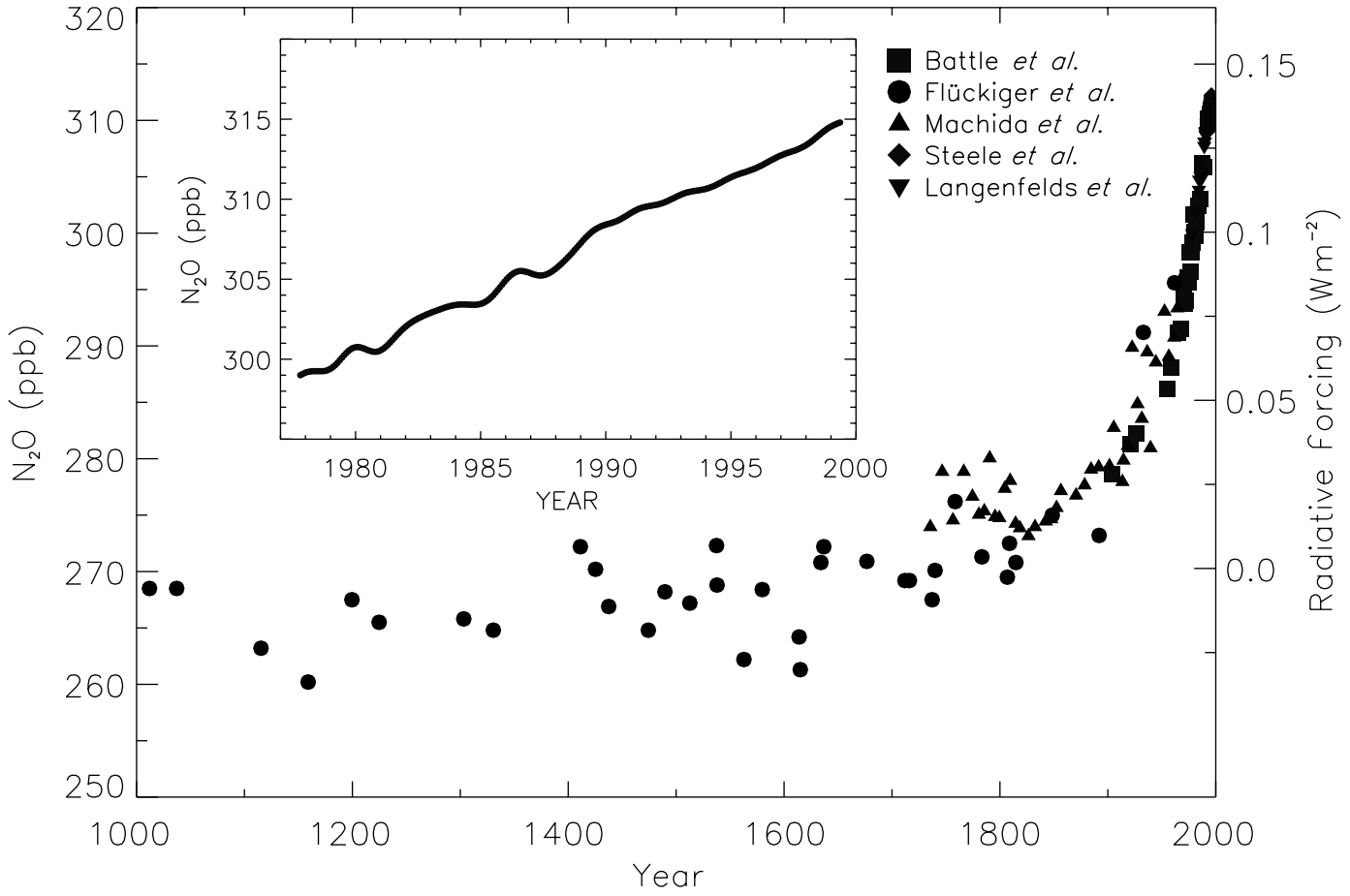

Figure 4.2: Change in N_2O abundance for the last 1,000 years as determined from ice cores, firn, and whole air samples. Data sets are from: Machida *et al.* (1995); Battle *et al.* (1996); Langenfelds *et al.* (1996); Steele *et al.* (1996); Flückiger *et al.* (1999). Radiative forcing, approximated by a linear scale, is plotted on the right axis. Deseasonalised global averages are plotted in the inset (Butler *et al.*, 1998b).

be 10.7 TgN/yr, which implies that current anthropogenic emissions are about 5.7 TgN/yr assuming no change in the natural emissions over this period. The average rate of increase during the period 1980 to 1998 determined from surface measurements was +0.8 ± 0.2 ppb/yr (+0.25 ± 0.05 %/yr) and is in reasonable agreement with measurements of the N_2O vertical column density above Jungfraujoch Station, +0.36 ± 0.06%/yr between 1984 and 1992 (Zander *et al.*, 1994). Large interannual variations in this trend are also observed. Thompson *et al.* (1994) report that the N_2O growth rate decreased from 1 ppb/yr in 1991 to 0.5 ppb/yr in 1993 and suggest that decreased use of nitrogen-containing fertiliser and lower temperatures in the Northern Hemisphere may have been in part responsible for lower biogenic soil emissions. Schauffler and Daniel (1994) suggest that the N_2O trend was affected by stratospheric circulation changes induced by massive increase in stratospheric aerosols following the eruption of Mt. Pinatubo. Since 1993, the N_2O increase has returned to rates closer to those observed during the 1980s.

The feedback of N_2O on its own lifetime (Prather, 1998) has been examined for this assessment with additional studies from established 2-D stratospheric chemical models. All models give similar results, see Table 4.5. The global mean atmospheric lifetime of N_2O decreases about 0.5% for every 10% increase in N_2O (s = –0.05). This shift is small but systematic, and it is included in Table 4.1a as a shorter perturbation lifetime for N_2O, 114 years instead of 120 years. For N_2O (unlike for CH_4) the time to mix the gas into the middle stratosphere where it is destroyed, about 3 years, causes a separation between PT (about 114 years) and the e-fold of the long-lived mode (about 110 years).

4.2.1.3 Hydrofluorocarbons (HFCs)

The HFCs with the largest measured atmospheric abundances are (in order), HFC-23 (CHF_3), HFC-134a (CF_3CH_2F), and HFC-152a (CH_3CHF_2). The recent rises in these HFCs are shown in Figure 4.3 along with some major HCFCs, the latter being controlled under the Montreal Protocol and its Amendments. HFC-23 is a by-product of HCFC-22 production. It has a long atmospheric lifetime of 260 years, so that most emissions, which have occurred over the past two decades, will have accumulated in the atmosphere. Between 1978 and 1995, HFC-23 increased from about 3 to 10 ppt; and it continues to rise even more rapidly (Oram *et al.*, 1996). HFC-134a is used primarily as a refrigerant, especially in car air conditioners. It has an atmospheric lifetime of 13.8 years, and its annual emissions have grown from near

Table 4.5: *Nitrous oxide lifetime feedback and residence time.*

Models	**Contributor**	**Lifetime LT** (yr)	**Sensitivity,** s=∂ln(LT)/ ∂ln(B)	**Decay Time of mode** (yr)
AER 2D	Ko and Weisenstein	111	–0.062	102
GSFC 2D	Jackman	137	–0.052	127
UCI 1D	Prather	119	–0.046	110
Oslo 2D	Rognerud	97	–0.061	

Lifetime (LT_B) is calculated at steady-state for an N_2O burden (B) corresponding to a tropospheric abundance of 330 ppb. The sensitivity coefficient (s) is calculated by increasing the N_2O burden approximately 10% to B+ΔB, calculating the new steady state atmospheric lifetime ($LT_{B+\Delta B}$), and then using a finite difference approximation for s, $\ln(LT_{B+\Delta B}/LT_B)/\ln(1+\Delta B/B)$. The perturbation lifetime (PT), i.e., the effective duration of an N_2O addition, can be derived as PT = LT/(1–s) or equivalently from the simple budget-balance equation: $(B+\Delta B)/LT_{B+\Delta B} = B/LT_B + \Delta B/PT$.

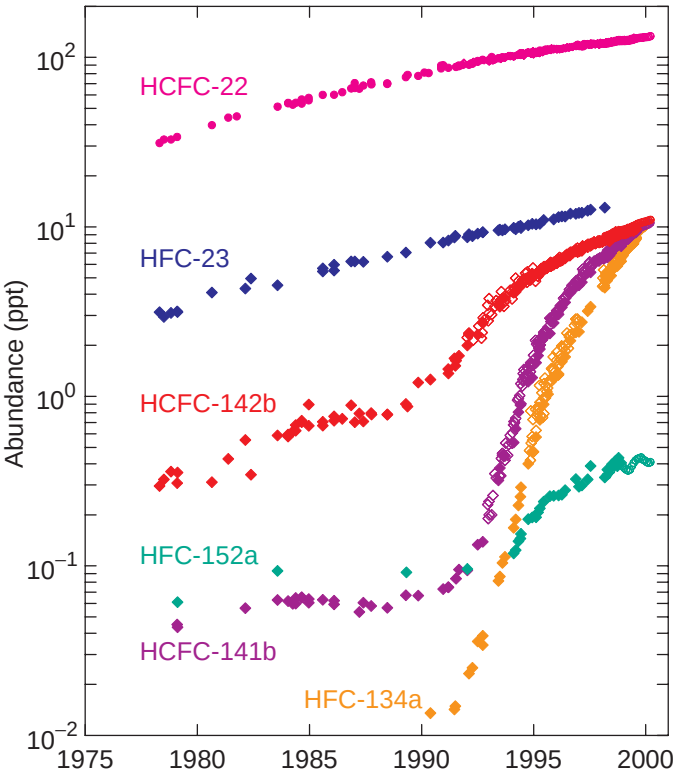

Figure 4.3: HFC-23 (blue, UEA scale), -152a (green, UEA scale), -134a (orange, NOAA scale), and HCFC-22 (magenta, SIO scale), -142b (red, NOAA scale), and -141b (purple, NOAA scale) abundances (ppt) at Cape Grim, Tasmania for the period 1978 to 1999. Different symbols are data from different measurement networks: SIO (filled circles), NOAA-CMDL (open diamonds, Montzka *et al.*, 1994, 1996a,b, 1999), UEA (filled diamonds, Oram *et al.*, 1995, 1996, 1998, 1999) and AGAGE (open circles, only for 1998 to 2000, all gases but HFC-23, Miller *et al.*, 1998; Sturrock *et al.*, 1999; Prinn *et al.*, 2000). Southern Hemisphere values (Cape Grim) are slightly lower than global averages.

zero in 1990 to an estimated 0.032 Tg/yr in 1996. The abundance continues to rise almost exponentially as the use of this HFC increases (Montzka *et al.*, 1996b; Oram *et al.*, 1996; Simmonds *et al.*, 1998). HFC-152a is a short-lived gas with a mean atmospheric lifetime of 1.4 years. Its rise has been steady, but its low emissions and a short lifetime have kept its abundance below 1 ppt.

4.2.1.4 Perfluorocarbons (PFCs) and sulphur hexafluoride (SF_6)

PFCs, in particular CF_4 and C_2F_6, as well as SF_6 have sources predominantly in the Northern Hemisphere, atmospheric lifetimes longer than 1,000 years, and large absorption cross-sections for terrestrial infra-red radiation. These compounds are far from a steady state between sources and sinks, and even small emissions will contribute to radiative forcing over the next several millennia. Current emissions of C_2F_6 and SF_6 are clearly anthropogenic and well quantified by the accumulating atmospheric burden. Harnisch and Eisenhauer (1998) have shown that CF_4 and SF_6 are naturally present in fluorites, and out-gassing from these materials leads to natural background abundances of 40 ppt for CF_4 and 0.01 ppt for SF_6. However, at present the anthropogenic emissions of CF_4 exceed the natural ones by a factor of 1,000 or more and are responsible for the rapid rise in atmospheric abundance. Atmospheric burdens of CF_4 and SF_6 are increasing as shown in Figures 4.4 and 4.5, respectively. Surface measurements show that SF_6 has increased by about 7%/yr during the 1980s and 1990s (Geller *et al.*, 1997; Maiss and Brenninkmeijer, 1998). Recent relative rates of increase are 1.3%/yr for CF_4 and 3.2%/yr for C_2F_6 (Harnisch *et al.*, 1996). The only important sinks for PFCs and SF_6 are photolysis or ion reactions in the mesosphere. These gases provide useful tracers of atmospheric transport in both troposphere and stratosphere.

A new, long-lived, anthropogenic greenhouse gas has recently been found in the atmosphere (Sturges *et al.*, 2000). Trifluoromethyl sulphur pentafluoride (SF_5CF_3) – a hybrid of PFCs and SF_6 not specifically addressed in Annex A of the Kyoto Protocol – has the largest radiative forcing, on a per molecule basis, of any gas found in the atmosphere to date. Its abundance has grown from near zero in the late 1960s to about 0.12 ppt in 1999.

4.2.2 Montreal Protocol Gases and Stratospheric Ozone (O_3)

The Montreal Protocol is an internationally accepted agreement whereby nations agree to control the production of ozone-depleting substances. Many of the chemicals that release chlorine atoms into the stratosphere, and deplete stratospheric O_3, are also greenhouse gases, so they are discussed briefly here. Detailed assessment of the current observations, trends, lifetimes, and emissions for substances covered by the protocol are in WMO (Kurylo and Rodriguez, 1999; Prinn and Zander, 1999). The ozone-depleting gases with the largest potential to influence climate are CFC-11 ($CFCl_3$), CFC-12 (CF_2Cl_2), and CFC-113 ($CF_2ClCFCl_2$). It is now clear from measurements in polar firn air that there are no natural sources of these compounds (Butler *et al.*, 1999). Surface measurements of these compounds show that their growth rates continue to decline. Growth rates are slightly negative for CFC-11 and CFC-113 (Montzka *et al.*, 1996a, 1999; Prinn *et al.*, 2000); see Figure 4.6. CFC-12 increased by 4 ppt/yr during 1995 to 1996, down from about 12 ppt/yr in the late 1980s, see Figure 4.7). Methyl chloroform (CH_3CCl_3) has decreased dramatically since the Montreal Protocol was invoked, due to its relatively short lifetime (about 5 years) and the rapidity with which emissions were phased out. Its decline was 13 ppt/yr during the period 1995 to 1996 (Prinn *et al.*, 1998, 2000). The halon abundances are small relative to the CFCs, and will never become large if the Montreal Protocol is adhered to. Atmospheric measurements show that growth rates of halon-1301 and halon-2402 decreased in response to the Montreal Protocol, but halon-1211 continues to increase at rates larger than expected based on industrial emissions data (Butler *et al.*, 1998a; Fraser *et al.*, 1999; Montzka *et al.*, 1999).

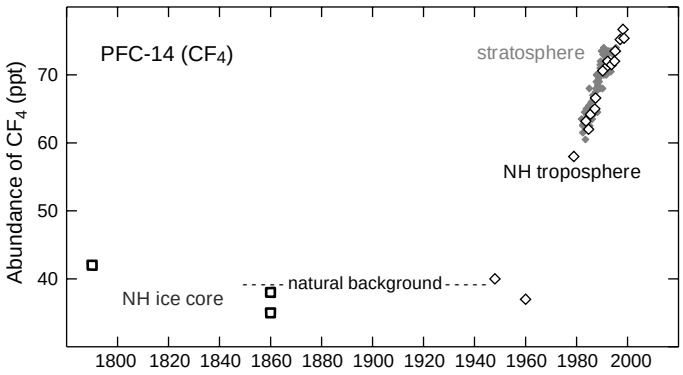

Figure 4.4: Abundance of CF_4 (ppt) over the last 200 years as measured in tropospheric air (open diamonds), stratospheric air (small filled diamonds), and ice cores (open squares) (Harnisch *et al.*, 1996; 1999).

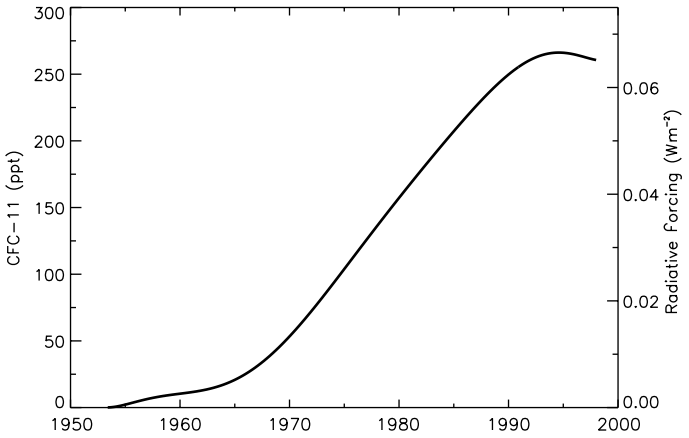

Figure 4.6: Global mean CFC-11 ($CFCl_3$) tropospheric abundance (ppt) from 1950 to 1998 based on smoothed measurements and emission models (Prinn *et al.*, 2000). CFC-11's radiative forcing is shown on the right axis.

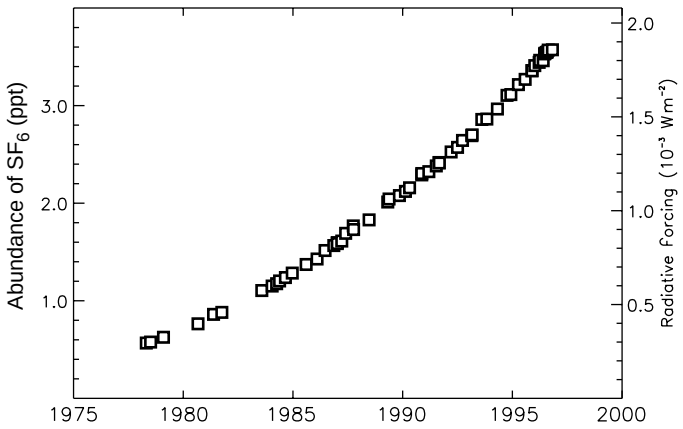

Figure 4.5: Abundance of SF_6 (ppt) measured at Cape Grim, Tasmania since 1978 (Maiss *et al.*, 1996; Maiss and Brenninkmeijer, 1998). Cape Grim values are about 3% lower than global averages.

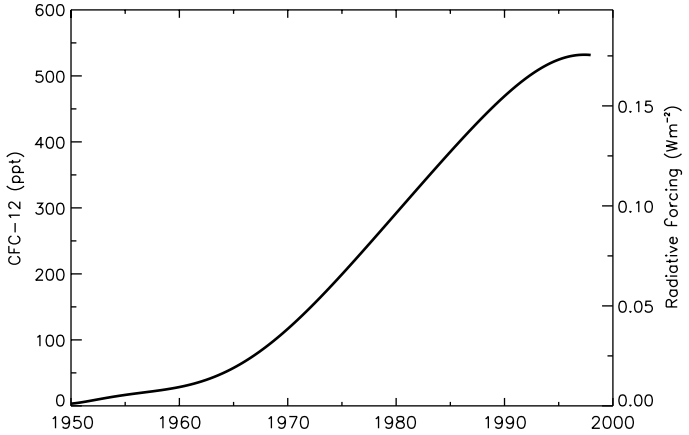

Figure 4.7: Global mean CFC-12 (CF_2Cl_2) tropospheric abundance (ppt) from 1950 to 1998 based on smoothed measurements and emission models (Prinn *et al.*, 2000). CFC-12's radiative forcing is shown on the right axis.

The depletion of stratospheric ozone over the past three decades has been substantial. Between 60°S and 60°N it averaged about 2%/decade. A thorough review of the direct and possible indirect effects of stratospheric ozone depletion are given in WMO (Granier and Shine, 1999). The depletion of O_3 (and its radiative forcing) is expected to follow the weighted halogen abundance in the stratosphere. Therefore, both will reach a maximum in about 2000 before starting to recover; however, detection of stratospheric O_3 recovery is not expected much before 2010 (Jackman *et al.*, 1996; Hofmann and Pyle, 1999). Methyl chloroform has been the main driver of the rapid turnaround in stratospheric chlorine during the late 1990s (Montzka *et al.*, 1999; Prinn *et al.*, 2000), and further recovery will rely on the more slowly declining abundances of CFC-11 and -12, and halons (Fraser *et al.*, 1999; Montzka *et al.*, 1999). It is expected that stratospheric ozone depletion due to halogens will recover during the next 50 to 100 years (Hofmann and Pyle, 1999). In the short run, climatic changes, such as cooling in the northern winter stratosphere, may enhance ozone depletion, but over the next century, the major uncertainties in stratospheric ozone lie with (i) the magnitude of future consumption of ozone-depleting substances by developing countries (Fraser and Prather, 1999; Montzka *et al.*, 1999), (ii) the projected abundances of CH_4 and N_2O, and (iii) the projected climate change impacts on stratospheric temperatures and circulation.

4.2.3 Reactive Gases

4.2.3.1 Carbon monoxide (CO) and hydrogen (H_2)

Carbon monoxide (CO) does not absorb terrestrial infrared radiation strongly enough to be counted as a direct greenhouse gas, but its role in determining tropospheric OH indirectly affects the atmospheric burden of CH_4 (Isaksen and Hov, 1987) and can lead to the formation of O_3. More than half of atmospheric CO emissions today are caused by human activities, and as a result the Northern Hemisphere contains about twice as much CO as the Southern Hemisphere. Because of its relatively short lifetime and distinct emission patterns, CO has large gradients in the atmosphere, and its global burden of about 360 Tg is more uncertain than those of CH_4 or N_2O. In the high northern latitudes, CO abundances vary from about 60 ppb during summer to 200 ppb during winter. At the South Pole, CO varies between about 30 ppb in summer and 65 ppb in winter. Observed abundances, supported by column density measurements, suggest that globally, CO was slowly increasing until the late 1980s, but has started to decrease since then (Zander *et al.* 1989; Khalil and Rasmussen, 1994), possibly due to decreased automobile emissions as a result of catalytic converters (Bakwin *et al.*, 1994). Measurements from a globally distributed network of sampling sites indicate that CO decreased globally by about 2 %/yr from 1991 to 1997 (Novelli *et al.*, 1998) but then increased in 1998. In the Southern Hemisphere, no long-term trend has been detected in CO measurements from Cape Point, South Africa for the period 1978 to 1998 (Labuschagne *et al.*, 1999).

Some recent evaluations of the global CO budget are presented in Table 4.6. The emissions presented by Hauglustaine *et al.* (1998) were used in a forward, i.e., top-down, modelling study of the CO budget; whereas Bergamasschi *et al.* (2000) used a model inversion to derive CO sources. These varied approaches do not yet lead to a consistent picture of the CO budget. Anthropogenic sources (deforestation, savanna and waste burning, fossil and domestic fuel use) dominate the direct emissions of CO, emitting 1,350 out of 1,550 Tg(CO)/yr. A source of 1,230 Tg(CO)/yr is estimated from *in situ* oxidation of CH_4 and other hydrocarbons, and about half of this source can be attributed to anthropogenic emissions. Fossil sources of CO have already been accounted for as release of fossil C in the CO_2 budget, and thus we do not double-count this CO as a source of CO_2.

It has been proposed that CO emissions should have a GWP because of their effects on the lifetimes of other greenhouse gases (Shine *et al.*, 1990; Fuglesvedt *et al.*, 1996; Prather, 1996). Daniel and Solomon (1998) estimate that the cumulative indirect radiative forcing due to anthropogenic CO emissions may be larger than that of N_2O. Combining these early box models with 3-D global CTM studies using models from OxComp (Wild and Prather, 2000; Derwent *et al.*, 2001) suggests that emitting 100 Tg(CO) is equivalent to emitting 5 Tg(CH_4): the resulting CH_4 perturbation appears after a few months and lasts 12 years as would a CH_4 perturbation; and further, the resulting tropospheric O_3 increase is global, the same as for a direct CH_4 perturbation. Effectively the CO emission excites the global 12-year chemical mode that is associated with CH_4 perturbations. This equivalency is not unique as the impact of CO appears to vary by as much as 20% with latitude of emission. Further, this equivalency systematically underestimates the impact of CO on greenhouse gases because it does not include the short-term tropospheric O_3 increase during the early period of very high CO abundances (< 6 months). Such O_3 increases are regional, however, and their magnitude depends on local conditions.

Molecular hydrogen (H_2) is not a direct greenhouse gas. But it can reduce OH and thus indirectly increase CH_4 and HFCs. Its atmospheric abundance is about 500 ppb. Simmonds *et al.* (2000) report a trend of $+1.2 \pm 0.8$ ppb/yr for background air at Mace Head, Ireland between 1994 and 1998; but, in contrast, Novelli *et al.* (1999) report a trend of -2.3 ± 0.1 ppb/yr based on a global network of sampling sites. H_2 is produced in many of the same processes that produce CO (e.g., combustion of fossil fuel and atmospheric oxidation of CH_4), and its atmospheric measurements can be used to constrain CO and CH_4 budgets. Ehhalt (1999) estimates global annual emissions of about 70 Tg(H_2)/yr, of which half are anthropogenic. About one third of atmospheric H_2 is removed by reaction with tropospheric OH, and the remainder, by microbial uptake in soils. Due to the larger land area in the Northern Hemisphere than in the Southern Hemisphere, most H_2 is lost in the Northern Hemisphere. As a result, H_2 abundances are on average greater in the Southern Hemisphere despite 70% of emissions being in the Northern Hemisphere (Novelli *et al.*, 1999; Simmonds *et al.*, 2000). Currently the impact of H_2 on tropospheric OH is small, comparable to some of the VOC. No scenarios for changing H_2 emissions are considered here; however, in a possible fuel-cell economy, future emissions may need to be considered as a potential climate perturbation.

Table 4.6: *Estimates of the global tropospheric carbon monoxide budget (in Tg(CO)/yr) from different sources compared with the values adopted for this report (TAR).*

Reference:	Hauglustaine *et al.* (1998)	Bergamasschi *et al.* (2000)	WMO (1999)	SAR (1996)	TAR[a]
Sources					
Oxidation of CH_4		795		400 – 1000	800
Oxidation of Isoprene		268		200 – 600[b]	270
Oxidation of Terpene		136			~0
Oxidation of industrial NMHC		203			110
Oxidation of biomass NMHC		–			30
Oxidation of Acetone		–			20
Sub-total *in situ* oxidation	**881**	**1402**			**1230**
Vegetation		–	100	60 – 160	150
Oceans		49	50	20 – 200	50
Biomass burning[c]		768	500	300 – 700	700
Fossil & domestic fuel		641	500	300 – 550	650
Sub-total direct emissions	**1219**	**1458**	**1150**		**1550**
Total sources	**2100**	**2860**		**1800 – 2700**	**2780**
Sinks					
Surface deposition	190			250 – 640	
OH reaction	1920			1500 – 2700	

Anthropogenic emissions by continent/region	Y2000	Y2100(A2p)
Africa	80	480
South America	36	233
Southeast Asia	44	203
India	64	282
North America	137	218
Europe	109	217
East Asia	158	424
Australia	8	20
Other	400	407
Sum	1036	2484

[a] Recommended for OxComp model calculations for year 2000.
[b] Includes all VOC oxidation.
[c] From deforestation, savannah and waste burning.

4.2.3.2 Volatile organic compounds (VOC)

Volatile organic compounds (VOC), which include non-methane hydrocarbons (NMHC) and oxygenated NMHC (e.g., alcohols, aldehydes and organic acids), have short atmospheric lifetimes (fractions of a day to months) and small direct impact on radiative forcing. VOC influence climate through their production of organic aerosols and their involvement in photochemistry, i.e., production of O_3 in the presence of NO_x and light. The largest source, by far, is natural emission from vegetation. Isoprene, with the largest emission rate, is not stored in plants and is only emitted during photosynthesis (Lerdau and Keller, 1997). Isoprene emission is an important component in tropospheric photochemistry (Guenther *et al.*, 1995, 1999) and is included in the OxComp simulations. Monoterpenes are stored in plant reservoirs, so they are emitted throughout the day and night. The monoterpenes play an important role in aerosol formation and are discussed in Chapter 5. Vegetation also releases other VOC at relatively small rates, and small amounts of NMHC are emitted naturally by the oceans. Anthropogenic sources of VOC include fuel production, distribution, and combustion, with the largest source being emissions (i) from motor vehicles due to either evaporation or incomplete combustion of fuel, and (ii) from biomass burning. Thousands of different compounds with varying lifetimes and chemical behaviour have been observed in the atmosphere, so most models of tropospheric chemistry include some chemical speciation of the VOC. Generally, fossil

Table 4.7(a): *Estimates of global VOC emissions (in TgC/yr) from different sources compared with the values adopted for this report (TAR).*

Ehhalt (1999)	**Isoprene (C_5H_8)**	**Terpene ($C_{10}H_{16}$)**	**C_2H_6**	**C_3H_8**	**C_4H_{10}**	**C_2H_4**	**C_3H_6**	**C_2H_2**	**Benzene (C_6H_6)**	**Toluene (C_7H_8)**
Fossil fuel [a]	–	–	4.8	4.9	8.3	8.6	8.6	2.3	4.6	13.7
Biomass burning	–	–	5.6	3.3	1.7	8.6	4.3	1.8	2.8	1.8
Vegetation	503	124	4.0	4.1	2.5	8.6	8.6	–	–	–
Oceans	–	–	0.8	1.1	–	1.6	1.4	–	–	–

TAR [b]	**Total**	**Isoprene**	**Terpene**	**Acetone**
Fossil fuel [a]	161			
Biomass burning	33			
Vegetation	377	220	127	30

[a] Fossil includes domestic fuel.
[b] TAR refers to recommended values for OxComp model calculations for the year 2000.

Table 4.7(b): *Detailed breakdown of VOC emissions by species adopted for this report (TAR).*

	Industrial		**Biomass burning**	
Species	wt%	#C atoms	wt%	#C atoms
Alcohols	3.2	2.5	8.1	1.5
Ethane	4.7	2.0	7.0	2.0
Propane	5.5	3.0	2.0	3.0
Butanes	10.9	4.0	0.6	4.0
Pentanes	9.4	5.0	1.4	5.0
Higher alkanes	18.2	7.5	1.3	8.0
Ethene	5.2	2.0	14.6	2.0
Propene	2.4	3.0	7.0	3.0
Ethyne	2.2	2.0	6.0	2.0
Other alkenes, alkynes, dienes	3.8	4.8	7.6	4.6
Benzene	3.0	6.0	9.5	6.0
Toluene	4.9	7.0	4.1	7.0
Xylene	3.6	8.0	1.2	8.0
Trimethylbenzene	0.7	9.0	–	–
Other aromatics	3.1	9.6	1.0	8.0
Esters	1.4	5.2	–	–
Ethers	1.7	4.7	5.5	5.0
Chlorinated HC's	0.5	2.6	–	–
Formaldehyde	0.5	1.0	1.2	1.0
Other aldehydes	1.6	3.7	6.1	3.7
Ketones	1.9	4.6	0.8	3.6
Acids	3.6	1.9	15.1	1.9
Others	8.1	4.9	–	–

wt% values are given for the individual VOC with the sums being: industrial, 210 Tg(VOC)/yr, corresponding to 161 TgC/yr; and biomass burning, 42 Tg(VOC)/yr, corresonding to 33 TgC/yr.

VOC sources have already been accounted for as release of fossil C in the CO_2 budgets and thus we do not count VOC as a source of CO_2.

Given their short lifetimes and geographically varying sources, it is not possible to derive a global atmospheric burden or mean abundance for most VOC from current measurements. VOC abundances are generally concentrated very near their sources. Natural emissions occur predominantly in the tropics (23°S to 23°N) with smaller amounts emitted in the northern mid-latitudes and boreal regions mainly in the warmer seasons. Anthropogenic emissions occur in heavily populated, industrialised regions (95% in the Northern Hemisphere peaking at 40°N to 50°N), where natural emissions are relatively low, so they have significant impacts on regional chemistry despite small global

emissions. A few VOC, such as ethane and acetone, are longer-lived and impact tropospheric chemistry on hemispheric scales. Two independent estimates of global emissions (Ehhalt, 1999; and TAR/OxComp budget based on the Emission Database for Global Atmospheric Research (EDGAR)) are summarised in Table 4.7a. The OxComp specification of the hydrocarbon mixture for both industrial and biomass-burning emissions is given in Table 4.7b.

One of the NMHC with systematic global measurements is ethane (C_2H_6). Rudolph (1995) have used measurements from five surface stations and many ship and aircraft campaigns during 1980 to 1990 to derive the average seasonal cycle for ethane as a function of latitude. Ehhalt *et al.* (1991) report a trend of +0.8%/yr in the column density above Jungfraujoch, Switzerland for the period 1951 to 1988, but in the following years, the trend turned negative. Mahieu *et al.* (1997) report a trend in C_2H_6 of -2.7 ± 0.3%/yr at Jungfraujoch, Switzerland for 1985 to 1993; Rinsland *et al.* (1998) report a trend of -1.2 ± 0.4%/yr at Kitt Peak, Arizona for 1977 to 1997 and -0.6 ± 0.8%/yr at Lauder, New Zealand for 1993 to 1997. It is expected that anthropogenic emissions of most VOC have risen since pre-industrial times due to increased use of gasoline and other hydrocarbon products. Due to the importance of VOC abundance in determining tropospheric O_3 and OH, systematic measurements and analyses of their budgets will remain important in understanding the chemistry-climate coupling.

There is a serious discrepancy between the isoprene emissions derived by Guenther *et al.* (1995) based on a global scaling of emission from different biomes, about 500 TgC/yr, and those used in OxComp for global chemistry-transport modelling, about 200 TgC/yr. When the larger isoprene fluxes are used in the CTMs, many observational constraints on CO and even isoprene itself are poorly matched. This highlights a key uncertainty in global modelling of highly reactive trace gases: namely, what fraction of primary emissions escapes immediate reaction/removal in the vegetation canopy or immediate boundary layer and participates in the chemistry on the scales represented by global models? For the isoprene budget, there are no measurements of the deposition of reaction products within the canopy. More detail on the scaling of isoprene and monoterpene emissions is provided in Chapter 5. Although isoprene emissions are likely to change in response to evolving chemical and climate environment over the next century, this assessment was unable to include a projection of such changes.

4.2.3.3 Nitrogen oxides (NO_x)

Nitrogen oxides ($NO_x = NO + NO_2$) do not directly affect Earth's radiative balance, but they catalyse tropospheric O_3 formation through a sequence of reactions, e.g.,

$$\begin{aligned} & OH + CO + O_2 \rightarrow CO_2 + HO_2 \\ & HO_2 + NO \rightarrow NO_2 + OH \\ & NO_2 + h\nu \rightarrow NO + O(^3P) \\ & O(^3P) + O_2 + M \rightarrow O_3 + M \\ \text{net:} \quad & CO + 2O_2 + h\nu \rightarrow CO_2 + O_3 \end{aligned}$$

By rapidly converting HO_2 to OH, NO enhances tropospheric OH abundances and thus indirectly reduces the atmospheric burdens of CO, CH_4, and HFCs. Much of recent understanding of the role of NO_x in producing tropospheric O_3 and changing OH abundances is derived from *in situ* measurement campaigns that sample over a wide range of chemical conditions in the upper troposphere or at the surface (see Section 4.2.6 on tropospheric OH). These atmospheric measurements generally support the current photochemical models. There is substantial spatial and temporal variability in the measured abundance of NO_x, which ranges from a few ppt near the surface over the remote tropical Pacific Ocean to >100 ppb in urban regions. The local chemical lifetime of NO_x is always short, but varies widely throughout the troposphere, being 1 day or less in the polluted boundary layer, day or night, and 5 to 10 days in the upper troposphere. As with VOC, it is not possible to derive a global burden or average abundance for NO_x from measurements of atmospheric abundances.

Most tropospheric NO_x are emitted as NO, which photochemically equilibrates with nitrogen dioxide (NO_2) within a few minutes. Significant sources, summarised in Table 4.8, include both surface and *in situ* emissions, and only a small amount is transported down from the stratosphere. NO_x emitted within polluted regions are more rapidly removed than those in remote regions. Emissions directly into the free troposphere have a disproportionately large impact on global greenhouse gases. The major source of NO_x is fossil fuel combustion, with 40% coming from the transportation sector. Benkovitz *et al.* (1996) estimated global emissions at 21 TgN/yr for 1985. The NO_x emissions from fossil fuel use used in model studies here for year 2000 are considerably higher, namely 33 TgN/yr. The large American and European emissions are relatively stable, but emissions from East Asia are increasing by about +4%/yr (Kato and Akimoto, 1992). Other important, but more uncertain surface sources are biomass burning and soil emissions. The soil source recently derived from a bottom-up compilation of over 100 measurements from various ecosystems is 21 TgN/yr (Davidson and Kingerlee, 1997), much higher than earlier estimates. Part of the discrepancy can be explained by the trapping of soil-emitted NO in the vegetation canopy. Inclusion of canopy scavenging reduces the NO_x flux to the free troposphere to 13 TgN/yr, which is still twice the flux estimated by another recent study (Yienger and Levy, 1995). Emissions of NO_x in the free troposphere include NO_x from aircraft (8 to 12 km), ammonia oxidation, and lightning (Lee *et al.*, 1997). Estimates of the lightning NO_x source are quite variable; some recent global estimates are 12 TgN/yr (Price *et al.*, 1997a,b), while other studies recommend 3 to 5 TgN/yr (e.g., Huntrieser *et al.*, 1998; Wang *et al.*, 1998a). Recent studies indicate that the global lightning frequency may be lower than previously estimated (Christian *et al.*, 1999) but that intra-cloud lightning may be much more effective at producing NO (DeCaria *et al.*, 2000). In total, anthropogenic NO_x emissions dominate natural sources, with fossil fuel combustion concentrated in northern industrial regions. However, natural sources may control a larger fraction of the globe. Overall, anthropogenic NO_x emissions are expected to undergo a fundamental shift from the current dominance of the

Table 4.8: *Estimates of the global tropospheric NO_x budget (in TgN/yr) from different sources compared with the values adopted for this report.*

Reference:	TAR	Ehhalt (1999)	Holland *et al.* (1999)	Penner *et al.* (1999)	Lee *et al.* (1997)
Base year	2000	~1985	~1985	1992	
Fossil fuel	33.0	21.0	20 – 24	21.0	22.0
Aircraft	0.7	0.45	0.23 – 0.6	0.5	0.85
Biomass burning	7.1	7.5	3 – 13	5 – 12	7.9
Soils	5.6	5.5	4 – 21	4 – 6	7.0
NH_3 oxidation	–	3.0	0.5 – 3	–	0.9
Lightning	5.0	7.0	3 – 13	3 – 5	5.0
Stratosphere	<0.5	0.15	0.1 –0.6	–	0.6
Total	**51.9**	**44.6**			**44.3**

Anthropogenic emissions by continent/region	Y2000	Y2100(A2p)
Africa	2.5	21.8
South America	1.4	10.8
Southeast Asia	1.2	6.8
India	1.7	10.0
North America	10.1	18.5
Europe	7.3	14.3
East Asia	5.6	24.1
Australia	0.5	1.1
Other	2.3	2.6
Sum	**32.6**	**110.0**

The TAR column was used in OxComp model calculations for year 2000; fossil fuel includes bio-fuels, but surface sources only; stratospheric source in TAR is upper limit and includes HNO_3; the range of values used in modelling for IPCC aviation assessment (Penner *et al.* 1999) is given.

Northern Hemisphere to a more tropical distribution of emissions. Asian emissions from fossil fuel are expected to drive an overall increase in NO_x emissions in the 21st century (Logan, 1994; Van Aardenne *et al.*, 1999).

The dominant sink of NO_x is atmospheric oxidation of NO_2 by OH to form nitric acid (HNO_3), which then collects on aerosols or dissolves in precipitation and is subsequently scavenged by rainfall. Other pathways for direct NO_x removal occur through canopy scavenging of NO_x and direct, dry deposition of NO_x, HNO_3, and particulate nitrates to the land surface and the ocean. Dry deposition can influence the surface exchanges and can thus alter the release of NO_x and N_2O to the atmosphere. Peroxyacetyl nitrate (PAN), formed by the reaction of $CH_3C(O)O_2$ with NO_2, can transport HO_x and NO_x to remote regions of the atmosphere due to its stability at the cold temperatures of the upper troposphere. In addition tropospheric aerosols provide surfaces on which reactive nitrogen, in the form of NO_3 (nitrate radical) or N_2O_5, is converted to HNO_3 (Dentener and Crutzen, 1993; Jacob, 2000).

Some CTM studies argue against either the large soil source or the large lightning source of NO_x. A climatology of NO_x measurements from aircraft was prepared by Emmons *et al.* (1997) and compared with six chemical transport models. They found that the processes controlling NO_x in the remote troposphere are not well modelled and that, of course, there is a paucity of global NO_x measurements. For short-lived gases like NO_x, resolution of budget discrepancies is even more challenging than for the long-lived species, because the limited atmospheric measurements offer few real constraints on the global budget. However, an additional constraint on the NO_x budget is emerging as the extensive measurements of wet deposition of nitrate over Northern Hemisphere continents are compiled and increasing numbers of surface measurements of dry deposition of HNO_3, NO_2, and particulate nitrate become available, and thus allow a much better estimate of the NO_x sink.

4.2.4 Tropospheric O_3

Tropospheric O_3 is a direct greenhouse gas. The past increase in tropospheric O_3 is estimated to provide the third largest increase in direct radiative forcing since the pre-industrial era. In addition, through its chemical impact on OH, it modifies the lifetimes of other greenhouse gases, such as CH_4. Its budget, however, is much more difficult to derive than that of a long-lived gas for

Table 4.9: *Estimates of the change in tropospheric ozone since the pre-industrial era from various sources compared with the values recommended in this report.*

Current climatology of tropospheric ozone (Park *et al.*, 1999)**:**

Global mean tropospheric O_3: 34 DU = 370 Tg(O)$_3$ content in the Northern Hemisphere = 36 DU, in the Southern Hemisphere = 32 DU.

SAR recommendation:

"50% of current Northern Hemisphere is anthropogenic" gives pre-industrial global mean content = 25 DU.

Increase = +9 DU

19th & early 20th century observations: [a]

Assume Northern Hemisphere tropospheric ozone has increased uniformly by >30 ppb.

Increase = +10 to +13 DU

Survey of CTM simulated change from pre-industrial: [b]

DU increase	*Model*	*Reference*
9.6	UIO	Berntsen *et al.* (1999)
7.9	GFDL	Haywood *et al.* (1998)
8.9	MOZART-1	Hauglustaine *et al.* (1998)
8.4	NCAR/2D	Kiehl *et al.* (1999)
9.5	GFDL-scaled	Levy *et al.* (1997)
12.0	Harvard/GISS	Mickley *et al.* (1999)
7.2	ECHAM4	Roelofs *et al.* (1997)
8.7	UKMO	Stevenson *et al.* (2000)
8.0	MOGUNTIA	VanDorland *et al.* (1997)

Increase = +7 to +12 DU (model range)

TAR recommendation:

Pre-industrial era global mean tropospheric O_3 has increased from 25 DU to 34 DU.

This increase, +9 DU, has a 67% likely range of 6 to 13 DU.

Increase = +9 DU (+6 to +13 DU)

The troposphere is defined as air with O_3 <150 ppb, see Logan (1999). The Dobson Unit is 1 DU = 2.687×10^{16} molecules of O_3 per square centimetre; globally 1 DU = 10.9 Tg(O_3) and 1 ppb of tropospheric O_3 = 0.65 DU. The change in CH_4 alone since pre-industrial conditions would give about +4 DU global increase in tropospheric O_3 alone (see Table 4.11).

[a] Early observations are difficult to interpret and do not provide coverage needed to derive the tropospheric burden of O_3 (see Harris *et al.*, 1997). The change in burden is derived here by shifting tropospheric O_3 uniformly in altitude to give 10 ppb at the surface in Northern Hemisphere mid-latitudes and 20 ppb at surface in Northern Hemisphere tropics (implies 10 DU), or by additionally reducing Southern Hemisphere tropics to 20 ppb and Southern Hemisphere mid-latitudes to 25 ppb at the surface (13 DU).

[b] From a survey of models by Hauglustaine and Solomon and Chapter 4. Except for Kiehl *et al.*, these were all CTMs; they used widely varying assumptions about pre-industrial conditions for CH_4, CO, NO_x, and biomass burning and they did not all report consistent diagnostics.

several reasons. Ozone abundances in the troposphere typically vary from less than 10 ppb over remote tropical oceans up to about 100 ppb in the upper troposphere, and often exceed 100 ppb downwind of polluted metropolitan regions. This variability, reflecting its rapid chemical turnover, makes it impossible to determine the tropospheric burden from the available surface sites, and we must rely on infrequent and sparsely sited profiles from ozone sondes (e.g., Logan, 1999). The total column of ozone is measured from satellites, and these observations have been used to infer the tropospheric ozone column after removing the much larger stratospheric column (e.g., Fishman and Brackett, 1997; Hudson and Thompson, 1998; Ziemke *et al.*, 1998). The current burden of tropospheric O_3 is about 370 Tg(O_3), which is equivalent to a globally averaged column density of 34 DU (Dobson Units, 1 DU = 2.687×10^{16} molecules/cm^{-2}) or a mean abundance of about 50 ppb, see Table 4.9.

The sources and sinks of tropospheric ozone are even more difficult to quantify than the burden. Influx of stratospheric air is a source of about 475 Tg(O_3)/yr based on observed correlations with other gases (Murphy and Fahey, 1994; McLinden *et al.*, 2000). The *in situ* photochemical sources are predicted to be many times larger, but are nearly balanced by equally large *in situ* chemical sinks (see discussion on CTM modelling of tropospheric O_3 in Sections 4.4 and 4.5, Table 4.12). Photochemical production of ozone is tied to the abundance of pollutants and thus varies widely over a range of spatial scales, the most important of which (e.g., biomass burning plumes, urban plumes, aircraft corridors, and convective outflows) are not well represented in most global CTMs and cannot be quantified globally with regional models. The dominant photochemical sinks for tropospheric O_3 are the catalytic destruction cycle involving the $HO_2 + O_3$ reaction and photolytic destruction by pathways involving the reaction of $O(^1D)$, a product of O_3 photodissociation. The other large sink, comparable in magnitude to the stratospheric source, is surface loss mainly to vegetation. Another loss of O_3 is observed under certain conditions in the polar marine boundary layer, notably at the end of Arctic winter. It indicates reactions involving halogen radicals and aerosols (Oum *et al.*, 1998; Dickerson *et al.*, 1999; Impey *et al.*, 1999; Platt and Moortgat, 1999; Prados *et al.*, 1999; Vogt *et al.*, 1999). The contribution of these processes to the global budget is not yet quantified, but is probably small.

Atmospheric measurement campaigns, both at surface sites and with aircraft, have focused on simultaneous observations of the many chemical species involved in tropospheric O_3 production. Primary areas of O_3 production are the mid-latitude industrialised and tropical biomass burning regions. For example, the North Atlantic Regional Experiment (NARE) and the Atmosphere Ocean Chemistry Experiment (AEROCE) showed that the prevailing westerly winds typically carry large quantities of ozone and precursors from the eastern USA over the North Atlantic, reaching Bermuda and beyond (e.g., Dickerson *et al.*, 1995; Penkett *et al.*, 1998; Prados *et al.*, 1999). The Pacific Exploratory Missions (PEM: Hoell *et al.*, 1997, 1999) measured extensive plumes of pollution including ozone and its precursors downwind of eastern Asia. Convective transport of emissions from biomass burning affect the abundance of O_3 in the mid- and upper troposphere (Pickering *et al.*, 1996). Emissions by tropical fires in South America and southern Africa have been identified as the cause of enhanced O_3 over the South Atlantic (Thompson *et al.*, 1996), and the effects of biomass burning were seen in the remote South Pacific in PEM Tropics A (Schultz *et al.*, 1999; Talbot *et al* ., 1999). Due to the widely varying chemical environments, these extensive studies provide a statistical sampling of conditions along with a critical test of the photochemistry in CTM simulations, but they do not provide an integrated budget for tropospheric O_3. An example of such model-and-measurements study is given in the Section 4.2.6 discussion of tropospheric OH.

Recent trends in global tropospheric O_3 are extremely difficult to infer from the available measurements, while trends in the stratosphere are readily identified (Randel *et al.*, 1999; WMO, 1999). With photochemistry producing local lifetimes as short as a few days in the boundary layer, the local measurement of tropospheric O_3 does not reflect the abundance over the surrounding continent, and a surface measurement is not representative of the bulk of the troposphere above. Thus it is not contradictory for decadal trends in different atmospheric regions to be different, e.g., driven by the regional changes in pollutants, particularly NO_x. Ozone sondes offer the best record of O_3 throughout the troposphere, although measurements at many stations are made only weekly (infrequently for a variable gas like O_3). Weekly continuous data since 1970 are available from only nine stations in the latitude range 36°N to 59°N (Logan *et al.*, 1999; WMO, 1999). Different trends are seen at different locations for different periods. Most stations show an increase from 1970 to 1980, but no clear trend from 1980 to 1996. A composite record of the mid-tropospheric O_3 abundance from 1970 to 1996 from the nine stations is taken from the analysis of Logan *et al.* (1999) and presented in Figure 4.8. There is no obvious linear increase in O_3 abundance over this period, although the second half of this record (about 57 ppb) is clearly greater than the first half (about 53 ppb). Of the fourteen stations with records since 1980, only two, one in Japan and one in Europe, had statistically significant increases in mid-tropospheric O_3 between 1980 and 1995. By contrast, the four Canadian stations, all at high latitudes, had significant decreases for the same time period. Surface O_3 measurements from seventeen background stations also show no clear trend, even in the northern mid-latitudes (Oltmans *et al.*, 1998; WMO, 1999). The largest negative trend in surface O_3 was $-0.7 \pm 0.2\%$/yr at the South Pole (1975 to 1997), while the largest positive trend was $+1.5 \pm 0.5\%$/yr at Zugspitze, Germany (1978 to 1995). This ambiguous record of change over the past two decades may possibly be reconciled with the model predictions (see Section 4.4) of increasing tropospheric O_3 driven regionally by increasing emissions of pollutants: the growth in NO_x emissions is expected to have shifted from North America and Europe to Asia.

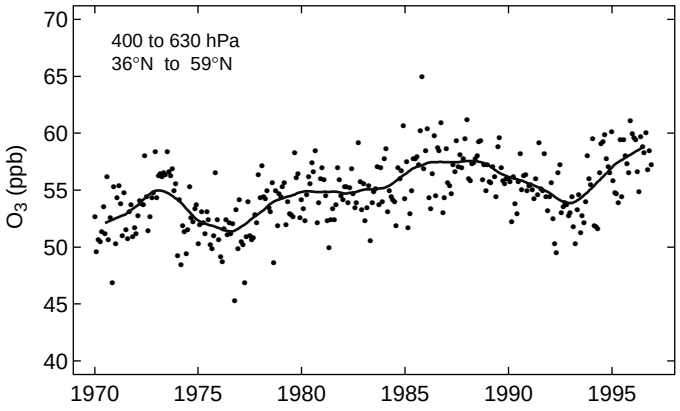

Figure 4.8: Mid-tropospheric O_3 abundance (ppb) in northern mid-latitudes (36°N-59°N) for the years 1970 to 1996. Observations between 630 and 400 hPa are averaged from nine ozone sonde stations (four in North America, three in Europe, two in Japan), following the data analysis of Logan *et al.* (1999). Values are derived from the residuals of the trend fit with the trend added back to allow for discontinuities in the instruments. Monthly data (points) are shown with a smoothed 12-month-running mean (line).

The change in tropospheric O_3 since the pre-industrial era is even more difficult to evaluate on the basis of measurements alone. Since O_3 is reactive, atmospheric abundances cannot be retrieved from ice cores. Recent evaluations of surface measurements in the 19th and early 20th century in Europe (Volz and Kley, 1988; Staehelin *et al.*, 1994, 1998; Harris *et al.*, 1997) indicate much lower O_3 abundances than today, yet the scaling of these data to a tropospheric O_3 burden, even for northern mid-latitudes, is not obvious. In the SAR, these data were used to make a rough estimate that O_3 abundances in the Northern Hemispheric troposphere have doubled since the pre-industrial era. A similar difference, of 10 to 13 DU when globally averaged, is obtained using the climatology given by Park *et al.* (1999) for tropospheric O_3 today and a parallel one with abundances adjusted to match the 19th century measurements in the Northern Hemisphere. CTM calculations predict that current anthropogenic emissions of NO_x, CO, and VOC, as well as the increase in CH_4 should have increased tropospheric O_3 by a similar amount, primarily in the Northern Hemisphere. A recent survey of CTM studies gives global average increases ranging from 8 to 12 DU, although this small range does not adequately represent the uncertainty. These results are summarised in Table 4.9. Based on measurements, analyses, and models, the most likely increase in tropospheric O_3 was 9 DU globally averaged, with a 67% confidence range of 6 to 13 DU. For some of the emissions scenarios considered here, tropospheric O_3 is expected to increase even more in the 21st century as emissions of its precursors – NO_x, CO and VOC – continue to grow (see Section 4.4).

4.2.5 Stratospheric H_2O

Water vapour in the lower stratosphere is a very effective greenhouse gas. Baseline levels of stratospheric H_2O are controlled by the temperature of the tropical tropopause, a parameter that changes with climate (Moyer *et al.*, 1996; Rosenlof *et al.*, 1997; Dessler, 1998; Mote *et al.*, 1998). The oxidation of CH_4 is a source of mid-stratospheric H_2O and currently causes its abundance to increase from about 3 ppm at the tropopause to about 6 ppm in the upper stratosphere. In addition, future direct injections of H_2O from high-flying aircraft may add H_2O to the lower stratosphere (Penner *et al.*, 1999). Oltmans and Hofmann (1995) report statistically significant increases in lower stratospheric H_2O above Boulder, Colorado between 1981 and 1994. The vertical profile and amplitude of these changes do not correspond quantitatively with that expected from the recognised anthropogenic sources (CH_4 oxidation). Analyses of satellite and ground-based measurements (Nedoluha *et al.*, 1998; Michelsen *et al.*, 2000) find increases in upper stratospheric H_2O from 1985 to 1997, but at rates (>1%/yr) that exceed those from identified anthropogenic sources (i.e., aviation and methane increases) and that obviously could not have been maintained over many decades. In principle such a temporary trend could be caused by a warming tropopause, but a recent analysis indicates instead a cooling tropopause (Simmons *et al.*, 1999). It is important to resolve these apparent discrepancies; since, without a physical basis for this recent trend, no recommendation can be made here for projecting changes in lower stratospheric H_2O over the 21st century.

*4.2.6 Tropospheric OH and Photochemical Modelling

The hydroxyl radical (OH) is the primary cleansing agent of the lower atmosphere, in particular, it provides the dominant sink for CH_4 and HFCs as well as the pollutants NO_x, CO and VOC. Once formed, tropospheric OH reacts with CH_4 or CO within a second. The local abundance of OH is controlled by the local abundances of NO_x, CO, VOC, CH_4, O_3, and H_2O as well as the intensity of solar UV; and thus it varies greatly with time of day, season, and geographic location.

The primary source of tropospheric OH is a pair of reactions that start with the photodissociation of O_3 by solar UV.

$$O_3 + h\nu \rightarrow O(^1D) + O_2$$
$$O(^1D) + H_2O \rightarrow OH + OH$$

Although in polluted regions and in the upper troposphere, photodissociation of other trace gases such as peroxides, acetone and formaldehyde (Singh *et al.*, 1995; Arnold *et al.*, 1997) may provide the dominant source (e.g., Folkins *et al.*, 1997; Prather and Jacob, 1997; Wennberg *et al.*, 1998; Müller and Brasseur, 1999). OH reacts with many atmospheric trace gases, in most cases as the first and rate-determining step of a reaction chain that leads to more or less complete oxidation of the compound. These chains often lead to formation of an HO_2 radical, which then reacts with O_3 or NO to recycle back to OH. Tropospheric OH is lost through reactions with other radicals, e.g., the reaction with HO_2 to form H_2O or with NO_2 to form HNO_3. In addition to providing the primary loss for CH_4 and other pollutants, HO_x radicals (OH and HO_2) together with NO_x are key catalysts in the production of tropospheric O_3 (see Section 4.2.3.3). The sources and sinks of OH involve most of the fast photochemistry of the troposphere.

Pre-industrial OH is likely to have been different than today, but because of the counteracting effects of lower CO and CH_4 (increasing OH) and reduced NO_x and O_3 (decreasing OH), there is no consensus on the magnitude of this change (e.g., Wang and Jacob, 1998). Trends in the current OH burden appear to be <1%/yr. Separate analyses of the CH_3CCl_3 observations for the period 1978 to 1994 report two different but overlapping trends in global OH: no trend within the uncertainty range (Prinn *et al.*, 1995), and 0.5 ± 0.6%/yr (Krol *et al.*, 1998). Based on the OxComp workshop, the SRES projected emissions would lead to future changes in tropospheric OH that ranging from +5% to –20% (see Section 4.4).

4.2.6.1 Laboratory data and the OH lifetime of greenhouse gases

Laboratory data on the rates of chemical reactions and photodissociation provide a cornerstone for the chemical models used here. Subsequent to the SAR there have been a number of updates to the recommended chemical rate databases of the International Union of Pure and Applied Chemistry (IUPAC 1997a,b, 1999) and the Jet Propulsion Laboratory (JPL) (DeMore *et al.*, 1997; Sander *et al.*, 2000). The CTMs in the OxComp workshop generally used the JPL-1997 database (JPL, 1997) with some updated rates similar to JPL-2000 (JPL, 2000). The most significant changes or additions to the databases include: (i) revision of the low temperature reaction rate coefficients for OH + NO_2 leading to enhancement of HO_x

and NO_x abundances in the lower stratosphere and upper troposphere; (ii) extension of the production of $O(^1D)$ from O_3 photodissociation to longer wavelengths resulting in enhanced OH production in the upper troposphere; and (iii) identification of a new heterogeneous reaction involving hydrolysis of $BrONO_2$ which serves to enhance HO_x and suppress NO_x in the lower stratosphere. These database improvements, along with many other smaller refinements, do not change the overall understanding of atmospheric chemical processes but do impact the modelled tropospheric OH abundances and the magnitude of calculated O_3 changes by as much as 20% under certain conditions.

Reaction rate coefficients used in this chapter to calculate atmospheric lifetimes for gases destroyed by tropospheric OH are from the 1997 and 2000 NASA/JPL evaluations (DeMore *et al.*, 1997; Sander *et al.*, 2000) and from Orkin *et al.* (1999) for HFE-356mff2. These rate coefficients are sensitive to atmospheric temperature and can be ten times faster near the surface than in the upper troposphere. The global mean abundance of OH cannot be directly measured, but a weighted average of the OH sink for certain synthetic trace gases (whose budgets are well established and whose total atmospheric sinks are essentially controlled by OH) can be derived. The ratio of the atmospheric lifetimes against tropospheric OH loss for a gas is scaled to that of CH_3CCl_3 by the inverse ratio of their OH-reaction rate coefficients at an appropriate scaling temperature. A new analysis of the modelled global OH distribution predicts relatively greater abundances at mid-levels in the troposphere (where it is colder) and results in a new scaling temperature for the rate coefficients of 272K (Spivakovsky *et al.*, 2000), instead of 277K (Prather and Spivakovsky, 1990; SAR). The atmospheric lifetimes reported in Table 4.1 use this approach, adopting an "OH lifetime" of 5.7 years for CH_3CCl_3 (Prinn *et al.*, 1995; WMO, 1999). Stratospheric losses for all gases are taken from published values (Ko *et al.*, 1999; WMO, 1999) or calculated as 8% of the tropospheric loss (with a minimum lifetime of 30 years). The only gases in Table 4.1 with surface losses are CH_4 (a soil-sink lifetime of 160 years) and CH_3CCl_3 (an ocean-sink lifetime of 85 years). The lifetime for nitrogen trifluoride (NF_3) is taken from Molina *et al.* (1995). These lifetimes agree with the recent compendium of Naik *et al.* (2000).

Analysis of the CH_3CCl_3 burden and trend (Prinn *et al.*, 1995; Krol *et al.*, 1998; Montzka *et al.*, 2000) has provided a cornerstone of our empirical derivations of the OH lifetimes of most gases. Quantification of the "OH-lifetime" of CH_3CCl_3 has evolved over the past decade. The SAR adopted a value of 5.9 ± 0.7 years in calculating the lifetimes of the greenhouse gases. This range covered the updated analysis of Prinn *et al.* (1995), 5.7 years, which was used in WMO (1999) and adopted for this report. Montzka *et al.* (2000) extend the atmospheric record of CH_3CCl_3 to include the rapid decay over the last five years following cessation of emissions and derive an OH lifetime of 6.3 years. The new information on the CH_3CCl_3 lifetime by Montzka *et al.* (2000) has not been incorporated into this report, but it falls within the ±15% uncertainty for these lifetimes. If the new value of 6.3 years were adopted, then the lifetime of CH_4 would increase to 9.2 yr, and all lifetimes, perturbation lifetimes, and GWPs for gases controlled by tropospheric OH would be about 10% greater.

4.2.6.2 Atmospheric measurements and modelling of photochemistry

Atmospheric measurements provide another cornerstone for the numerical modelling of photochemistry. Over the last five years direct atmospheric measurements of HO_x radicals, made simultaneously with the other key species that control HO_x, have been conducted over a wide range of conditions: the upper troposphere and lower stratosphere (e.g., SPADE, ASHOE/MAESA, STRAT; SUCCESS, SONEX, PEM-TROPICS A & B), the remote Pacific (MLOPEX), and the polluted boundary layer and its outflow (POPCORN, NARE, SOS). These intensive measurement campaigns provide the first thorough tests of tropospheric OH chemistry and production of O_3 for a range of global conditions. As an example here, we present an analysis of the 1997 SONEX (Subsonic assessment program Ozone and Nitrogen oxide EXperiment) aircraft campaign over the North Atlantic that tests one of the chemical models from the OxComp workshop (HGIS).

The 1997 SONEX aircraft campaign over the North Atlantic provided the first airborne measurements of HO_x abundances concurrent with the controlling chemical background: H_2O_2, CH_3OOH, CH_2O, O_3, NO_x, H_2O, acetone and hydrocarbons. These observations allowed a detailed evaluation of our understanding of HO_x chemistry and O_3 production in the upper troposphere. Figure 4.9 (panels 1-3) shows a comparison between SONEX measurements and model calculations (Jaeglé *et al.*, 1999) for OH and HO_2 abundances and the ratio HO_2/OH. At each point the model used the local, simultaneously observed chemical abundances. The cycling between OH and HO_2 takes place on a time-scale of a few seconds and is mainly controlled by reaction of OH with CO producing HO_2, followed by reaction of HO_2 with NO producing OH. This cycle also leads to the production of ozone. As seen in Figure 4.9, the HO_2/OH ratio is reproduced by model calculations to within the combined uncertainties of observations (±20%) and those from propagation of rate coefficient errors in the model (±100%), implying that the photochemical processes driving the cycling between OH and HO_2 appear to be understood (Wennberg *et al.*, 1998; Brune *et al.*, 1999). The absolute abundances of OH and HO_2 are matched by model calculations to within 40% (the reported accuracy of the HO_x observations) and the median model-to-observed ratio for HO_2 is 1.12. The model captures 80% of the observed variance in HO_x, which is driven by the local variations in NO_x and the HO_x sources (Faloona *et al.*, 2000, Jaeglé *et al.*, 2000;). The predominant sources of HO_x during SONEX were reaction of $O(^1D)$ with H_2O and photodissociation of acetone; the role of H_2O_2 and CH_3OOH as HO_x sources was small. This was not necessarily the case in some of the other airborne campaigns, where large differences between measured and modelled OH, up to a factor of 5, were observed in the upper troposphere. In these campaigns the larger measured OH concentrations were tentatively ascribed to enhanced levels of OH precursors, such as H_2O_2, CH_3OOH, or CH_2O, whose concentrations had not been measured.

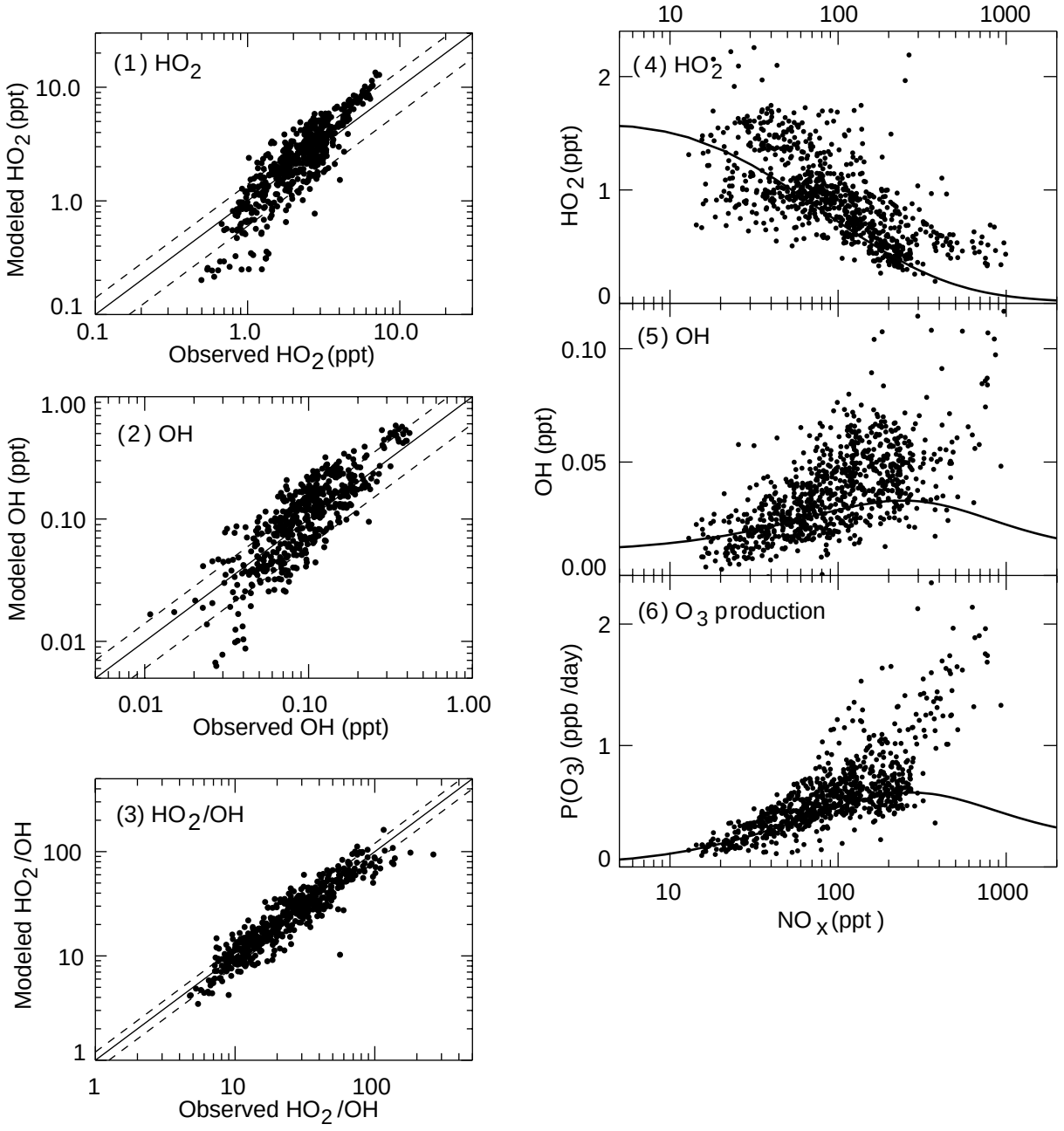

Figure 4.9: (left panel) Observed versus modelled (1) HO_2 abundance (ppt), (2) OH abundance (ppt), and (3) HO_2/OH ratio in the upper troposphere (8 to 12 km altitude) during SONEX. Observations are for cloud-free, daytime conditions. Model calculations are constrained with local observations of the photochemical background (H_2O_2, CH_3OOH, NO, O_3, H_2O, CO, CH_4, ethane, propane, acetone, temperature, pressure, aerosol surface area and actinic flux). The 1:1 line (solid) and instrumental accuracy range (dashed) are shown. Adapted from Brune *et al.* (1999). (right panel) Observed (4) HO_2 abundance (ppt), (5) OH abundance (ppt), and (6) derived O_3 production rate (ppb/day) as a function of the NO_x ($NO+NO_2$) abundance (ppt). Data taken from SONEX (8 to 12 km altitude, 40° to 60°N latitude) and adapted from Jaeglé *et al.* (1999). All values are 24-hour averages. The lines correspond to model-calculated values as a function of NO_x using the median photochemical background during SONEX rather than the instantaneous values (points).

Tropospheric O_3 production is tightly linked to the abundance of NO_x, and Figure 4.9 (panel 6) shows this production rate (calculated as the rate of the reaction of HO_2 with NO) for each set of observations as function of NO_x during the SONEX mission. Also shown in Figure 4.9 (panels 4-5) are the measured abundances of OH and HO_2 as a function of NO_x. The smooth curve on each panel 4-6 is a model simulation of the expected relationship if the chemical background except for NO_x remained unchanged at the observed median abundances. This curve shows the "expected" behaviour of tropospheric chemistry when only NO_x is increased: OH increases with NO_x abundances up to 300 ppt because HO_2 is shifted into OH; it decreases with increasing NO_x at higher NO_x abundances because the OH reaction with NO_2 forming HNO_3 becomes the dominant sink for HO_x radicals.

Production of O_3 is expected to follow a similar pattern with rates suppressed at NO_x abundances greater than 300 ppt under these atmospheric conditions (e.g., Ehhalt, 1998). These SONEX observations indicate, however, that both OH abundance and O_3 production may continue to increase with NO_x concentrations up to 1,000 ppt because the high NO_x abundances were often associated with convection and lightning events and occurred simultaneously with high HO_x sources. By segregating observations according to HO_x source strengths, Jaeglé *et al.* (1999) identified the approach to NO_x-saturated conditions predicted by the chemical models when HO_x sources remain constant. A NO_x-saturated environment was clearly found for the POPCORN (Photo-Oxidant formation by Plant emitted Compounds and OH Radicals in north-eastern Germany) boundary layer measurements in Germany (Rohrer *et al.*, 1998; Ehhalt and Rohrer, 2000). The impact of NO_x-saturated conditions on the production of O_3 is large in the boundary layer, where much of the NO_x is removed within a day, but may be less important in the upper troposphere, where the local lifetime of NO_x is several days and the elevated abundances of NO_x are likely to be transported and diluted to below saturation levels. This effective reduction of the NO_x-saturation effect due to 3-D atmospheric mixing is seen in the CTM modelling of aviation NO_x emissions where a linear increase in tropospheric O_3 is found, even with large NO_x emissions in the upper troposphere (Isaksen and Jackman, 1999).

4.3 Projections of Future Emissions

The IPCC SRES (Nakićenović *et al.*, 2000) developed 40 future scenarios that are characterised by distinctly different levels of population, economic, and technological development. Six of these scenarios were identified as illustrative scenarios and these were used for the analyses presented in this chapter. The SRES scenarios define only the changes in anthropogenic emissions and not the concurrent changes in natural emissions due either to direct human activities such as land-use change or to the indirect impacts of climate change. The annual anthropogenic emissions for all greenhouse gases, NO_x, CO, VOC and SO_2 (sulphur dioxide) are given in the SRES for the preliminary marker scenarios (Nakićenović *et al.*, 2000, Appendix VI) and the final marker/illustrative scenarios (Nakićenović *et al.*, 2000, Appendix VII). Much of these data is also tabulated in Appendix II to this report. There are insufficient data in the published SRES (Nakićenović *et al.*, 2000) to break down the individual contributions to HFCs, PFCs, and SF_6, but these emissions were supplied by Lead Authors of the SRES (available at sres.ciesin.org) and are also reproduced in this Appendix. The geographic distribution of emissions of the short-lived compounds – NO_x, CO, VOC, and SO_2 – is an important factor in their greenhouse forcing, and the preliminary gridded emissions were likewise supplied by the SRES Lead Authors (Tom Kram and Steven Smith, December 1998) and used in the OxComp model studies. A synopsis of the regional shift in CO and NO_x emissions projected by 2100 is given in Tables 4.6 and 4.8.

This chapter evaluates the SRES emissions from year 2000 to year 2100 in terms of their impact on the abundances of non-CO_2 greenhouse gases. A new feature of this report, i.e., use of NO_x, CO and VOC emissions to project changes in tropospheric O_3 and OH, represents a significant advance over the level-of-science in the SAR. The original four preliminary marker scenarios (December 1998) are included here because they have been used in preliminary model studies for the TAR and are designated A1p, A2p, B1p, B2p. In January 1999, these emissions were converted into greenhouse gas abundances using the level-of-science and methodology in the SAR, and the radiative forcings from these greenhouse gas abundances were used in this report for some climate model simulations.

The recently approved six marker/illustrative scenarios (March 2000) are also evaluated and are designated A1B-AIM, A1T-MESSAGE, A1FI-MiniCAM, A2-ASF, B1-IMAGE, B2-MESSAGE (hereafter abbreviated as A1B, A1T, A1FI, A2, B1, B2). For comparison with the previous assessment, we also evaluate the IPCC emissions scenario IS92a used in the SAR; for the full range of IS92 scenarios, see the SAR. An agreed-upon property of all SRES scenarios is that there is no intervention to reduce greenhouse gases; but, in contrast, regional controls on SO_2 emissions across the illustrative SRES scenarios lead to emissions in the last two decades of the century that are well below those of 1990 levels. There appear to be few controls on NO_x, CO and VOC emissions across all scenarios; however, the large increases in surface O_3 abundances implied by these results may be inconsistent with the SRES storylines that underpin the emissions scenarios. As understanding of the relationship between emissions and tropospheric O_3 abundances improves, particularly on regional scales, more consistent emissions scenarios can be developed. The SRES scenarios project substantial emissions of HFC-134a as in IS92a, but only half as much HFC-125, and no emissions of HFC-152a. The SRES emissions scenarios do include a much larger suite of HFCs plus SF_6 and PFCs, which are not included in IS92a. The emissions of greenhouse gases under the Montreal Protocol and its Amendments (CFCs, HCFCs, halons) have been evaluated in WMO (Madronich and Velders, 1999). This report adopts the single WMO baseline Montreal Protocol Scenario A1 (no relation to SRES A1) for emissions and concentrations of these gases, while the SRES adopted a similar WMO Scenario A3 (maximum production); however, the differences between scenarios in terms of climate forcing is inconsequential. The resulting abundances of greenhouse gases are given in Appendix II and discussed in Section 4.4.5.

4.3.1 The Adjusted/Augmented IPCC/SRES Emission Scenarios

Among the four SRES preliminary marker scenarios, A2p has overall the highest emissions. For model simulations of future atmospheric chemistry in the OxComp workshop, we needed to focus on a single test case and chose scenario A2p in the year 2100 since it represents the largest increase in emissions of CH_4, CO, NO_x, and VOC. Once the response of O_3 and OH to these extreme emissions is understood, other scenarios and intermediate years can be interpolated with some confidence.

Y2000

For the OxComp workshop, we adopt Y2000 emissions that

include both natural and anthropogenic sources. The OxComp Y2000 anthropogenic emissions are roughly consistent with, but different in detail from, the anthropogenic emissions provided by SRES. These adjustments were necessary to be consistent with current budgets, to include natural sources as discussed previously, and to provide more detailed information on source categories, including temporal and spatial distribution of emissions that are not specified by SRES. Emissions of NO_x, CO and VOC for the year 2000 are based on GEIA(Global Emissions Inventory Activity)/EDGAR emissions for 1990 (Graedel *et al.*, 1993; Olivier *et al.*, 1999) projected to year 2000. Tropospheric abundances of long-lived gases such as CH_4 were fixed from recent observations. The difference between SRES and OxComp Y2000 emissions are nominally within the range of uncertainty for these quantities. The OxComp Y2000 simulations provide a "current" atmosphere to compare with observations.

Y2100(A2p)
Since the OxComp Y2000 emissions differ somewhat from the A2p emissions for the year 2000, we define Y2100(A2p) emissions by the sum of our adjusted Y2000 emissions plus the difference between the SRES-A2p emissions for the years 2100 and 2000. Thus our absolute increase in emissions matches that of SRES-A2p. In these Y2100(A2p) simulations, natural emissions were not changed.

4.3.2 Shifting Regional Emissions of NO_x CO, and VOC in 2100

A shift of the growth of anthropogenic emissions of NO_x, CO and VOC, such as that from North America and Europe to Southern and Eastern Asia over the past decades, is changing the geographic pattern of emissions, which in turn will change the distribution of the O_3 increases in the troposphere predicted for the year 2100. In contrast, for long-lived greenhouse gases, shifting the location of emissions has little impact. We use the SRES emission maps, to take into account such changes in emissions patterns. For Y2000 and Y2100(A2p) the emissions of CO and NO_x, broken down by continents, are given in Tables 4.6 and 4.8, respectively. In terms of assessing future changes in tropospheric OH and O_3, it is essential to have a coherent model for emissions scenarios that consistently projects the spatial patterns of the emissions along with the accompanying changes in urbanisation and land use.

4.3.3 Projections of Natural Emissions in 2100

SRES scenarios do not consider the changes in natural emissions and sinks of reactive gases that are induced by alterations in land use and agriculture or land-cover characteristics. (Land-use change statistics, however, are reported, and these could, in principle, be used to estimate such changes.) In some sense these altered emissions must be considered as anthropogenic changes. Examples of such changes may be increased NO_x, N_2O and NH_3 emissions from natural waters and ecosystems near agricultural areas with intensified use of N-fertiliser. A change of land cover, such as deforestation, may lead to reduced isoprene emissions but to increases in soil emissions of NO_x. At present we can only point out the lack of projecting these parallel changes in once natural emissions as an uncertainty in this assessment.

4.4 Projections of Atmospheric Composition for the 21st Century

4.4.1 Introduction

Calculating the abundances of chemically reactive greenhouse gases in response to projected emissions requires models that can predict how the lifetimes of these gases are changed by an evolving atmospheric chemistry. This assessment focuses on predicting changes in the oxidative state of the troposphere, specifically O_3 (a greenhouse gas) and OH (the sink for many greenhouse gases). Many research groups have studied and predicted changes in global tropospheric chemistry, and we seek to establish a consensus in these predictions, using a standardised set of scenarios in a workshop organised for this report. The projection of stratospheric O_3 recovery in the 21st century – also a factor in radiative forcing and the oxidative state of the atmosphere – is reviewed extensively in WMO (Hofmann and Pyle, 1999), and no new evaluation is made here. The only stratospheric change included implicitly is the N_2O feedback on its lifetime. Overall, these projections of atmospheric composition for the 21st century include the most extensive set of trace gas emissions for IPCC assessments to date: greenhouse gases (N_2O, CH_4, HFCs, PFCs, SF_6) plus pollutants (NO_x, CO, VOC).

4.4.2 The OxComp Workshop

In the SAR, the chapter on atmospheric chemistry included two modelling studies: PhotoComp (comparison of ozone photochemistry in box models) and Delta-CH_4 (methane feedbacks in 2-D and 3-D tropospheric chemistry models). These model studies established standard model tests for participation in IPCC. They resulted in a consensus regarding the CH_4 feedback and identified the importance (and lack of uniform treatment) of NMHC chemistry on tropospheric O_3 production. This synthesis allowed for the SAR to use the CH_4-lifetime feedback and a simple estimate of tropospheric O_3 increase due solely to CH_4. The SAR noted that individual CTMs had calculated an impact of changing NO_x and CO emissions on global OH and CH_4 abundances, but that a consensus on predicting future changes in O_3 and OH did not exist.

Since 1995, considerable research has gone into the development and validation of tropospheric CTMs. The IPCC Special Report on Aviation and the Global Atmosphere (Derwent and Friedl, 1999) used a wide range of global CTMs to predict the enhancement of tropospheric O_3 due to aircraft NO_x emissions. The results were surprisingly robust, not only for the hemispheric mean O_3 increase, but also for the increase in global mean OH reported as a decrease in the CH_4 lifetime. The current state-of-modelling in global tropospheric chemistry has advanced since PhotoComp and Delta-CH_4 in the SAR and now includes as standard a three-dimensional synoptic meteorology and treatment of non-methane hydrocarbon chemistry. A survey of

Table 4.10: *Chemistry-Transport Models (CTM) contributing to the OxComp evaluation of predicting tropospheric O_3 and OH.*

CTM	Institute	Contributing authors	References
GISS	GISS	Shindell /Grenfell	Hansen *et al.* (1997b)
HGEO	Harvard U.	Bey / Jacob	Bey *et al.* (1999)
HGIS	Harvard U.	Mickley / Jacob	Mickley *et al.* (1999)
IASB	IAS/Belg.	Mülller	Müller and Brasseur (1995, 1999)
KNMI	KNMI/Utrecht	van Weele	Jeuken *et al.* (1999), Houweling *et al.* (2000)
MOZ1	NCAR/CNRS	Hauglustaine / Brasseur	Brasseur *et al.* (1998b), Hauglustaine *et al.* (1998)
MOZ2	NCAR	Horowitz/ Brasseur	Brasseur *et al.* (1998b), Hauglustaine *et al.* (1998)
MPIC	MPI/Chem	Kuhlmann / Lawrence	Crutzen *et al.* (1999), Lawrence *et al.* (1999)
UCI	UC Irvine	Wild	Hannegan *et al.* (1998), Wild and Prather (2000)
UIO	U. Oslo	Berntsen	Berntsen and Isaksen (1997), Fuglestvedt *et al.* (1999)
UIO2	U. Oslo	Sundet	Sundet (1997)
UKMO	UK Met Office	Stevenson	Collins *et al.* (1997), Johnson *et al.* (1999)
ULAQ	U. L. Aquila	Pitari	Pitari *et al.* (1997)
UCAM	U. Cambridge	Plantevin /Johnson	Law *et al.* (1998, 2000)(TOMCAT)

recent CTM-based publications on the tropospheric O_3 budget, collected for this report, is discussed in Section 4.5.

This assessment, building on these developments, organised a workshop to compare CTM results for a few, well-constrained atmospheric simulations. An open invitation, sent out in March 1999 to research groups involved in 3-D global tropospheric chemistry modelling, invited participation in this report's assessment of change in tropospheric oxidative state through a model intercomparison and workshop (OxComp). This workshop is an IPCC-focused follow-on to the Global Integration and Modelling (GIM) study (Kanakidou *et al.*, 1999). The infrastructure for OxComp (ftp site, database, graphics, and scientific support) was provided by the University of Oslo group, and the workshop meeting in July 1999 was hosted by the Max Planck Institute for Meteorology (MPI) Hamburg. Participating models are described by publications in peer-reviewed literature as summarised in Table 4.10; all include 3-D global tropospheric chemistry including NMHC; and assessment results are based on models returning a sufficient number of OxComp cases. The two goals of OxComp are (i) to build a consensus on current modelling capability to predict changes in tropospheric OH and O_3 and (ii) to develop a useful parametrization to calculate the greenhouse gases (including tropospheric O_3 but not CO_2) using the IPCC emissions scenarios.

4.4.3 Testing CTM Simulation of the Current (Y2000) Atmosphere

The OxComp workshop defined a series of atmospheres and emission scenarios. These included Y2000, a new reference atmosphere meant to represent year 2000 that provides a baseline from which all changes in greenhouse gases were calculated. For Y2000, abundances of long-lived gases were prescribed by 1998 measurements (Table 4.1a), and emissions of short-lived pollutants, NO_x, CO and VOC, were based primarily on projections to the year 2000 of GEIA/EDGAR emissions for 1990 (Olivier *et al.*, 1998, 1999), see Section 4.3.1. Stratospheric O_3 was calculated in some models and prescribed by current observation in others. The predicted atmospheric quantities in all these simulations are therefore short-lived tropospheric gases: O_3, CO, NO_x, VOC, OH and other radicals. Following the GIM model study (Kanakidou *et al.*, 1999), we use atmospheric measurement of O_3 and CO to test the model simulations of the current atmosphere. The Y2000 atmosphere was chosen because of the need for an IPCC baseline, and it does not try to match conditions over the l980s and 1990s from which the measurements come. Although the observed trends in tropospheric O_3 and CO are not particularly large over this period and thus justify the present approach, a more thorough comparison of model results and measurements would need to use the regional distribution of the pollutant emissions for the observation period.

The seasonal cycle of O_3 in the free troposphere (700, 500, and 300 hPa) has been observed over the past decade from more than thirty ozone sonde stations (Logan, 1999). These measurements are compared with the OxComp Y2000 simulations for Resolute (75°N), Hohenpeissenberg (48°N), Boulder (40°N), Tateno (36°N), and Hilo (20°N) in Figure 4.10. Surface measurements from Cape Grim (40°S), representative of the marine boundary layer in southern mid-latitudes, are also compared with the models in Figure 4.10. With the exception of a few outliers, the model simulations are within ±30% of observed tropospheric O_3 abundance, and they generally show a maximum in spring to early summer as observed, although they often miss the month of maximum O_3. At 300 hPa the large springtime variation at many stations is due to the influence of stratospheric air that is approximately simulated at Resolute, but, usually overestimated at the other stations. The CTM simulations in the tropics (Hilo) at 700 to 500 hPa show much greater spread and hence generally worse agreement with observations. The mean concentration of surface O_3 observed at Cape Grim is well matched by most models, but the seasonality is underestimated.

Observed CO abundances are compared with the Y2000 model simulations in Figure 4.11 for surface sites at various altitudes and latitudes: Cape Grim (CGA, 94 m), Tae Ahn (KOR,

Table 4.11: *Changes in tropospheric O_3 (DU) and OH (%) relative to year 2000 for various perturbations to the atmosphere. Individual values calculated with chemistry transport-models (CTMs) plus the average values adopted for this report (TAR).*

	Y2000	A2x: Y2100 – Y2000		
	+10% CH_4	All A2x	$-NO_x$	$-NO_x-VOC-CH_4$
CTM	Case A	Case B	Case C	Case D
Effective[a] tropospheric O_3 change (DU):				
HGIS		26.5		
GISS		25.2		
IASB	0.66	18.9	9.2	0.4
KNMI	0.63	18.0	9.0	
MOZ1		16.6		
MOZ2		22.4		
MPIC	0.40			
UCI	0.69	23.3	10.2	2.8
UIO	0.51	26.0	6.0	2.1
UKMO		18.9	4.6	3.1
ULAQ	0.85	22.2	14.5	5.9
TAR[b]	**0.64**	**22.0**	**8.9**	**2.0**
Tropospheric OH change (%)				
IASB	–2.9%	–7%		
KNMI	–3.3%	–25%	–41%	
MOZ1		–21%		
MOZ2		–18%		
MPIC	–2.7%			
UCI	–3.2%	–15%	–39%	–16.0%
UIO	–3.1%	–6%	–37%	–12.3%
UKMO	–2.9%	–12%	–37%	–10.8%
ULAQ	–2.7%	–17%	–43%	–22.0%
TAR[b]	**–3.0%**	**–16%**	**–40%**	**–14%**

Model results from OxComp workshop; all changes (DU for O_3 and % for OH) are relative to the year Y2000. Tropospheric mean OH is weighted by CH_4 loss rate. Mean O_3 changes (all positive) are derived from the standard reporting grid on which the CTMs interpolated their results. See Table 4.10 for the model key. The different cases include (A) a 10% increase in CH_4 to 1,920 ppb and (B) a full 2100 simulation following SRES draft marker scenario A2 (based on February 1999 calculations for preliminary work of this report). Case C drops the NO_x emissions back to Y2000 values; and case D drops NO_x, VOC, and CH_4 likewise.

Adopted CH_4 abundances and pollutant emissions from Y2000 to Y2100 are:

Y2000: CH_4=1,745 ppb, e–NO_x=32.5 TgN/yr, e–CO=1,050 Tg/yr, e–VOC=150 Tg/yr.

Y2100: CH_4=4,300 ppb, e–NO_x=110.0 TgN/yr, e–CO=2,500 Tg/yr, e–VOC=350 Tg/yr.

[a] N.B. Unfortunately, after the government review it was discovered that the method of integrating O_3 changes on the reporting grid was not well defined and resulted in some unintentional errors in the values reported above. Thus, the values here include in effect the O_3 increases predicted/expected in the lower stratosphere in addition to the troposphere. In terms of climate change, use of these values may not be unreasonable since O_3 changes in the lower stratosphere do contribute to radiative forcing. Nevertheless, the troposphere-only changes are about 25 to 33% less than the values above.

$$\delta(\text{tropospheric } O_3) = +5.0\times\delta\ln(CH_4) + 0.125\times\delta(e-NO_x) + 0.0011\times\delta(e-CO) + 0.0033\times\delta(e-VOC) \text{ in DU.}$$

[b] TAR adopts the weighted average for cases A to D as shown, where the weighting includes factors about model formulation and comparison with observations. A linear interpolation is derived from these results and used in the scenarios:

$$\delta\ln(\text{tropospheric OH}) = -0.32\times\delta\ln(CH_4) + 0.0042\times\delta(e-NO_x) - 1.05e-4\times\delta(e-CO) - 3.15e-4\times\delta(e-VOC),$$

$$\delta(\text{effective } O_3) = +6.7\times\delta\ln(CH_4) + 0.17\times\delta(e-NO_x) + 0.0014\times\delta(e-CO) + 0.0042\times\delta(e-VOC) \text{ in DU.}$$

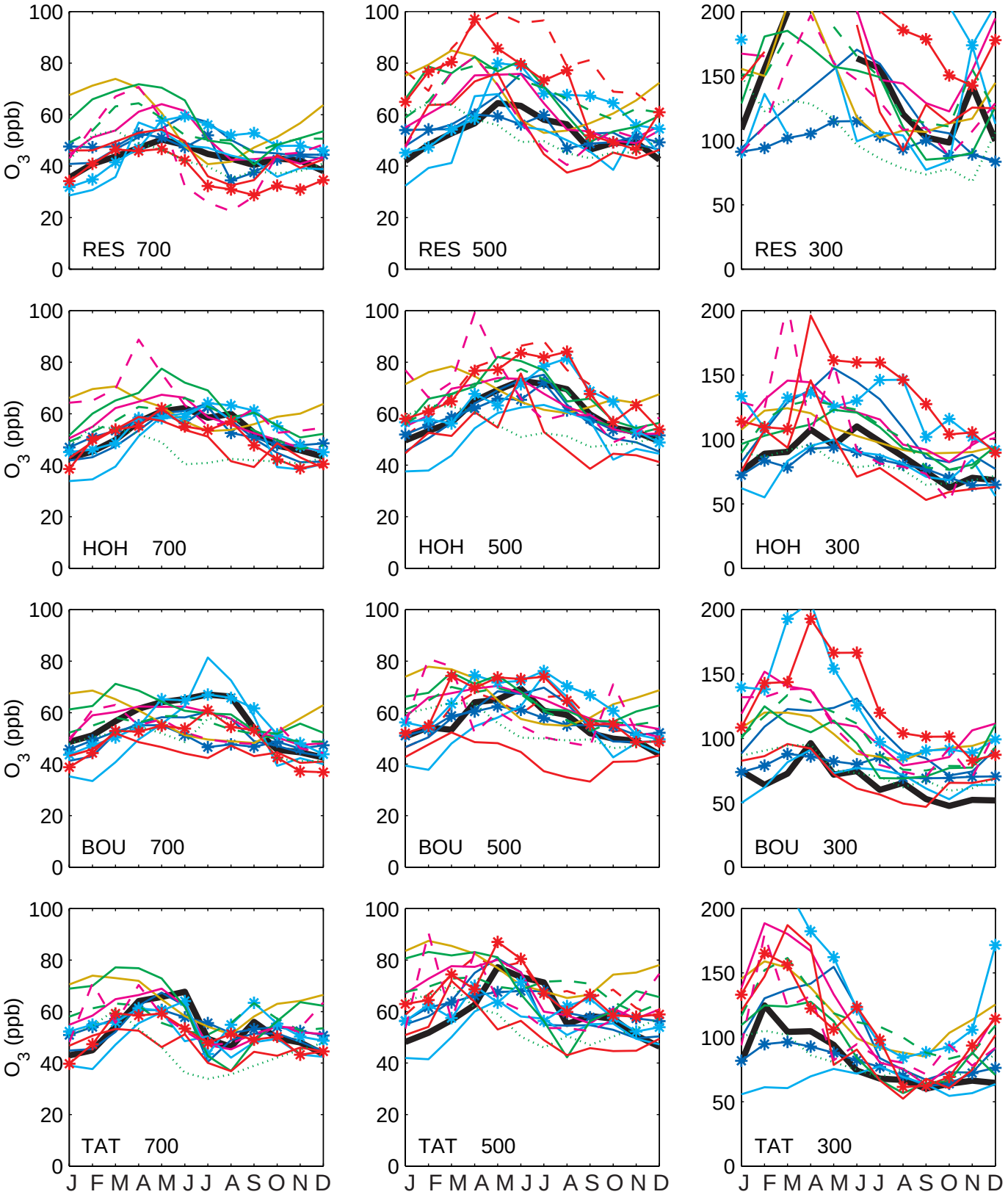

Figure 4.10: Observed monthly mean O_3 abundance (ppb) from sondes at 700 hPa (left column), 500 hPa (centre) and 300 hPa (right) from a sample of stations (thick black line) compared with Y2000 model simulations from OxComp (thin coloured lines, see model key in legend and Table 4.10). The sonde stations include RESolute (75°N, 95°W), HOHenpeissenberg (48ºN, 11°E), BOUlder (40°N, 105°W), TATeno (36°N, 140°E), and HILo (20°N, 155°W). Surface monthly O_3 observations (thick black line) at Cape Grim Observatory (CGA, 40°S, 144°E, 94 m above mean sea level) are also compared with the models. (Continues opposite.)

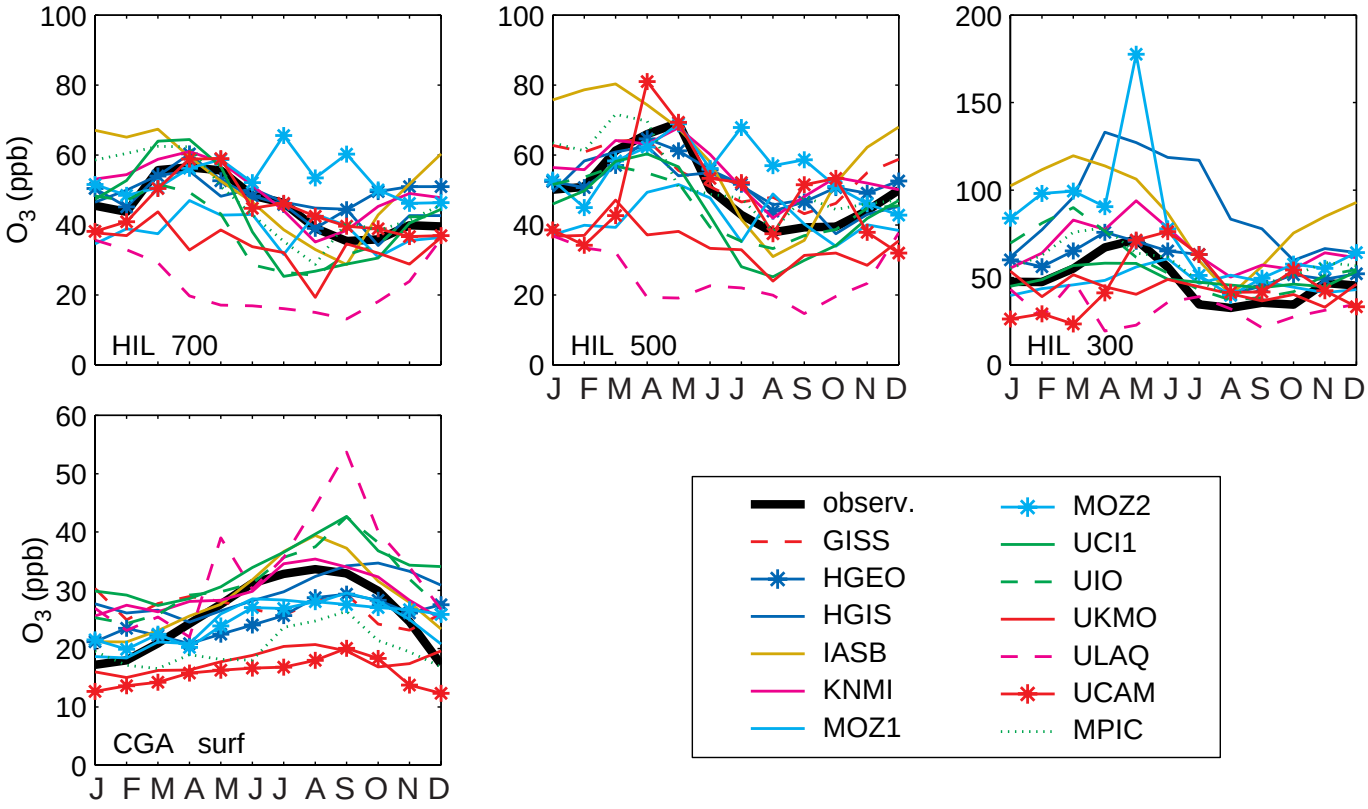

20 m), Mauna Loa (MLH, 3397 m), Alert (ALT, 210 m), and Niwot Ridge (NWR, 3475 m). The Alert abundances are well matched by most but not all models. Niwot Ridge and Mauna Loa are reasonably well modelled except for the February to March maximum. At Tae Ahn, the models miss the deep minimum in late summer, but do predict the much larger abundances downwind of Asian sources. At Cape Grim the seasonal cycle is matched, but the CO abundance is uniformly overestimated (30 to 50%) by all the models, probably indicating an error in Southern Hemisphere emissions of CO.

Overall, this comparison with CO and O_3 observations shows good simulations by the OxComp models of the global scale chemical features of the current troposphere as evidenced by CO and O_3; however, the critical NO_x chemistry emphasises variability on much smaller scales, such as biomass burning plumes and lightning storms, that are not well represented by the global models. With this large variability and small scales, the database of NO_x measurements needed to provide a test for the global models, equivalent to CO and O_3, would need to be much larger.

The current NO_x database (e.g., Emmons *et al.*, 1997; Thakur *et al.*, 1999) does not provide critical tests of CTM treatment of these sub-grid scales.

4.4.4 Model Simulations of Perturbed and Y2100 Atmospheres

The OxComp workshop also defined a series of perturbations to the Y2000 atmosphere for which the models reported the monthly averaged 3-D distribution of O_3 abundances and the budget for CH_4, specifically the loss due to reaction with tropospheric OH. From these diagnostics, the research group at Oslo calculated the change in global mean tropospheric O_3 (DU) and in OH (%) relative to Y2000, as shown in Table 4.11. For each model at every month, the "troposphere" was defined as where O_3 abundances were less than 150 ppb in the Y2000 simulation, a reasonably conservative diagnostic of the tropopause (see Logan, 1999). Because O_3 is more effective as a greenhouse gas when it lies above the surface boundary layer (SAR; Hansen *et al.*, 1997a; Prather and Sausen, 1999; Chapter 6 of this report), the model study diagnosed the O_3 change occurring in the 0 to 2 km layers of the model. This amount is typically 20 to 25% of the total change and is consistent across models and types of perturbations here.

Case A, a +10% increase in CH_4 abundance for Y2000, had consistent results across reporting models that differed little from the SAR's Delta-CH_4 model study. The adopted values for this report are –3% change in OH and +0.64 DU increase in O_3, as listed under the "TAR" row in Table 4.11.

The Y2100 atmosphere in OxComp mimics the increases in pollutant emissions in SRES A2p scenario from year 2000 to year 2100 with the year 2100 abundance of CH_4, 4,300 ppb, calculated with the SAR technology and named here A2x. (See discussion in section 4.4.5; for the SAR, only the CH_4-OH feedback is included.) The long-lived gases CO_2 and N_2O have no impact on these tropospheric chemistry calculations as specified.

Cases B-C-D are a sequence of three Y2100 atmospheres based on A2x: Case B is the full Y2100-A2x scenario; Case C is the same Y2100-A2x scenario but with unchanged (Y2000) NO_x

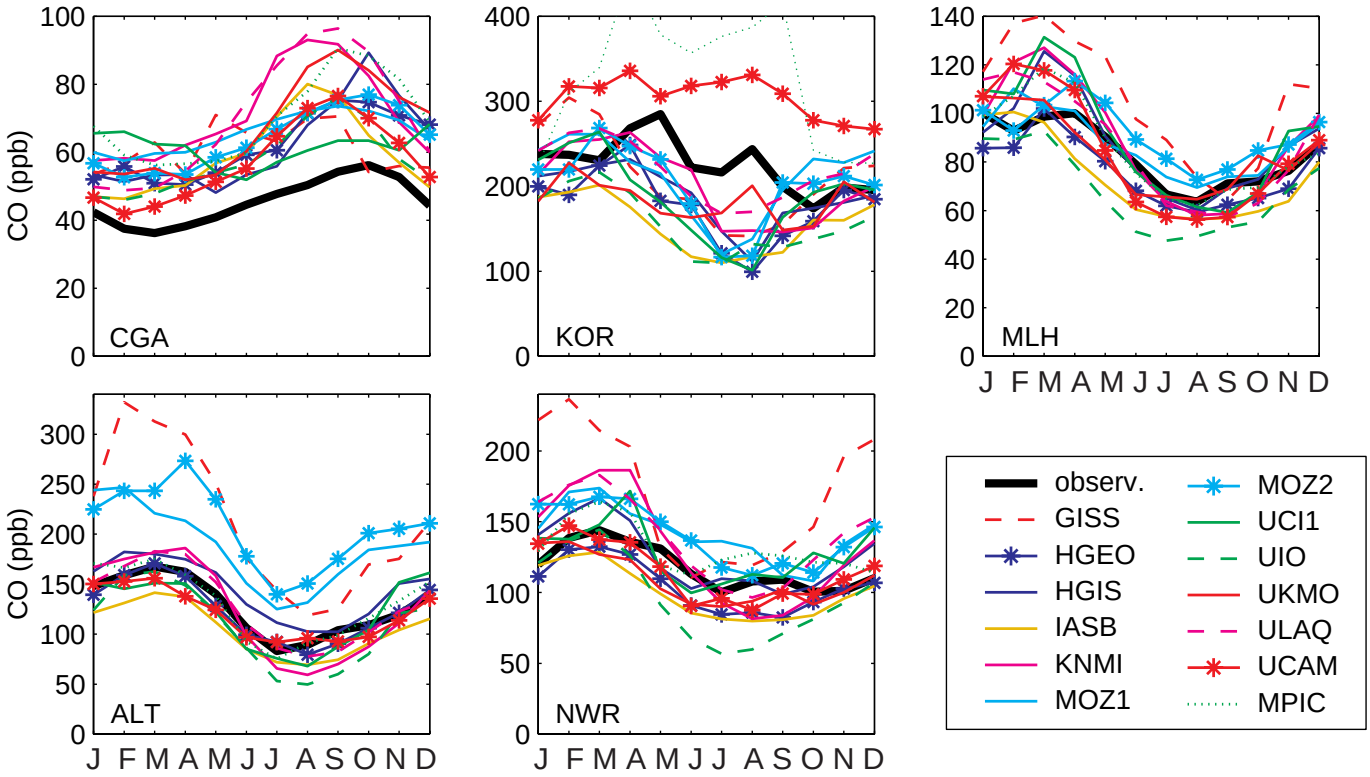

Figure 4.11: Observed seasonal surface CO abundance (ppb, thick black lines) at Cape Grim (CGA: 40°S, 144°E, 94 m above mean sea level), Tae Ahn (KOR: 36°N, 126°E, 20 m), Mauna Loa (MLH: 19°N, 155°W, 3397 m), Alert (ALT: 82°N, 62°W, 210 m), and Niwot Ridge (NWR: 40°N, 105°W, 3475 m) are compared with the OxComp model simulations from Y2000, see Figure 4.10.

emissions; and Case D is the same but with NO_x, VOC and CH_4 unchanged since Y2000 (i.e., only CO emissions change). Case B (Y2100-A2x) results are available from most OxComp participants. All models predict a decrease in OH, but with a wide range from –6 to –25%, and here we adopt a decrease of –16%. Given the different distributions of the O_3 increase from the OxComp models (Figures 4.12-13), the increases in globally integrated O_3 were remarkably consistent, ranging from +16.6 to +26.5 DU, and we adopt +22 DU. Without the increase in NO_x emissions (Case C) the O_3 increase drops substantially, ranging from +4.6 to +14.5 DU; and the OH decrease is large, –37 to –43%. With only CO emissions (Case D) the O_3 increase is smallest in all models, +0.4 to +5.9 DU.

This report adopts a weighted, rounded average of the changes in OH and O_3 for cases A-D as shown in the bold rows in Table 4.11. The weighting includes factors about model formulation and comparison with observations. This sequence of calculations (Y2000 plus Cases A-B-C-D) allows us to define a simple linear relationship for the absolute change in tropospheric O_3 and the relative change in OH as a function of the CH_4 abundance and the emission rates for NO_x, for CO, and for VOC. These two relationships are given in Table 4.11. Since the change in CH_4 abundance and other pollutant emissions for Y2100-A2x are among the largest in the SRES scenarios, we believe that interpolation of the O_3 and OH changes for different emission scenarios and years introduces little additional uncertainty.

The possibility that future emissions of CH_4 and CO overwhelm the oxidative capacity of the troposphere is tested (Case E, see Table 4.3 footnote &) with a +10% increase in CH_4 on top of Y2100-A2x (Case B). Even at 4,300 ppb CH_4, the decrease in OH calculated by two CTMs is only slightly larger than in Case A, and thus, at least for SRES A2p, the CH_4-feedback factor does not become as large as in the runaway case (Prather, 1996). This report assumes that the CH_4 feedback remains constant over the next century; however, equivalent studies for the low-NO_x future scenarios are not assessed.

The apparent agreement on predicting the single global, annual mean tropospheric O_3 increase, e.g., Case B in Table 4.11, belies the large differences as to where this increase occurs and what is its peak magnitude. The spatial distributions of the tropospheric O_3 increases in July for Case B are shown in Figure 4.12 (latitude by altitude zonal average abundance, ppb) and Figure 4.13 (latitude by longitude column density, DU) for nine CTMs. The largest increase in abundance occurs near the tropopause at 40°N latitude; yet some models concentrate this increase in the tropics and others push it to high latitudes. In terms of column density, models generally predict large increases along the southern edge of Asia from Arabia to eastern China; although the increases in tropical, biomass-burning regions varies widely from model to model.

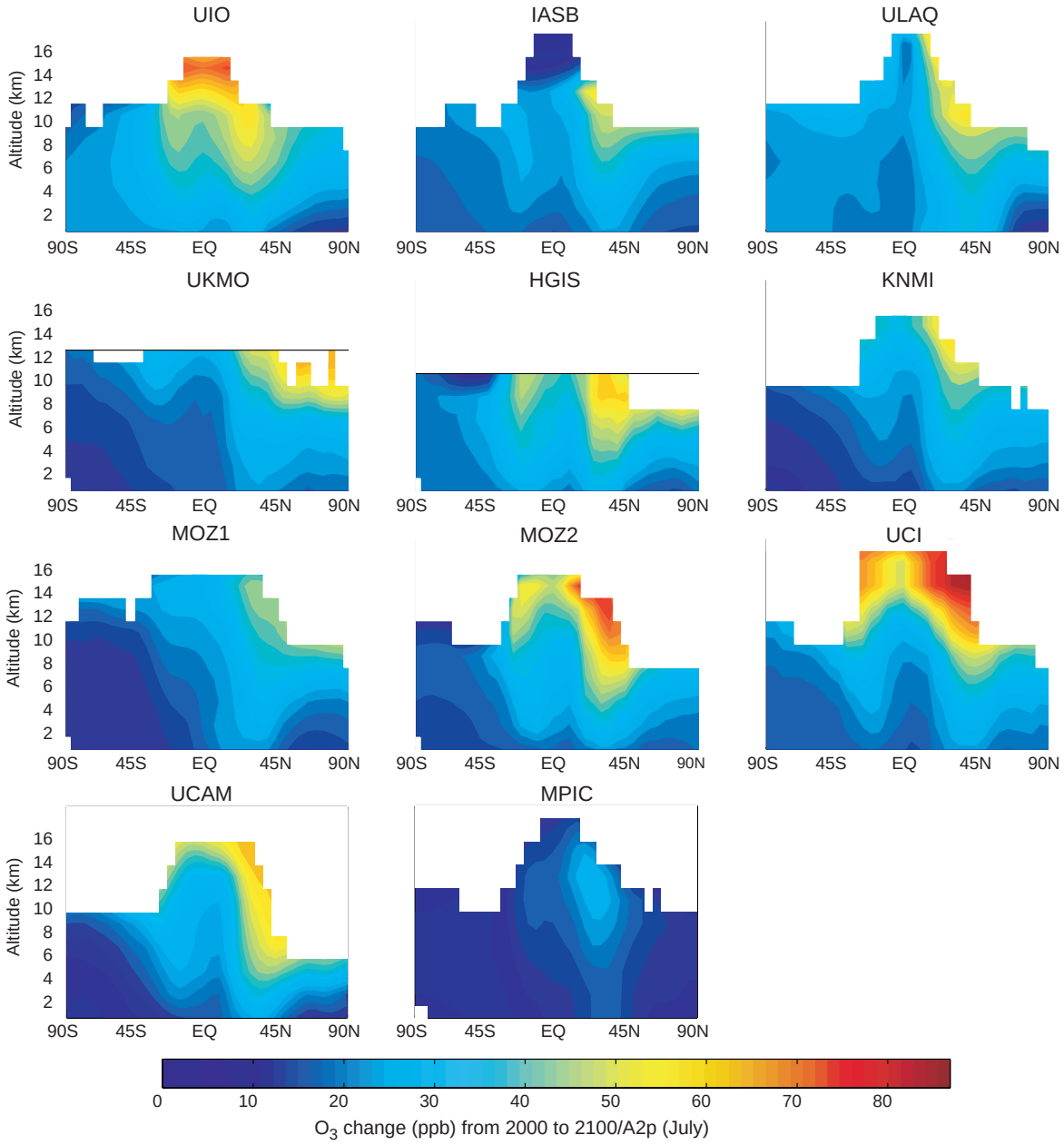

Figure 4.12: July zonal mean increase in tropospheric O_3 (ppb) as a function of latitude and altitude from Y2000 to Y2100 adopting SRES A2p projections for CH_4, CO, VOC, and NO_x. Results are shown for a sample of the chemistry-transport models (CTM) participating in IPCC OxComp workshop. Increases range from 0 to more than 80 ppb. Changes in the stratosphere (defined as O_3 > 150 ppb in that model's Y2000 simulation) are masked off, as are also regions in the upper troposphere for some CTMs (UKMO, HGIS) where O_3 is not explicitly calculated. See Table 4.10 for participating models.

This similarity in the total, but difference in the location, of the predicted O_3 increases is noted in Isaksen and Jackman (1999) and is probably due to the different transport formulations of the models as documented in previous CTM intercomparisons (Jacob *et al.*, 1997). Possibly, the agreement on the average O_3 increase may reflect a more uniform production of O_3 molecules as a function of NO_x emissions and CH_4 abundance across all models. Nevertheless, the large model range in the predicted patterns of O_3 perturbations leads to a larger uncertainty in climate impact than is indicated by Table 4.11.

The projected increases in tropospheric O_3 under SRES A2 and A1FI will have serious consequences on the air quality of most of the Northern Hemisphere by year 2100. Taking only the global numbers from Figure 4.14, the mean abundance of tropospheric O_3 will increase from about 52 ppb (typical mid-tropospheric abundances) to about 84 ppb in year 2100. Similar increases of about +30 ppb are seen near the surface at 40°N on a zonal average in Figure 4.12. Such increases will raise the "background" levels of O_3 in the northern mid-latitudes to close to the current clean-air standard.

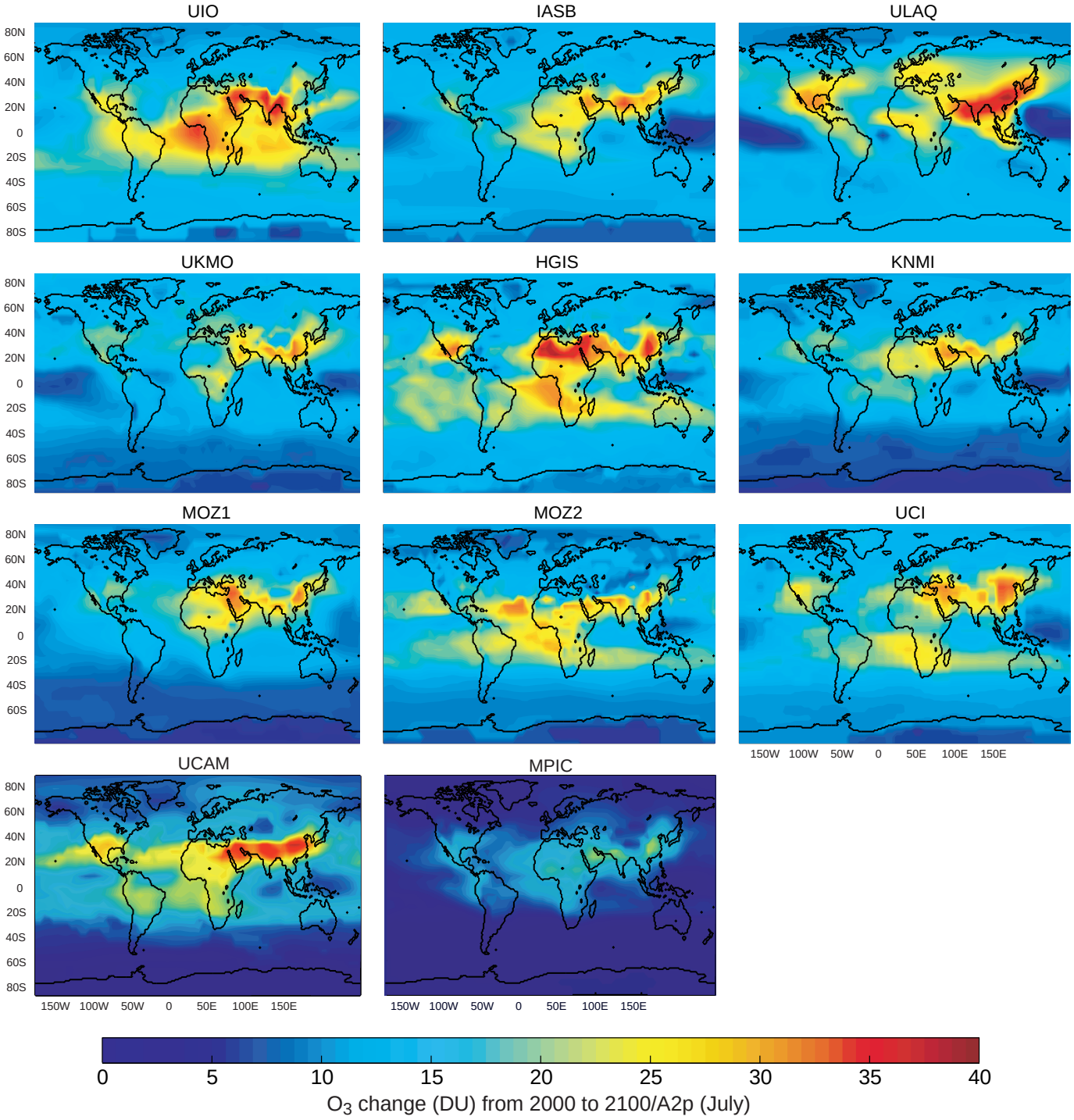

Figure 4.13: July column increase in tropospheric O_3 (DU) as a function of latitude and longitude from Y2000 to Y2100 adopting SRES A2p projections for CH_4, CO, VOC, and NO_x is shown for some OxComp simulations. See Figure 4.12.

4.4.5 Atmospheric Composition for the IPCC Scenarios to 2100

Mean tropospheric abundances of greenhouse gases and other chemical changes in the atmosphere are calculated by this chapter for years 2000 to 2100 from the SRES scenarios for anthropogenic emissions of CH_4, N_2O, HFCs, PFCs, SF_6, NO_x, CO, and VOC (corresponding emissions of CO_2 and aerosol precursors are not used). The emissions from the six SRES marker/illustrative scenarios (A1B, A1T, A1FI, A2, B1, B2) are tabulated in Appendix II, as are the resulting greenhouse gas abundances, including CO_2 and aerosol burdens. Chlorine- and bromine-containing greenhouse gases are not calculated here, and we adopt the single baseline scenario from the WMO assessment (Montreal Protocol Scenario A1 of Madronich and Velders, 1999), which is reproduced in Appendix II. Also given in Appendix II are the parallel data for the SRES preliminary

marker scenarios (A1p, A2p, B1p, B2p) and, in many cases, the SAR scenario IS92a as a comparison with the previous assessment.

Greenhouse gas abundances are calculated using a methodology similar to the SAR: (1) The troposphere is treated as a single box with a fill-factor for each gas that relates the burden to the tropospheric mean abundance (e.g., Tg/ppb). (2) The atmospheric lifetime for each gas is recalculated each year based on conditions at the beginning of the year and the formulae in Table 4.11. (Changes in tropospheric OH are used to scale the lifetimes of CH_4 and HFCs, and the abundance of N_2O is used to calculate its new lifetime.) (3) The abundance of a gas is integrated exactly over the year assuming that emissions remain constant for 12 months. (4) Abundances are annual means, reported at the beginning of each year (e.g., year 2100 = 1 January 2100).

In the SAR, the only OH feedback considered was that of CH_4 on its own lifetime. For this report, we calculate the change in tropospheric OH due to CH_4 abundance as well as the immediate emissions of NO_x, CO and VOC. Likewise, the increase in tropospheric O_3 projected in the SAR considered only increases in CH_4; whereas now it includes the emissions of NO_x, CO and VOC. Thus the difference between IS92a in the SAR and in this report is similar to that noted by Kheshgi *et al.* (1999). Also, the feedback of N_2O on its lifetime is included here for the first time and shows up as reduction of 14 ppb by year 2100 in this report's IS92a scenario as compared to the SAR.

The 21st century abundances of CH_4, N_2O, tropospheric O_3, HFC-134a, CF_4, and SF_6 for the SRES scenarios are shown in Figure 4.14. Historical data are plotted before year 2000; and the SRES projections, thereafter to year 2100. CH_4 continues to rise in B2, A1FI, and A2 (like IS92a), with abundances reaching 2,970 to 3,730 ppb, in order. For A1B and A1T, CH_4 peaks in mid-century at about 2,500 ppb and then falls. For B1, CH_4 levels off and eventually falls to 1980-levels by year 2100. N_2O continues to rise in all scenarios, reflecting in part its long lifetime, and abundances by the end of the century range from 350 to 460 ppb. Most scenarios lead to increases in tropospheric O_3, with scenarios A1FI and A2 projecting the maximum tropospheric O_3 burdens of 55 DU by year 2100. This increase of about 60% from today is more than twice the change from pre-industrial to present. Scenario B1 is alone in projecting an overall decline in tropospheric O_3 over most of the century: the drop to 30 DU is about halfway back to pre-industrial values. HFC-134a, the HFC with the largest projected abundance, is expected to reach about 900 ppt by year 2100 for all scenarios except B1. Likewise by 2100, the abundance of CF_4 rises to 340 to 400 ppt in all scenarios except B1. The projected increase in SF_6 is much smaller in absolute abundance, reaching about 60 ppt in scenarios A1 and A2. For the major non-CO_2 greenhouse gases, the SRES A2 and A1FI increases are similar to, but slightly larger than, those of IS92a. The SRES mix of lesser greenhouse gases (HFCs, PFCs, SF_6) and their abundances are increased substantially relative to IS92a. The summed radiative forcings from these gases plus CO_2 and aerosols are given in Chapter 6.

The chemistry of the troposphere is changing notably in these scenarios, and this is illustrated in Figure 4.14 with the lifetime (LT) of CH_4 and the change in mean tropospheric OH relative to year 2000. In all scenarios except B1, OH decreases 10% or more by the end of the century, pushing the lifetime of CH_4 up from 8.4 years, to 9.2 to 10.0 years. While increasing emissions of NO_x in most of these scenarios increases O_3 and would tend to increase OH (see notes to Table 4.11), the increase in CH_4 abundance and the greater CO emissions appear to dominate, driving OH down. In such an atmosphere, emissions of CH_4 and HFCs persist longer with greater greenhouse impact. In contrast the B1 atmosphere is more readily able to oxidise these compounds and reduce their impact.

4.4.6 Gaps in These Projections – the Need for Coupled Models

There are some obvious gaps in these projections where processes influencing the greenhouse gas abundances have been omitted. One involves coupling of tropospheric chemistry with the stratosphere. For one, we did not include the recovery of stratospheric ozone expected over the next century. The slow recovery of stratospheric ozone depletion from the halogens will lead to an increase in the flux of ozone into the troposphere and also to reduced solar UV in the troposphere, effectively reversing over the next century what has occurred over the past two decades. A more important impact on the Y2100 stratosphere, however, is the response to increases in CH_4 and N_2O projected by most scenarios (see Hofmann and Pyle, 1999), which in terms of coupled stratosphere-troposphere chemistry models could be evaluated in only one of the OxComp models (ULAQ, Université degli studi dell' Aguila) and is not included here.

Another major gap in these projections is the lack of global models coupling the atmospheric changes with biogeochemical models. There have been studies that tackled individual parts of the problem, e.g., deposition of reactive N (Holland *et al.*, 1997), crop damage from O_3 (Chameides *et al.*, 1994). Integrated assessment studies have coupled N_2O and CH_4 emission models with lower dimension or parametrized climate and chemistry models (e.g., Alcamo, 1994; Holmes and Ellis, 1999; Prinn *et al.*, 1999). However, the inherent local nature of this coupling, along with the possible feedbacks through, for example NO and VOC emissions, point to the need for coupled 3-D global chemistry and ecosystem models in these assessments.

Finally, there is an obvious need to couple the physical changes in the climate system (water vapour, temperature, winds, convection) with the global chemical models. This has been partially accomplished for some cases that are highlighted here (Section 4.5.2), but like other gaps presents a major challenge for the next assessment.

4.4.7 Sensitivity Analysis for Individual Sectors

In order to assess the overall impact of changing industry or agriculture, it would be necessary to combine all emissions from a specific sector or sub-sector as has been done with the IPCC assessment of aviation (Penner *et al.*, 1999). Further, the impact on natural emissions and land-use change (e.g., albedo, aerosols) would also need to be included. Such a sector analysis would cut across Chapters 3, 4, 5 and 6 of this report (e.g., as in Prather and

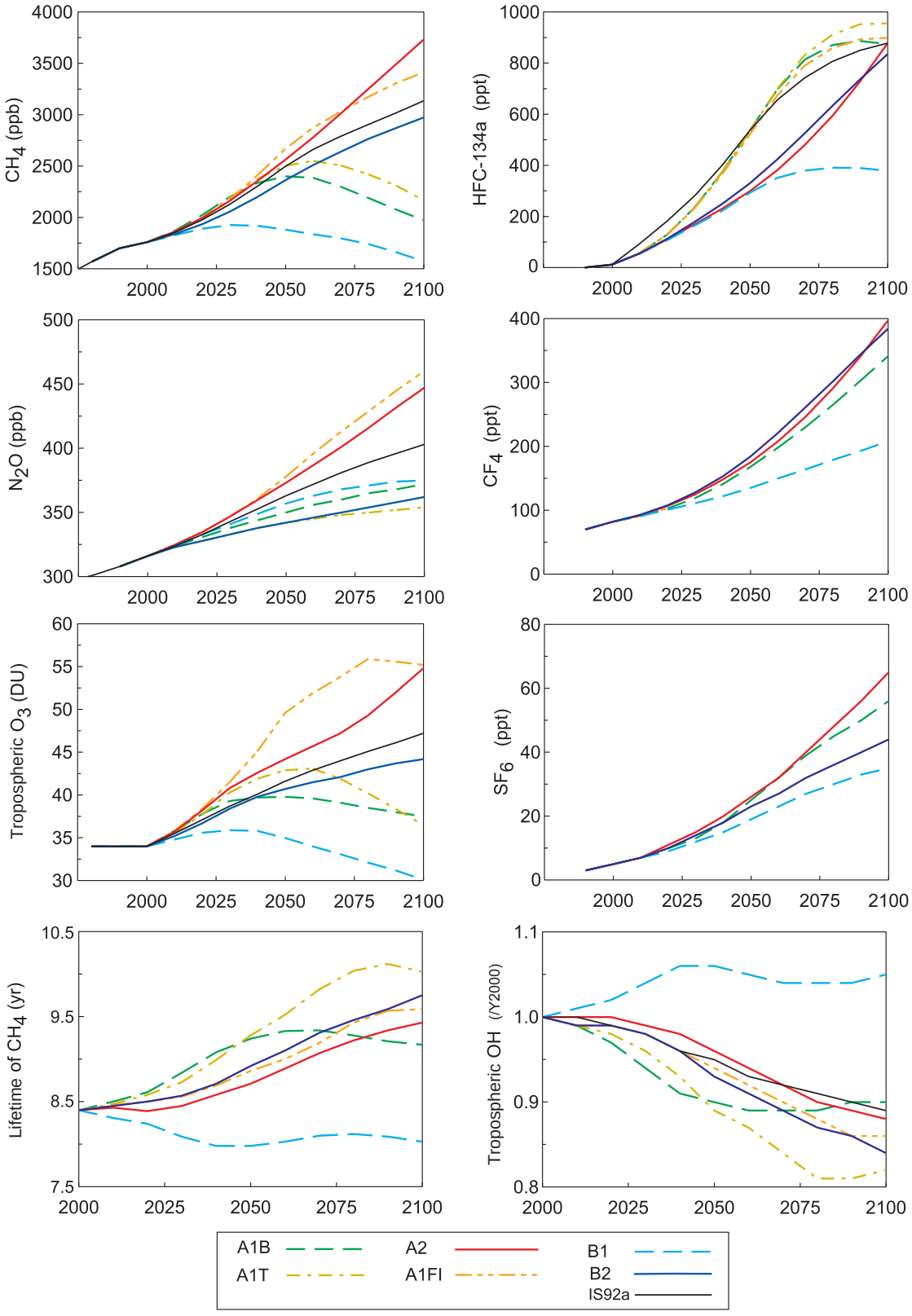

Figure 4.14: Atmospheric composition and properties predicted using the six SRES Marker-Illustrative scenarios for anthropogenic emissions: A1B (green dashed line), A1T (yellow dash-dotted), A1FI (orange dash-dot-dotted), A2 (red solid), B1 (cyan dashed), B2 (solid dark blue). Abundances prior to year 2000 are taken from observations, and the IS92a scenario computed with current methodology is shown for reference (thin black line). Results are shown for CH_4 (ppb), N_2O (ppb), tropospheric O_3 (DU), HFC-134a (ppt), CF_4 (ppt), SF_6 (ppt), the lifetime of CH_4 (yr), and the global annual mean abundance of tropospheric OH (scaled to year 2000 value). All SRES A1-type scenarios have the same emissions for HFCs, PFCs, and SF_6 (appearing a A1B), but the HFC-134a abundances vary because the tropospheric OH values differ affecting its lifetime. The IS92a scenario did not include emissions of PFCs and SF_6. For details, see chapter text and tables in Appendix II.

Sausen, 1999). Such an analysis cannot be done for the SRES emissions scenarios, which lack a breakdown by sector and also lack numbers for the changes in the land area of agriculture or urbanisation.

4.5 Open Questions

Many processes involving atmospheric chemistry, and the coupling of atmospheric chemistry with other elements of global change, have been proposed in the scientific literature. These are generally based on sound physical and chemical principles, but unfortunately, there is no consensus on their quantitative role in atmospheric chemistry on a global scale (e.g., the effects of clouds on tropospheric ozone: Lelieveld and Crutzen (1990) vs. Liang and Jacob (1997)), on the magnitude of possible compensating effects (e.g., net settling of HNO_3 on cloud particles: Lawrence and Crutzen (1999) vs. full cloud-scale dynamics), or even on how to implement them or whether these are already effectively included in many of the model calculations. While many of these processes may be important, there is inadequate information or consensus to make a quantitative evaluation in this assessment. This assessment is not a review, and so this section presents only a few examples of recent publications studying feedbacks or chemical processes, which are not included, but which are potentially important in this assessment.

4.5.1 Chemical Processes Important on the Global Scale

4.5.1.1 Missing chemistry, representation of small scales, and changing emission patterns

Analyses and observations (see Section 4.2.6) continue to test and improve the chemistry and transport used in the global CTMs. In terms of the chemistry, recent studies have looked, for example, at the representation of NMHC chemistry (Houweling *et al.* 1998; Wang *et al.* 1998b), the role of halogens in the O_3 budget of the remote marine troposphere, and the acetone source of upper tropospheric OH (see Sections 4.2.4 and 4.2.6). Most of these improvements in understanding will eventually become adopted as standard in the global CTMs, but at this stage, for example, the role of tropospheric halogen chemistry on the Y2100 predictions has not been evaluated in the CTMs.

Convection, as well as urban pollution and biomass burning plumes, occur on horizontal scales not resolved in global CTMs. These sub-grid features appear to be important in calculating OH abundances and O_3 production for biomass burning emissions (Pickering *et al.*, 1996; Folkins *et al.*, 1997), for the remote upper troposphere (Jaeglé *et al.*, 1997; Prather and Jacob, 1997; Wennberg *et al.*, 1998), and in urban plumes (e.g., Sillman *et al.*, 1990). Convection is represented in all CTMs here (e.g., Collins *et al.*, 1999; Müller and Brasseur, 1999) but in quite different ways, and it still involves parametrization of processes occurring on a sub-grid scale. A substantial element of the differences in CTM simulations appears to lie with the different representations of convection and boundary layer transport, particularly for the short-lived gases such as NO_x.

A change in the geographic emission pattern of the pollutants (NO_x, CO and VOC) can by itself alter tropospheric O_3 and OH abundances and in turn the abundances of CH_4 and HFCs. In one study of regional NO_x emissions and control strategy, Fuglestvedt *et al.* (1999) find that upper tropospheric O_3 is most sensitive to NO_x reductions in Southeast Asia and Australia and least to those in Scandinavia. Understanding trends in CO requires knowledge not only of the *in situ* chemistry of CO (e.g., Granier *et al.*, 1996; Kanakidou and Crutzen, 1999), but also of how local pollution control has altered the global pattern of emissions (e.g., Hallock-Waters *et al.*, 1999). These shifts have been included to some extent in the SRES emissions for year 2100 used here; however, the projected change in emission patterns have not been formally evaluated within the atmospheric chemistry community in terms of uncertainty in the Y2100 global atmosphere.

4.5.1.2 Aerosol interactions with tropospheric O_3 and OH

Over the past decade of assessments, stratospheric O_3 chemistry has been closely linked with aerosols, and global models in the recent WMO assessments have included some treatment of the stratospheric sulphate layer and polar stratospheric clouds. In the troposphere, studies have identified mechanisms that couple gas-phase and aerosol chemistry (Jacob, 2000). Many aerosols are photochemically formed from trace gases, and at rates that depend on the oxidative state of the atmosphere. Such processes are often included in global aerosol models (see Chapter 5). The feedback of the aerosols on the trace gas chemistry includes a wide range of processes: conversion of NO_x to nitrates, removal of HO_x, altering the UV flux and hence photodissociation rates (e.g., Dickerson *et al.*, 1997; Jacobson, 1998), and catalysing more exotic reactions leading to release of NO_x or halogen radicals. These processes are highly sensitive to the properties of the aerosol and the local chemical environment, and their importance on a global scale is not yet established. Only the first example above of aerosol chemistry is generally included in many of the CTMs represented here; however, the surface area of wet aerosols (that converts NO_x to HNO_3 via the intermediate species NO_3 and N_2O_5) is usually specified and not interactively calculated. More laboratory and field research is needed to define the processes so that implementation in global scale models can evaluate their quantitative impact on these calculations of greenhouse gases.

4.5.1.3 Stratosphere-troposphere coupling

The observed depletion of stratospheric ozone over the past three decades, which can be attributed in large part but not in total to the rise in stratospheric chlorine levels, has been reviewed extensively in WMO (1999). This depletion has lead to increases in tropospheric UV and hence forces tropospheric OH abundances upward (Bekki *et al.*, 1994). The total effect of such a change is not simple and involves the coupled stratosphere-troposphere chemical system; for example, ozone depletion may also have reduced the influx of O_3 from the stratosphere, which would reduce tropospheric O_3 (Karlsdottir *et al.*, 2000) and tend to reverse the OH trend. Such chemical feedbacks are reviewed as "climate-chemistry" feedbacks in WMO 1999 (Granier and Shine, 1999). There is insufficient understanding or quantitative consensus on these effects to be included in this assessment. While chlorine-driven O_3 depletion becomes much less of an issue

in the latter half of the 21st century, the projected increases in CO_2, CH_4, and N_2O may cause even larger changes in stratospheric O_3. The lack of coupled CTMs that include stratospheric changes adds uncertainty to these projections.

4.5.1.4 Uncertainties in the tropospheric O_3 budget

An updated survey of global tropospheric CTM studies since the SAR focuses on the tropospheric O_3 budget and is reported in Table 4.12. In this case authors were asked for diagnostics that did not always appear in publication. The modelled tropospheric O_3 abundances generally agree with observations; in most cases the net budgets are in balance; and yet the individual components vary greatly. For example, the stratospheric source ranges from 400 to 1,400 Tg/yr, while the surface sink is only slightly more constrained, 500 to 1,200 Tg/yr. If absolute production is diagnosed as the reactions of HO_2 and other peroxy radicals with NO, then the globally integrated production is calculated to be very large, 2,300 to 4,300 Tg/yr and is matched by an equally large sink (see Sections 4.2.3.3 and 4.2.6). The differences between the flux from the stratosphere and the destruction at the surface is balanced by the net *in situ* photochemical production. In this survey, the net production varies widely, from −800 to +500 Tg/yr, indicating that in some CTMs the troposphere is a large chemical source and in others a large sink. Nevertheless, the large differences in the stratospheric source are apparently the driving force behind whether a model calculates a chemical source or sink of tropospheric O_3. Individual CTM studies of the relative roles of stratospheric influx versus tropospheric chemistry in determining the tropospheric O_3 abundance (e.g., Roelofs and Lelieveld, 1997; Wang *et al.*, 1998a; Yienger *et al.*, 1999) will not represent a consensus until all CTMs develop a more accurate representation of the stratospheric source consistent with observations (Murphy and Fahey, 1994).

4.5.2 Impacts of Physical Climate Change on Atmospheric Chemistry

As global warming increases in the next century, the first-order atmospheric changes that impact tropospheric chemistry are the anticipated rise in temperature and water vapour. For example, an early 2-D model study (Fuglestvedt *et al.*, 1995) reports that tropospheric O_3 decreases by about 10% in response to a warmer, more humid climate projected for year 2050 as compared to an atmosphere with current temperature and H_2O. A recent study based on NCAR (National Center for Atmospheric Research) CCM (Community Climate Model) projected year 2050 changes in tropospheric temperature and H_2O (Brasseur *et al.*, 1998a) finds a global mean 7% increase in the OH abundance and a 5% decrease in tropospheric O_3, again relative to the same calculation with the current physical climate.

A 3-D tropospheric chemistry model has been coupled to the Hadley Centre Atmosphere-Ocean General Circulation Model (AOGCM) and experiments performed using the SRES preliminary marker A2p emissions (i) as annual snapshots (Stevenson *et al.*, 2000) and (ii) as a 110-year, fully coupled experiment (Johnson *et al.*, 1999) for the period 1990 to 2100. By 2100, the experiments with coupled climate change have increases in CH_4 which are only about three-quarters those of the simulation without climate change and increases in Northern Hemisphere mid-latitude O_3 which are reduced by half. The two major climate-chemistry feedback mechanisms identified in these and previous studies were (1) the change of chemical reaction rates with the average 3°C increase in tropospheric temperatures and (2) the enhanced photochemical destruction of tropospheric O_3 with the approximately 20% increase in water vapour. The role of changes in the circulation and convection appeared to play a lesser role but have not been fully evaluated. These studies clearly point out the importance of including the climate-chemistry feedbacks, but are just the beginning of the research that is needed for adequate assessment.

Thunderstorms, and their associated lightning, are a component of the physical climate system that provides a direct source of a key chemical species, NO_x. The magnitude and distribution of this lightning NO_x source controls the magnitude of the anthropogenic perturbations, e.g., that of aviation NO_x emissions on upper tropospheric O_3 (Berntsen and Isaksen, 1999). In spite of thorough investigations of the vertical distribution of lightning NO_x (Huntrieser *et al.*, 1998; Pickering *et al.* 1998), uncertainty in the source strength of lightning NO_x cannot be easily derived from observations (Thakur *et al.*, 1999; Thompson *et al.*, 1999). The link of lightning with deep convection (Price and Rind, 1992) opens up the possibility that this source of NO_x would vary with climate change, however, no quantitative evaluation can yet be made.

4.5.3 Feedbacks through Natural Emissions

Natural emissions of N_2O and CH_4 are currently the dominant contributors to their respective atmospheric burdens, with terrestrial emissions greatest in the tropics. Emissions of both of these gases are clearly driven by changes in physical climate as seen in the ice-core record (Figure 4.1e). Soil N_2O emissions are sensitive to temperature and soil moisture and changes in rates of carbon and nitrogen cycling (Prinn *et al.*, 1999). Similarly, methane emissions from wetlands are sensitive to the extent of inundation, temperature rise, and changes in rates of carbon and nitrogen cycling. Natural emissions of the pollutants NO_x, CO, and VOC play an important role in production of tropospheric O_3 and the abundance of OH; and these emissions are subject to similar forcings by both the physical and chemical climates. Terrestrial and aquatic ecosystems in turn respond to near-surface pollution (O_3, NO_2, acidic gases and aerosols) and to inadvertent fertilisation through deposition of reactive nitrogen (often emitted from the biosphere as NO or NH_3). This response can take the form of die back, reduced growth, or changed species composition competition that may alter trace gas surface exchange and ecosystem health and function. The coupling of this feedback system – between build-up of greenhouse gases, human-induced climate change, ecosystem responses, trace gas exchange at the surface, and back to atmospheric composition – has not been evaluated in this assessment. The variety and complexity of these feedbacks relating to ecosystems, beyond simple increases with rising temperatures and changing precipitation, argues strongly for the full interactive coupling of biogeochemical models of trace gas emissions with chemistry and climate models.

Table 4.12: *Tropospheric ozone budgets for circa 1990 conditions from a sample of global 3-D CTMs since the SAR.*

CTM	STE	Prod	Loss	P–L	SURF	Burden	Reference
	(Tg/yr)					(Tg)	
MATCH	1440	2490	3300	–810	620		Crutzen *et al.* (1999)
MATCH-MPIC	1103	2334	2812	–478	621		Lawrence *et al.* (1999)
ECHAM/TM3	768	3979	4065	–86	681	311	Houweling *et al.* (1998)
ECHAM/TM3[a]	740	2894	3149	–255	533	266	Houweling *et al.* (1998)
HARVARD	400	4100	3680	+420	820	310	Wang *et al.* (1998a)
GCTM	696			+128	825	298	Levy *et al.* (1997)
UIO	846			+295	1178	370	Berntsen *et al.* (1996)
ECHAM4	459	3425	3350	+75	534	271	Roelofs and Lelieveld (1997)
MOZART[b]	391	3018	2511	+507	898	193	Hauglustaine *et al.* (1998)
STOCHEM	432	4320	3890	+430	862	316	Stevenson *et al.* (2000)
KNMI	1429	2864	3719	–855	574		Wauben *et al.* (1998)
UCI	473	4229	3884	+345	812	288	Wild and Prather (2000)

STE = stratosphere-troposphere exchange (net flux from stratosphere) (Tg/yr).
Prod & Loss = *in situ* tropospheric chemical terms, P–L = net. (Tg/yr).
SURF = surface deposition (Tg/yr). Burden = total content (Tg, 34DU = 372Tg).
Budgets should balance exactly (STE+P–L=SURF), but may not due to roundoff.
[a] Results using CH_4-only chemistry without NMHC.
[b] Budget/burden calculated from surface to 250 hPa (missing part of upper troposphere).

4.6 Overall Impact of Global Atmospheric Chemistry Change

The projected growth in emissions of greenhouse gases and other pollutants in the IPCC SRES scenarios for the 21st century is expected to increase the atmospheric burden of non-CO_2 greenhouse gases substantially and contribute a sizable fraction to the overall increase in radiative forcing of the climate. These changes in atmospheric composition may, however, degrade the global environment in ways beyond climate change.

The impact of metropolitan pollution, specifically O_3 and CO, on the background air of the Atlantic and Pacific Oceans has been highlighted by many studies over the past decade. These have ranged from observations of anthropogenic pollution reaching across the Northern Hemisphere (e.g., Parrish *et al.*, 1993; Jaffe *et al.*, 1999) to analyses of rapidly increasing emissions of pollutants (NO_x, CO, VOC) in, for example, East Asia (Kato and Akimoto 1992; Elliott *et al.*, 1997). CTM studies have tried to quantify some of these projections for the near term: Berntsen *et al.* (1999) predict notable increases in CO and O_3 coming into the north-west USA from a doubling of current Asian emissions; Jacob *et al.* (1999) calculate that monthly mean O_3 abundances over the USA will increase by 1 to 6 ppb from a tripling of these emissions between 1985 and 2010; and Collins *et al.* (2000) project a 3 ppb increase from 1990 to 2015 in monthly mean O_3 over north-west Europe due to rising North American emissions. The impact of metropolitan pollution will expand over the coming decades as urban areas grow and use of resources intensifies.

What is new in this IPCC assessment is the extension of these projections to the year 2100, whereupon the cumulative impact of all Northern Hemisphere emissions, not just those immediately upwind, may for some scenarios double O_3 abundances over the northern mid-latitudes. Surface O_3 abundances during July over the industrialised continents of the Northern Hemisphere are about 40 ppb with 2000 emissions; and under SRES scenarios A2 and A1FI they would reach 45 to 50 ppb with 2030 emissions, 60 ppb with 2060 emissions, and >70 ppb with 2100 emissions. Since regional ozone episodes start with these background levels and build upon them with local smog production, it may be impossible under these circumstances to achieve a clean-air standard of <80 ppb over most populated regions. This problem reaches across continental boundaries and couples emissions of NO_x on a hemispheric scale. In the 21st century a global perspective will be needed to meet regional air quality objectives. The impact of this threatened degradation of air quality upon societal behaviour and policy decisions will possibly change the balance of future emissions impacting climate change (e.g., more fuel burn (CO_2) to achieve lower NO_x as in aviation; Penner *et al.*, 1999).

Under some emission scenarios, the large increases in tropospheric O_3 combined with the decreases in OH may alter the oxidation rate and the degradation paths for hydrocarbons and other hazardous substances. The damage caused by higher O_3 levels to both crops and natural systems needs to be assessed, and societal responses to this threat would likely change the emissions scenarios evaluated here (e.g., the current SRES scenarios anticipate the societal demand to control urban aerosols and acid rain by substantially cutting sulphur emissions) .

Coupling between atmospheric chemistry, the biosphere, and the climate are not at the stage that these feedbacks can be included in this assessment. There are indications, however, that the evolution of natural emissions and physical climate projected over the next century will change the baseline atmospheric chemistry and lead to altered biosphere-atmosphere exchanges and continued atmospheric change independent of anthropogenic emissions.

References

Alcamo, J. (ed.), 1994: IMAGE 2.0: Integrated Modeling of Global Climate Change. Special issue of *Water, Air and Soil Pollution*, **76**(1-2).

Arnold, F., J. Schneider, K. Gollinger, H. Schlager, P. Schulte, D.E. Hagen, P.D. Whitefield and P. van Velthoven, 1997: Observation of upper tropospheric sulfur dioxide and acetone pollution: potential implications for hydroxyl radical and aerosol formation. *Geophys. Res. Lett.*, **24**, 57-60.

Bakwin, P.S., P.P. Tans and P.C. Novelli, 1994: Carbon monoxide budget in the northern hemisphere. *Geophys. Res. Lett.*, **21**, 433-436.

Battle, M., M. Bender, T. Sowers, P.P. Tans, J.H. Butler, J.W. Elkins, T. Conway, N. Zhang, P. Lang and A.D. Clarke, 1996: Atmospheric gas concentrations over the past century measured in air from firn at South Pole. *Nature*, **383**, 231-235.

Becker, K.H., J.C. Lörzer, R. Kurtenbach, P. Wiesen, T.E. Jensen and T.J. Wallington, 1999: Nitrous oxide emissions from vehicles. *Envir. Sci. Tech.*, **33**, 4134-4139.

Bekki, S., K.S. Law and J.A. Pyle, 1994: Effect of ozone depletion on atmospheric CH_4 and CO concentrations. *Nature*, **371**, 595-597.

Benkovitz, C.M., M.T. Scholtz, J. Pacyna, L. Tawasou, J. Dignon, E.C. Voldner, P.A. Spiro, J.A. Logan and T.E. Graedel, 1996: Global gridded inventories of anthropogenic emissions of sulfur and nitrogen. *J. Geophys. Res.*, **101**, 29239-29252.

Bergamaschi, P., R. Hein, M. Heimann and P.J. Crutzen, 2000: Inverse modeling of the global CO cycle 1. Inversion of CO mixing ratios. *J. Geophys. Res.*, **105**, 1909-1927.

Berges, M.G.M., R.M. Hofmann, D. Schafre and P.J. Crutzen, 1993: Nitrous oxide emissions from motor vehicles in tunnels and their global extrapolation. *J. Geophys. Res.*, **98**, 18527-18531.

Berntsen, T. and I.S.A. Isaksen, 1997: A global three-dimensional chemical transport model for the troposphere. 1. Model description and CO and ozone results. *J. Geophys. Res.*, **102**, 21239-21280.

Berntsen, T. and I.S.A. Isaksen, 1999: Effects of lightning and convection on changes in tropospheric ozone due to NOx emissions from aircraft. *Tellus*, **51B**, 766-788.

Berntsen, T., I.S.A. Isaksen, W.-C. Wang and X.-Z. Liang, 1996: Impacts of increased anthropogenic emissions in Asia on tropospheric ozone and climate. A global 3-D model study. *Tellus*, **48B**, 13-32.

Berntsen, T.K., S. Karlsdottir and D.A. Jaffe, 1999: Influence of Asian emissions on the composition of air reaching the North Western United States. *Geophys. Res. Lett.*, **26**, 2171-2174.

Bey, I., R.M. Yantosca and D.J. Jacob, 1999: Export of pollutants from eastern Asia: a simulation of the PEM - West (B) aircraft mission using a 3-D model driven by assimilated meteorological fields. Presented at AGU spring meeting, 1999.

Bolin, B. and H. Rodhe, 1973: A note on the concepts of age distribution and transit time in natural reservoirs. *Tellus*, **25**, 58-62.

Blunier, T., J. Chappellaz, J. Schwander, J.-M. Barnola, T. Desperts, B. Stauffer and D. Raynaud, 1993: Atmospheric methane, record from a Greenland ice core over the last 1000 years. *J. Geophys. Res.*, **20**, 2219-2222.

Blunier, T., J. Chappellaz, J. Schwander, B. Stauffer and D. Raynaud, 1995: Variations in atmospheric methane concentration during the Holocene epoch. *Nature*, **374**, 46-49.

Brasseur, G.P., J.T. Kiehl, J.-F. Muller, T. Schneider, C. Granier, X.X. Tie and D. Hauglustaine, 1998a: Past and future changes in global tropospheric ozone: impact on radiative forcing. *Geophys. Res. Lett.*, **25**, 3807-3810.

Brasseur, G.P., D.A. Hauglustaine, S. Walters, P.J. Rasch, J.-F. Müller, C. Granier and X.X. Tie, 1998b: MOZART, a global chemical transport model for ozone and related chemical tracers: 1. Model description. *J. Geophys. Res.*, **103**, 28265-28289.

Brook, E.J., S. Harder, J. Severinghaus, E.J. Steig and C.M. Sucher, 2000: On the origin and timing of rapid changes in atmospheric methane during the last glacial period. *Global Biogechem. Cycles*, **14**, 559-572.

Brune, W.H., D. Tan, I.F. Faloona, L. Jaeglé, D.J. Jacob, B.G. Heikes, J. Snow, Y. Kondo, R. Shetter, G.W. Sachse, B. Anderson, G.L. Gregory, S. Vay, H.B. Singh, D.D. Davis, J.H. Crawford and D.R. Blake, 1999: OH and HO_2 chemistry in the north Atlantic free troposphere. *Geophys. Res. Lett.*, **26**, 3077-3080.

Butler, J.H., S.A. Montzka, A.D. Clarke, J.M. Lobert and J.W. Elkins, 1998a: Growth and distribution of halons in the atmosphere. *J. Geophys. Res.*, **103**, 1503-1511.

Butler, J.H. et al., 1998b: Nitrous oxide and halocompounds. In "Climate Monitoring and Diagnostics Laborartory Summary Report No. 24, 1996-1997," edited by D.J. Hofmann, J.T. Peterson and R.M. Rosson, pp. 91-121.

Butler, J.H., M. Battle, M.L. Bender, S.A. Montzka, A.D. Clark, E.S. Saltzman, C.M. Sucher, J.P. Severinghaus and J.W. Elkins, 1999: A record of atmospheric halocarbons during the twentieth century from polar firn air. *Nature*, **399**, 749-755.

Cao, M., K. Gregson and S. Marshall, 1998: Global methane emission from wetlands and its sensitivity to climate change. *Atmos. Env.*, **32**, 3293-3299.

Chameides, W.L., P.S. Kasibhatla, J. Yienger and H. Levy, 1994: Growth of continental-scale metro-agro-plexes, regional ozone pollution, and world food-production. *Science*, **264**, 74-77.

Chappellaz, J., T. Blunier, S. Kints, A. Dällenbach, J.-M. Barnola, J. Schwander, D. Raynaud and B. Stauffer, 1997: Changes in the atmospheric CH_4 gradient between Greenland and Antarctica during the Holocene. *J. Geophys. Res.*, **102**, 15987-15999.

Christian, H.J. et al., 1999: Global frequency and distribution of lightning as observed by the optical transient detector (OTD). 11th International Conference on Atmospheric Electricity, Guntersville, AL NASA/CP-1999-209261.

Collins, W.J., D.S. Stevenson, C.E. Johnson and R.G. Derwent, 1997: Tropospheric ozone in a global-scale three-dimensional Lagrangian model and its response to NOx emission controls. *J. Atmos. Chem.*, **26**, 223-274.

Collins, W.J., D.S. Stevenson, C.E. Johnson and R.G. Derwent, 1999: The role of convection in determining the budget of odd hydrogen in the upper troposphere. *J. Geophys. Res.*, **104**, 26927-26941.

Collins, W.J., D.S. Stevenson, C.E. Johnson and R.G. Derwent, 2000: The European regional ozone distribution and its links with the global scale for the years 1992 and 2015. *Atmos. Env.*, **34**, 255-267.

Crutzen, P.J., M.G. Lawrence and U. Poschl, 1999: On the background photochemistry of tropospheric ozone. *Tellus*, **51A-B**, 123-146.

Daniel, J.S. and S. Solomon, 1998: On the climate forcing of carbon monoxide. *J. Geophys. Res.*, **103**, 13249-13260.

Davidson, E.A and W. Kingerlee, 1997: A global inventory of nitric oxide emissions form soils. **48**, 37-50.

DeCaria, A., K.E. Pickering, G.L. Stenchikov, J.R. Scala, J.E. Dye, B.A. Ridley and P. Laroche, 2000: A cloud-scale model study of lightning-generated NOx in an individual thunderstorm during STERAO-A. *J. Geophys. Res.*, **105**, 11601-11616.

DeMore, W.B., S.P. Sander, D.M. Goldan, R.F. Hampson, M.J. Kurylo, C.J. Howard, A.R. Ravishankara, C.E. Kolb and M.J. Molina, 1997: Chemical kinetics and photochemical data for use in stratospheric modeling. Evaluation No. 12, JPL Publication 97-4, Jet Propulsion Laboratory, California Institute of Technology, Pasadena, CA.

Dentener, F.J. and P.J. Crutzen, 1993: Reaction of N_2O_5 on tropospheric aerosols: Impact on the global distribution of NOx, O_3, and OH. *J. Geophys. Res.*, **98**, 7149-7163.

Derwent, R. and R. Friedl, 1999: Chapter 2. Impacts of Aircraft Emissions on Atmospheric Ozone. In: Aviation and the Global Atmosphere, edited by J.E. Penner *et al.*, Cambridge University Press, pp 29-64.

Derwent, R.G., W.J. Collins, C.E. Johnson and D.S. Stevenson, 2001: Transient behaviour of tropospheric ozone precursors in a global 3-D CTM and their indirect greenhouse effects. *Clim Change*, **49:4**, in press.

Dessler, A.E., 1998: A reexamination of the 'stratospheric fountain' hypothesis. *Geophys. Res. Lett.*, **25**, 4165-4168.

Dickens, G.R., 1999: The blast in the past. *Nature*, **401**, 752-755.

Dickens, G., 2001: On the fate of past gas: what happens to methane released from a bacterially mediated gas hydrate capacitor? Geochem. Geophys. Geosyst., **2**, 2000GC000131.

Dickerson, R.R., B.G. Doddridge, P.K. Kelley and K.P. Rhoads, 1995: Large-scale pollution of the atmosphere over the North Atlantic Ocean: Evidence from Bermuda. *J. Geophys Res.*, **100**, 8945-8952.

Dickerson, R.R., S. Kondragunta, G. Stenchikov, K.L. Civerolo, B.G. Doddridge and B.N. Holben, 1997: The impact of aerosols on solar radiation and photochemical smog. *Science*, **278**, 827-830.

Dickerson, R.R., K.P. Rhoads, T.P. Carsey, S.J. Oltmans, J.P. Burrows and P.J, Crutzen, 1999: Ozone in the remote marine boundary layer: A possible role for halogens. *J. Geophys. Res.*, **104**, 21385-21395.

Ding, A. and M.X. Wang, 1996: A Model for methane emission from rice field and its application in southern China. *Advances in Atmospheric Sciences*, **13**, 159-168.

Dlugokencky, E.J., E.G. Dutton, P.C. Novelli, P.P. Tans, K.A. Masarie, K.O. Lantz and S. Madronich, 1996: Changes in CH_4 and CO growth rates after the eruption of Mt. Pinatubo and their link with changes in tropical tropospheric UV flux. *Geophys. Res. Lett.*, **23**, 2761-2764.

Dlugokencky, E.J., K.A. Masarie, P.M. Lang and P.P. Tans, 1998: Continuing decline in the growth rate of the atmospheric methane burden. *Nature*, **393**, 447-450.

Ehhalt, D.H., 1998: Radical ideas. *Science*, **279**, 1002-1003.

Ehhalt, D.H., 1999: Gas phase chemistry of the troposphere. Chapter 2 in "Global Aspects of Atmospheric Chemistry", edited by Deutsche Bunsen-Gesellschaft fûr Physikalische Chemie e.V., R. Zellner guest editor, Darmstadt Steinkopff, New York, Springer, pp. 21-109.

Ehhalt, D.H. and F. Rohrer, 2000: Dependence of the OH concentration on solar UV. *J. Geophys. Res.*, **105**, 3565-3571.

Ehhalt, D.H., U. Schmidt, R. Zander, P. Demoulin and C.P. Rinsland, 1991: Seasonal cycle and secular trend of the total and tropospheric column abundance of ethane above Jungfraujoch. *J. Geophys. Res.*, **96**, 4985-4994.

Elkins, J.W., J.H. Butler, D.F. Hurst, S.A. Montzka, F.L. Moore, T.M. Thompson and B.D. Hall, 1998: Halocarbons and other Atmospheric Trace Species Group/Climate Monitoring and Diagnostics Laboratory (HATS/CMDL), http://www.cmdl.noaa.gov/hats or anonymous ftp://ftp.cmdl.noaa.gov/hats, Boulder, Colorado, USA.

Elliott, S., D.R. Blake, R.A. Duce, C.A. Lai, I. McCreary, L.A. McNair, F.S. Rowland, A.G. Russell, G.E. Streit and R.P. Turco, 1997: Motorization of China implies changes in Pacific air chemistry and primary production. *Geophys. Res. Lett.*, **24**, 2671-2674.

Emmons, L.K., M.A. Carroll, D.A. Hauglustaine, G.P. Brasseur, C. Atherton, J. Penner, S. Sillman, H. Levy II, F. Rohrer, W.M.F. Wauben, P.F.J. Van Velthoven, Y. Wang, D. Jacob, P. Bakwin, R. Dickerson, B. Doddridge, C. Gerbig, R. Honrath, G. Hûbler, D. Jaffee, Y. Kondo, J.W. Munger, A. Torres and A. Volz-Thomas, 1997: Climatologies of NOx and NOy: A comparison of data and models. *Atmos. Env.*, **31**, 1851-1904.

Etheridge, D.M., L.P. Steele, R.J. Francey and R.L. Langenfelds, 1998: Atmospheric methane between 1000 A.D. and present: Evidence of anthropogenic emissions and climatic variability. *J. Geophys. Res.*, **103**, 15979-15993.

Faloona, I., D. Tan, W.H. Brune, L. Jaeglé, D.J. Jacob, Y. Kondo, M. Koike, R. Chatfield, R. Pueschel, G. Ferry, G. Sachse, S. Vay, B. Anderson, J. Hannon and H. Fuelberg, 2000: Observations of HOx and its relationship with NOx in the upper troposphere during SONEX. *J. Geophys. Res.*, **105**, 3771-3783.

Fishman, J. and V.G. Brackett, 1997: The climatological distribution of tropospheric ozone derived from satellite measurements using version 7 Total Ozone Mapping Spectrometer and Stratospheric Aerosol and Gas Experiment data sets. *J. Geophys. Res.*, **102**: 19275-19278.

Flückiger, J., A. Dällenbach, T. Blunier, B. Stauffer, T.F. Stocker, D. Raynaud and J.-M. Barnola, 1999: Variations in atmospheric N_2O concentration during abrupt climatic changes. *Science*, **285**, 227-230.

Folkins, I., P.O. Wennberg, T.F. Hanisco, J.G. Anderson and R.J. Salawitch, 1997: OH, HO_2 and NO in two biomass burning plumes: Sources of HOx and implications for ozone production. *Geophys. Res. Lett.*, **24**, 3185-3188.

Francey, R.J., M.R. Manning, C.E. Allison, S.A. Coram, D.M. Etheridge, R.L. Langenfelds, D.C. Lowe and L.P. Steele, 1999: A history of $\delta^{13}C$ in atmospheric CH_4 from the Cape Grim air archive and Antarctic firn air. *J. Geophys. Res.*, **104**, 23631-23643.

Fraser, P.J. and M.J. Prather, 1999: Uncertain road to ozone recovery. *Nature*, **398**, 663-664.

Fraser, P.J., D.E. Oram, C.E. Reeves, S.A. Penkett and A. McCulloch, 1999: Southern Hemisphere halon trends (1978-1998) and global halon emissions. *J. Geophys. Res.*, **104**, 15985-15999.

Frolking, S.E., A.R. Mosier, D.S. Ojima, C. Li, W.J. Parton, C.S. Potter, E. Priesack, R. Stenger, C. Haberbosch, P. Dorsch, H. Flessa, K.A. Smith, 1998: Comparison of N_2O emissions from soils at three temperate agricultural sites: simulations of year-round measurements by four models. *Nutr. Cycl. Agroecosys.*, **52**, 77-105.

Fuglestvedt, J.S., J.E. Jonson and I.S.A. Isaksen, 1994: Effects of reduction in stratospheric ozone on tropospheric chemistry through changes in photolysis rates. *Tellus*, **46B**, 172-192.

Fuglestvedt, J.S., J.E. Jonson, W.-C. Wang and I.S.A. Isaksen, 1995: Climate change and its effect on tropospheric ozone. In: Atmospheric Ozone as a Climate Gas, edited by W.C. Wang and I.S.A. Isaksen, pp. 145-162, NATO ASI Series vol. 132, Springer-Verlag, Berlin.

Fuglestvedt, J.S., I.S.A. Isaksen and W.-C. Wang, 1996: Estimates of indirect global warming potentials for CH_4, CO, and NOx. *Clim. Change*, **34**, 405-437.

Fuglestvedt, J.S., T. Berntsen, I.S.A. Isaksen, M. Liang and W.-C. Wang, 1999: Climatic forcing of nitrogen oxides through changes in tropospheric ozone and methane; global 3-D model studies. *Atmos. Env.*, **33**, 961-977.

Fung, I., J. John, J. Lerner, E. Matthews, M. Prather, L.P. Steele and P.J. Fraser, 1991: Three-dimensional model synthesis of the global methane cycle. *J. Geophys. Res.*, **96**, 13033-13065.

Geller, L.S., J.W. Elkins, J.M. Lobert, A.D. Clarke, D.F. Hurst, J.H. Butler and R.C. Myers, 1997: Tropospheric SF_6: observed latitudinal distribution and trends, dervived emissions, and interhemispheric exchange time. *Geophys. Res. Lett.*, **24**, 675-678.

Graedel, T.E., T.S. Bates, A.F. Bouwman, D. Cunnold, J. Dignon, I. Fung, D.J. Jacob, B.K. Lamb, J.A. Logan, G. Marland, P. Middleton, J.M. Pacyna, M. Placet and C. Veldt , 1993: A compilation of inventories of emissions to the atmosphere. *Global Biogeochemical Cycles*, **7**, 1-26.

Granier, C. and K.P. Shine, 1999: Chapter 10. Climate Effects of Ozone and Halocarbon Changes. In: Scientific Assessment of Ozone Depletion: 1998. Global Ozone Research and Monitoring Project - Report No. 44, World Meteorological Organization, Geneva, Switzerland, pp. 10.1-10.38.

Granier, C., J.-F. Müller, S. Madronich and G.P. Brasseur, 1996: Possible causes of the 1990-1993 decrease in the global tropospheric CO abundances: A three-dimensional sensitivity study. *Atmos. Env.*, **30**, 1673-1682.

Guenther, A., C. Hewitt, D. Erickson, R. Fall, C. Geron, T. Graedel, P. Harley, L. Klinger, M. Lerdau, W. McKay, T. Pierce, B. Scholes, R. Steinbrecher, R. Tallamraju, J. Taylor and P. Zimmerman, 1995: A global model of natural volatile organic compound emissions. *J. Geophys. Res.*, **100**, 8873-8892.

Guenther, A., B. Baugh, G. Brasseur, J. Greenberg, P. Harley, L. Klinger, D. Serca and L. Vierling, 1999: Isoprene emission estimates and uncertainties for the Central African EXPRESSO study domain. *J. Geophys. Res*., **104**, 30625-30639.

Hall, S. J. and P.A. Matson, 1999: Nitrogen oxide emissions after N additions in tropical forests. *Nature*, **400**, 152-155.

Hallock-Waters, K.A., B.G. Doddridge, R.R. Dickerson, S. Spitzer and J.D. Ray, 1999: Carbon monoxide in the U.S. mid-Atlantic troposphere: Evidence for a decreasing trend. *Geophys. Res. Lett*., **26**, 2816-2864.

Hannegan, B., S. Olsen, M. Prather, X. Zhu, D. Rind and J. Lerner, 1998: The dry stratosphere: A limit on cometary water influx. *Geophys.Res.Lett*., **25**, 1649-1652.

Hansen, J., M. Sato and R. Ruedy, 1997a: Radiative forcing and climate response. *J. Geophys. Res*., **102**, 6831-6864.

Hansen, J., M. Sato, R. Ruedy, A. Lacis, K. Asamoah and 38 others, 1997b: Forcings and chaos in interannual to decadal climate change. *J. Geophys. Res*., **102**, 25679-25720.

Harnisch, J. and A. Eisenhauer, 1998: Natural CF_4 and SF_6 on Earth. *Geophys. Res. Lett*., **25**, 2401-2404.

Harnisch, J., R. Borchers, P. Fabian and M. Maiss, 1996: Tropospheric trends for CF_4 and CF_3CF_3 since 1982 derived from SF_6 dated stratospheric air. *Geophys. Res. Lett*., **23**, 1099-1102.

Harnisch, J., R. Borchers, P. Fabian and M. Maiss, 1999: CF_4 and the age of mesospheric and polar vortex air. *Geophys. Res. Lett*., **26**, 295-298.

Harris, N.R.P., G. Ancellet, L. Bishop, D.J. Hofmann, J.B. Kerr, R.D. McPeters, M. Prendez, W.J. Randel, J. Staehelin, B.H. Subbaraya, A. Volz-Thomas, J. Zawodny and C.S. Zerefos, 1997: Trends in stratospheric and free tropospheric ozone. *J. Geophys. Res*., **102**, 1571-1590.

Hauglustaine, D.A., G.P. Brasseur, S. Walters, P.J. Rasch, J.-F. Müller, L.K. Emmons and M.A. Carroll, 1998: MOZART, a global chemical transport model for ozone and related chemical tracers: 2. Model results and evaluation. *J. Geophys. Res*., **103**, 28291-28335.

Haywood, J.M., M.D. Schawrzkopf and V. Ramaswamy, 1998: Estimates of radiative forcing due to modeled increases in tropospheric ozone. *J. Geophys. Res*., **103**, 16999-17007.

Hein, R., P.J. Crutzen and M. Heinmann, 1997: An inverse modeling approach to investigate the global atmospheric methane cycle. *Global Biogeochem. Cycles*, **11**, 43-76.

Hoell, J.M., D.D. Davis, S.C. Liu, R.E. Newell, H. Akimoto, R.J. McNeal and R.J. Bendura, 1997: The Pacific Exploratory Mission-West, Phase B: Feb-March, 1994. *J. Geophys. Res*., **102**, 28223-28239.

Hoell, J.M., D.D. Davis, D.J. Jacob, M.O. Rogers, R.E. Newell, H.E. Fuelberg, R.J. McNeal,. J.L. Raper and R.J. Bendura, 1999: Pacific Exploratory Mission in the tropical Pacific: PEM-Tropics A, August-September 1996. *J. Geophys. Res*., **104**, 5567-5583.

Hofmann, D.J. and J.A. Pyle, 1999: Chapter 12. Predicting Future Ozone Changes and Detection of Recovery. In: Scientific Assessment of Ozone Depletion: 1998. Global Ozone Research and Monitoring Project - Report No. 44, World Meteorological Organization, Geneva, Switzerland, pp. 12.1-57.

Hogan, K.B. and R.C. Harriss, 1994: Comment on 'A dramatic decrease in the growth rate of atmospheric methane in the northern hemisphere during 1992' by Dlugokencky et al. *Geophys. Res. Lett*., **21**, 2445-2446.

Holland, E.A., B.H. Braswell, J.F. Lamarque, A. Townsend, J. Sulzman, J.F. Muller, F. Dentener, G. Brasseur, H. Levy, J.E. Penner and G.J. Roelofs, 1997: Variations in the predicted spatial distribution of atmospheric nitrogen deposition and their impact on carbon uptake by terrestrial ecosystems. *J. Geophys. Res*., **102**, 15849-15866.

Holland, E.A., F.J. Dentener, B.H. Braswell and J.M. Sulzman, 1999: Contemporary and pre-industrial reactive nitrogen budgets. *Biogeochemistry*, **46**, 7-43.

Holmes, K.J. and J.H. Ellis, 1999: An integrated assessment modeling framework for assessing primary and secondary impacts from carbon dioxide stabilization scenarios. *Env. Modeling and Assessment*, **4**, 45-63.

Houweling, S., F. Dentener and J. Lelieveld, 1998: The impact of non-methane hydrocarbon compounds on tropospheric photochemistry. *J. Geophys. Res*., **103**, 10673-10696.

Houweling, S., T. Kaminski, F. Dentener, J. Lelieveld and M. Heimann, 1999: Inverse modeling of methane sources and sinks using the adjoint of a global transport model. *J. Geophys. Res*., **104**, 26137-26160.

Houweling, S., F. Dentener, J. Lelieveld, B. Walter and E. Dlugokencky, 2000: The modeling of tropospheric methane: how well can point measurements be reproduced by a global model? *J. Geophys. Res*., **105**, 8981-9002.

Hudson, R.D. and A.M. Thompson. 1998: Tropical tropospheric ozone from total ozone mapping spectrometer by a modified residual method. *J. Geophys. Res*., **103**, 22129-22145.

Huntrieser, H., H. Schlager, C. Feigl and H. Höller, 1998: Transport and production of NOx in electrified thunderstorms: survey of previous studies and new observations at midlatitudes. *J. Geophys. Res*., **103**, 28247-28264.

Impey, G.A., C.M. Mihele, K.G. Anlauf, L.A. Barrie, D.R. Hastie and P.B. Shepson, 1999: Measurements of photolyzable halogen compounds and bromine radicals during the Polar Sunrise Experiment 1997. *J. Atmos. Chem*., **34**, 21-37.

IPCC, 1996: Climate Change 1995: The Science of Climate Change. Contribution of Working Group I to the Second Assessment Report of the Intergovernmental Panel on Climate Change [Houghton, J.T., L.G. Meira Filho, B.A. Callander, N. Harris, A. Kattenberg, and K. Maskell (eds.)]. Cambridge University Press, Cambridge, United Kingdom and New York, NY, USA, 572 pp.

Isaksen, I.S.A. and O. Hov, 1987: Calculations of trends in the tropospheric concentrations of O_3, OH, CO, CH_4 and NOx. *Tellus*, **39B**, 271-283.

Isaksen, I. and C. Jackman, 1999: Chapter 4. Modeling the Chemical Composition of the Future Atmosphere. In: Aviation and the Global Atmosphere, edited by J.E. Penner et al., Cambridge University Press, pp 121-183.

IUPAC, 1997a: Evaluated kinetic and photochemical data for atmospheric chemistry: Supplement V, IUPAC subcommittee on gas kinetic data evaluation for atmospheric chemistry. *Journal of Physical Chemistry Reference Data*, **26**, 512-1011.

IUPAC, 1997b: Evaluated kinetic and photochemical data for atmospheric chemistry: Supplement VI, IUPAC subcommittee on gas kinetic data evaluation for atmospheric chemistry. *Journal of Physical Chemistry Reference Data*, **26**, 1329-1499.

IUPAC, 1999: Evaluated kinetic and photochemical data for atmospheric chemistry: Supplement VII, IUPAC subcommittee on gas kinetic data evaluation for atmospheric chemistry. *Journal of Physical Chemistry Reference Data*, **28**, 191-393.

Jackman, C.H., E.L. Fleming, S. Chandra, D.B. Considine and J.E. Rosenfield, 1996: Past, present, and future modeled ozone trends with comparisons to observed trends. *J. Geophys. Res.*, **101**, 28753-28767.

Jacob, D.J., 2000: Heterogeneous chemistry and tropospheric ozone. *Atmos. Env*., **34**, 2131-2159.

Jacob, D.J. *et al*. (30 authors), 1997: Evaluation and intercomparison of global atmospheric transport models using 222Rn and other short-lived tracers. *J. Geophys. Res*., **102**, 5953-5970.

Jacob, D.J., J.A. Logan and P.P. Murti, 1999: Effect of rising Asian emissions on surface ozone in the United States. *Geophys. Res. Lett*., **26**, 2175-2178.

Jacobson, M.Z., 1998: Studying the effects of aerosols on vertical photolysis rate coefficient and temperature profiles over an urban airshed. *J. Geophys. Res*., **103**, 10593-10604.

Jaeglé, L., D.J. Jacob, P.O. Wennberg, C.M. Spivakovsky, T.F. Hanisco, E.L. Lanzendorf, E.J. Hintsa, D.W. Fahey, E.R. Keim, M.H. Proffitt, E. Atlas, F. Flocke, S. Schauffler, C.T. McElroy, C. Midwinter, L. Pfister and J.C. Wilson, 1997: Observed OH and HO2 in the upper troposphere suggest a major source from convective injection of peroxides. *Geophys. Res. Lett.*, **24**, 3181-3184.

Jaeglé, L., D.J. Jacob, W.H. Brune, I. Faloona, D. Tan, Y. Kondo, G. Sachse, B. Anderson, G.L. Gregory, S. Vay, H.B. Singh, D.R. Blake and R. Shetter, 1999: Ozone production in the upper troposphere and the influence of aircraft during SONEX: approach of NOx-saturated conditions. *Geophys. Res. Lett.*, **26**, 3081-3084.

Jaeglé, L., D.J. Jacob, W.H. Brune, I. Faloona, D. Tan, B.G. Heikes, Y. Kondo, G. W. Sachse, B. Anderson, G.L. Gregory, H.B. Singh, R. Pueschel, G. Ferry, D.R. Blake and R.Shetter, 2000: Photochemistry of HOx in the upper troposphere at northern midlatitudes. *J. Geophys. Res.*, **105**, 3877-3892.

Jaffe, D.A., T. Anderson, D. Covert, R. Kotchenruther, B.Trost J. Danielson, W. Simpson, T. Berntsen, S. Karlsdottir, D. Blake, J. Harris and G. Carmichael, 1999: Transport of Asian air pollution to North America. *Geophys. Res. Lett.*, **26**, 711-714.

Jeuken, A.B.M., H.J. Eskes, P.F.J. van Velthoven, H.M. Kelder and E.V. Hólm, 1999: Assimilation of total ozone satellite measurements in a three-dimensional tracer transport model. *J. Geophys. Res.*, **104**, 5551-5563.

Jiménez, J.L., J.B. McManus, J.H. Shorter, D.D. Nelson, M.S. Zahniser, M. Koplow, G.J. McRae and C.E. Kolb, 2000: Cross road and mobile tunable infrared laser measurements of nitrous oxide emissions from motor vehicles. *Chemosphere: Global Change Science*, (in press).

Johnson, C.E., W.J. Collins, D.S. Stevenson and R.G. Derwent, 1999: The relative roles of climate and emissions changes on future oxidant concentrations. *J. Geophys. Res.*, **104**, 18631-18645.

JPL, 1997: Chemical Kinetics and Photochemical Data for Use in Stratospheric Modeling: Evaluation 12. JPL-97-4, NASA Panel for Data Evaluation, Jet Propulsion Laboratory, NASA Aeronautics and Space Administration, Pasadena, CA, USA, 266 pp.

JPL, 2000: Chemical Kinetics and Photochemical Data for Use in Stratospheric Modeling: Evaluation 13. JPL-00-3, NASA Panel for Data Evaluation, Jet Propulsion Laboratory, NASA Aeronautics and Space Administration, Pasadena, CA, USA, 73 pp.

Kanakidou, M. and P.J. Crutzen, 1999: The photochemical source of carbon monoxide: importance, uncertainties and feedbacks. *Chemosphere: Global Change Science*, **1**, 91-109.

Kanakidou, M., F.J. Dentener, G.P. Brasseur, T.K. Berntsen, W.J. Collins, D.A. Hauglustaine, S. Houweling, I.S.A. Isaksen, M. Krol, M.G. Lawrence, J.-F. Müller, N. Poisson, G.J. Roelofs, Y. Wang and W.M.F. Wauben, 1999: 3-D global simulations of tropospheric CO distributions - results of the GIM/IGAC intercomparison 1997 exercise. *Chemosphere: Global Change Science*, **1**, 263-282.

Karlsdottir, S. and I.S.A. Isaksen, 2000: Changing methane lifetime: Possible cause for reduced growth. *Geophys. Res. Lett.*, **27**, 93-96.

Karlsdottir, S., I.S.A. Isaksen, G. Myhre and T.K. Berntsen, 2000: Trend analysis of O_3 and CO in the period 1980 to 1996: A 3-D model study. *J. Geophys. Res.*, **105**, 28907-28933.

Kato, N. and H. Akimoto, 1992: Anthropogenic emissions of SO2 and NOx in Asia: emission inventories. *Atmos. Env.*, **26A**, 2997-3017.

Kennett, J.P., K.G. Cannariato, I.L. Hendy and R.J. Behl, 2000: Carbon isotopic evidence for methane hydrate instability during quaternary interstadials. *Science*, **288**, 128-133.

Khalil, M.A.K. and R. Rasmussen, 1994: Global decrease in atmospheric carbon monoxide. *Nature*, **370**, 639-641.

Kheshgi, H.S., A.K. Jain, R. Kotamarthi and D.J. Wuebbles, 1999: Future atmospheric methane concentrations in the context of the stabilization of greenhouse gas concentrations. *J. Geophys. Res.*, **104**, 19183-19190.

Kiehl, J.T., T.L. Schneider, R.W. Portmann and S. Solomon, 1999: Climate forcing due to tropospheric and stratospheric ozone. *J. Geophys. Res.*, **104**, 31239-31254.

Kim, K.-R. and H. Craig, 1990: Two-isotope characterization of N_2O in the Pacific Ocean and constraints on its origin in deep water. *Nature*, **347**, 58-61.

Kim, K.-R. and H. Craig, 1993: Nitrogen-15 and oxygen-18 characteristics of nitrous oxide: A global perspective. *Science*, **262**, 1855-1857.

Ko, M.K.W., R.-L. Shia, N.-D. Sze, H. Magid and R.G. Bray, 1999: Atmospheric lifetime and global warming potential of HFC-245fa. *J. Geophys. Res.*, **104**, 8173-8181.

Kroeze, C., A. Mozier and L. Bouwman, 1999: Closing the N_2O Budget: A retrospective analysis. *Global Biogeochem. Cycles*, **13**, 1-8.

Krol, M., P.J. Van Leeuwen and J. Lelieveld, 1998: Global OH trend inferred from methylchloroform measurements. *J. Geophys. Res.*, **103**, 10697-10711.

Kurylo, M.J. and J.M. Rodriguez, 1999: Chapter 2, Short-lived Ozone-Related Compounds. In: Scientific Assessment of Ozone Depletion: 1998. Global Ozone Research and Monitoring Project - Report No. 44, World Meteorological Organization, Geneva, Switzerland, pp 2.1-56.

Labuschagne, C., E.-G. Brunke, B. Parker and H.E. Scheel, 1999: Cape Point Trace Gas Observations Under Baseline and Non-Baseline Conditions. Poster Presentation at NOAA CMDL Annual Meeting, 12-13 May, 1999.

Langenfelds, R.L., P.J. Fraser, R.J. Francey, L.P. Steele, L.W. Porter and C.E. Allison, 1996: The Cape Grim Air Archive: The first seventeen years. In "Baseline Atmospheric Program Australia, 1994-95," edited by R.J. Francey, A.L. Dick and N. Derek, pp. 53-70.

Lassey, K.R., D.C. Lowe, C.A.M. Brenninkmeijer and A.J. Gomez, 1993: Atmospheric methane and its carbon isotopes in the southern hemisphere: Their time series and an instructive model. *Chemosphere: Global Change Science*, **26**, 95-100.

Law, K.S., P.-H. Plantevin, D.E. Shallcross, H.L.Rogers, J.A. Pyle, C.Grouhel, V. Thouret and A. Marenco, 1998: Evaluation of modelled O_3 using MOZAIC data. *J. Geophys. Res.*, **103**, 25721-25740.

Law, K.S., P.-H. Plantevin, V. Thouret, A. Marenco, W.A.H. Asman, M. Lawrence, P.J. Crutzen, J.F. Muller, D.A. Hauglustaine and M. Kanakidou, 2000: Comparison between global chemistry transport model results and MOZAIC data. *J. Geophys. Res.*, **105**, 1503-1525.

Lawrence, M. and P.J. Crutzen, 1999: The impact of cloud particle gravitational settling on soluble trace gas distributions. *Tellus*, **50B**, 263-289.

Lawrence, M.G., P.J. Crutzen, P.J. Rasch, B.E. Eaton and N.M. Mahowald, 1999: A model for studies of tropospheric photochemistry: description, global distributions and evaluation. *J. Geophys. Res.*, **104**, 26245-26277.

Lee, D.S., I. Köhler, E. Grobler, F. Rohrer, R. Sauen, L. Gallardo-Klenner, J.J.G. Olivier, F.J. Dentener and A.F. Bouwman, 1997: Estimates of global NOx emissions and their uncertainties. *Atmos. Env.*, **31**, 1735-1749.

Lelieveld, J. and P.J. Crutzen, 1990: Influences of cloud photochemical processes on tropospheric ozone. *Nature*, **343**, 227-233.

Lelieveld, J., P. Crutzen and F.J. Dentener, 1998: Changing concentration, lifetime and climate forcing of atmospheric methane. *Tellus*, **50B**, 128-150.

Lerdau, M. and M. Keller, 1997: Controls over isoprene emission from trees in a sub-tropical dry forest. *Plant, Cell, and Environment*, **20**, 569-578.

Levy II, H., P.S. Kasibhatla, W.J. Moxim, A.A. Klonecki, A.I. Hirsch, S.J. Oltmans and W.L. Chameides, 1997: The global impact of human activity on tropospheric ozone. *Geophys. Res. Lett.*, **24**, 791-794.

Li, C., S. Frolking and T.A. Frolking, 1992: A Model of nitrous oxide evolution from soil dirvben by rainfall events: I. Model structure and sensitivity. *J. Geophys. Res.*, **97**, 9759-9776.

Li, C., V. Narayanan and R. Harriss, 1996: Model estimates of nitrous oxide evoluation from soil agricultural lands in the United States. *Global Biogeochem. Cycles*, **10**, 297-306.

Liang, J. and D.J. Jacob, 1997: Effect of aqueous phase cloud chemistry on tropospheric ozone. *J. Geophys. Res*., **102**, 5993-6001.

Logan, J.A., 1994: Trends in the vertical distribution of ozone: an analysis of ozone sonde data. *J. Geophys. Res*., **99**, 25553-25585.

Logan, J.A., 1999: An analysis of ozonesonde data for the troposphere: recommendations for testing 3-D models and development of a gridded climatology for tropospheric ozone. *J. Geophys. Res*., **104**, 16115-16149.

Logan, J.A., I.A. Megretskaia, A.J. Miller, G.C. Tiao, D. Choi, L. Zhang, R.S. Stolarski, G.J. Labow, S.M. Hollandsworth, G.E. Bodeker, H. Claude, D. DeMuer, J.B. Kerr, D.W. Tarasick, S.J. Oltmans, B. Johnson, F. Schmidlin, J. Staehelin, P. Viatte and O. Uchino, 1999: Trends in the vertical distribution of ozone: A comparison of two analyses of ozonesonde data. *J. Geophys. Res.*, **104**, 26373-26399.

Lowe, D.C., C.A.M. Brenninkmeijer, G.W. Brailsford, K.R. Lassey and A.J. Gomez, 1994: Concentration and ^{13}C records of atmospheric methane in New Zealand and Antarctica: Evidence for changes in methane sources. *J. Geophys. Res*., **99**, 16913-16925.

Lowe, D.C., M.R. Manning, G.W. Brailsford and A.M. Bromley, 1997: The 1991-1992 atmospheric methane anomaly: Southern Hemisphere C-13 decrease and growth rate fluctuations. *Geophys. Res. Lett.*, **24**, 857-860.

Machida, T, T. Nakazawa, Y. Fujii, S. Aoki and O. Watanabe, 1995: Increase in the atmospheric nitrous oxide concentration during the last 250 years. *Geophys. Res. Lett*., **22**, 2921-2924.

Madronich, S. and G.J.M. Velders, 1999: Chapter 11, Halocarbon Scenarios for the Future Ozone Layer and Related Consequences. In: Scientific Assessment of Ozone Depletion: 1998. Global Ozone Research and Monitoring Project - Report No. 44, World Meteorological Organization, Geneva, Switzerland, pp 11.1-38.

Mahieu, E., R. Zander, L. Delbouille, P. Demoulin, G. Roland and C. Servais, 1997: Observed trends in total column abundances of atmospheric gases from IR solar spectra recorded at the Jungfraujoch. *J. Atmos. Chem*., **28**, 227-243.

Maiss, M. and C.A.M. Brenninkmeijer, 1998: Atmospheric SF_6: trends, sources, and prospects. *Envir. Sci. Tech*., **32**, 3077-3086.

Maiss, M., L.P. Steele, R.J. Francey, P.J. Fraser, R.L. Langenfelds, N.B.A. Trivett and I. Levin, 1996: Sulfur hexafluoride - A powerful new atmospheric tracer. *Atmos. Env*., **30**, 1621-1629.

Mak, J.E., M.R. Manning and D.C. Lowe, 2000: Aircraft observations of delta C-13 of atmospheric methane over the Pacific in August 1991 and 1993: Evidence of an enrichment in (CH_4)-C-13 in the Southern Hemisphere. *J. Geophys. Res*., **105**, 1329-1335.

Manning, M.R., 1999: Characteristic modes of isotopic variations in atmospheric chemistry. *Geophys. Res. Lett*., **26**, 1263-1266.

Matson, P.A., W.H. McDowell, A.R. Townsend and P.M. Vitousek, 1999: The globalization of N deposition: ecosystem consequences in tropical environments. *Biogeochemistry*, **46**, 67-83.

McElroy, M.B. and D.B.A. Jones, 1996: Evidence for an additional source of atmospheric N_2O. *Global Biogeochem. Cycles*, **10**, 651-659.

McLinden, C., S. Olsen, B. Hannegan, O. Wild, M. Prather and J. Sundet, 2000: Stratospheric ozone in 3-D models: a simple chemistry and the cross-tropopause flux. *J. Geophys. Res*., **105**, 14653-14665.

Michelsen, H.A., F.W. Irion, G.L. Manney, G.C. Toon and M.R. Gunson, 2000: Features and trends in ATMOS version 3 stratospheric water vapor and methane measurements. J. Geophys. Res., **105**, 22713-22724.

Mickley, L.J., P.P. Murti, D.J. Jacob, J.A. Logan, D. Rind and D. Koch, 1999: Radiative forcing from tropospheric ozone calculated with a unified chemistry-climate model. *J. Geophys. Res*., **104**, 30153-30172.

Miller, B., J. Huang, R. Weiss, R. Prinn and P. Fraser, 1998: Atmospheric trend and lifetime of chlorodifluoromethane (HCFC-22) and the global tropospheric OH concentration. *J. Geophys. Res*., **103**, 13237-13248.

Molina, L.T., P.J. Woodbridge and M.J. Molina, 1995: Atmospheric reactions and ultraviolet and infrared absorptivities of nitrogen trifluoride. *Geophys. Res. Lett*., **22**, 1873-1876.

Montzka, S.A., R.C. Myers, J.H. Butler and J.W. Elkins, 1994: Early trends in the global tropospheric abundance of hydrochlorofluorocarbon -141b and -142b. *Geophys. Res. Lett*., **21**, 2483-2486.

Montzka, S.A., J.H. Butler, R.C. Myers, T.M. Thompson. T.H. Swanson, A.D. Clarke, L.T. Lock and J.W. Elkins, 1996a: Decline in the tropospheric abundance of halogen from halocarbons: implications for stratospheric ozone depletion. *Science*, **272**, 1318-1322.

Montzka, S.A., R.C. Myers, J.H. Butler, J.W. Elkins, L.T. Lock, A.D. Clarke and A.H. Goldstein, 1996b: Observations of HFC-134a in the remote troposphere. *Geophys. Res. Lett*., **23**, 169-172.

Montzka, S.A., J.H. Butler, J.W. Elkins, T.M. Thompson, A.D. Clarke and L.T. Lock, 1999: Present and future trends in the atmospheric burden of ozone-depleting halogens. *Nature*, **398**, 690-694.

Montzka, S.A., C.M. Spivakovsky, J.H. Butler, J.W. Elkins, L.T. Lock and D.J. Mondeel, 2000: New observational constraints for atmospheric hydroxyl on global and hemispheric scales. *Science*, **288**, 500-503.

Mosier, A.R., J.M. Duxbury, J.R. Freney, O. Heinemeyer, K. Minami and D.E. Johnson, 1998a: Mitigating agricultural emissions of methane. *Clim. Change*, **40**, 39-80.

Mosier, A, C. Kroeze, C. Nevison, O. Oenema, S. Seitzinger and O. van Cleemput, 1998b: Closing the global N_2O budget: nitrous oxide emissions through the agricultural nitrogen cycle - OECD/IPCC/IEA phase II development of IPCC guidelines for national greenhouse gas inventory methodology. *Nutrient Cycling in Agroecosystems*, **52**, 225-248.

Mote, P.W., T.J. Dunkerton, M.E. McIntyre, E.A. Ray, P.H. Haynes and J.M. Russell, 1998: Vertical velocity, vertical diffusion, and dilution by midlatitude air in the tropical lower stratosphere. *J. Geophys. Res*., **103**, 8651-8666.

Moyer, E.J., F.W. Irion, Y.L. Yung and M.R. Gunson, 1996: ATMOS stratospheric deuterated water and implications for troposphere-stratosphere transport. *Geophys. Res. Lett*., **23**, 2385-2388.

Müller, J.-F. and G. Brasseur, 1995: IMAGES: A three-dimensional chemical transport model of the global troposphere. *J. Geophys. Res*., **100**, 16445-16490.

Müller, J.-F. and G. Brasseur, 1999: Sources of upper tropospheric HOx: A three-dimensional study. *J. Geophys. Res*., **104**, 1705-1715.

Murphy, D.M. and D.W. Fahey, 1994: An estimate of the flux of stratospheric reactive nitrogen and ozone into the troposphere. *J. Geophys. Res*., **99**, 5325-5332.

Naik, V., A.K. Jain, K.O. Patten, and D.J. Wuebbles, Consistent sets of atmospheric lifetimes and radiative forcing on climate for CFC replacements: HCFCs and HFCs, J. Geophys. Res., **105**, 6903-6914, 2000.

Nakićenović, N., J. Alcamo, G. Davis, B. de Vries, J. Fenhann, S. Gaffin, K. Gregory, A. Grübler, T. Y. Jung, T. Kram, E. L. La Rovere, L. Michaelis, S. Mori, T. Morita, W. Pepper, H. Pitcher, L. Price, K. Raihi, A. Roehrl, H-H. Rogner, A. Sankovski, M. Schlesinger, P. Shukla, S. Smith, R. Swart, S. van Rooijen, N. Victor, Z. Dadi, 2000: *IPCC Special Report on Emissions Scenarios*, Cambridge University Press, Cambridge, United Kingdom and New York, NY, USA, 599 pp.

Nedoluha, G.E., R.M. Bevilacqua, R.M. Gomez, D.E. Siskind, B.C. Hicks, J.M. Russell and B.J. Connor, 1998: Increases in middle atmospheric water vapor as observed by the Halogen Occultation Experiment and the ground-based Water Vapor Millimeter-wave Spectrometer from 1991 to 1997. *J. Geophys. Res*., **103**, 3531-3543.

Neue, H.-U. and R. Sass, 1998: The budget of methane from rice fields. *IGACtivities Newsletter*, **12**, 3-11.

Nevison C.D. and E.A. Holland, 1997: A reexamination of the impact of anthropogenically fixed nitrogen on atmospheric N_2O and the stratospheric O_3 layer. *J. Geophys. Res*., **102**, 25519-25536.

Norris, R.D. and U. Röhl, 1999: Carbon cycling and chronology of climate warming during the Palaeocene/Eocene transition. *Nature*, **401**, 775-778.

Novelli, P.C., K.A. Masarie and P.M. Lang, 1998: Distribution and recent changes of carbon monoxide in the lower troposphere. *J. Geophys. Res.*, **103**, 19015-19033.

Novelli, P.C., P.M. Lang, K.A. Masarie, D.F. Hurst, R. Myers and J.W. Elkins, 1999: Molecular hydrogen in the troposphere: Global distribution and budget. *J. Geophys. Res.*, **104**, 30427-30444.

Oltmans, S.J. and D.J. Hofmann, 1995: Increase in lower stratospheric water vapor at midlatitude northern hemisphere. *Nature*, **374**, 146-149.

Oltmans, S.J., A.S. Lefohn, H.E. Scheel, J.M. Harris, H. Levy, I.E. Galbally, E.G. Brunke, C.P. Meyer, J.A. Lathrop, B.J. Johnson, D.S. Shadwick, E. Cuevas, F.J. Schmidlin, D.W. Tarasick, H. Claude, J.B. Kerr, O. Uchino and V. Mohnen, 1998: Trends of ozone in the troposphere. *Geophys. Res. Lett*., **25**, 139-142.

Olivier, J.G.J., A.F. Bouwman, K.W. van der Hoek and J.J.M. Berdowski, 1998: Global Air Emission Inventories for Anthropogenic Sources of NOx, NH_3 and N_2O in 1990. *Environmental Poll.*, **102**, 135-148.

Olivier, J.G.J., A.F. Bouwman, J.J.M. Berdowski, C. Veldt, J.P.J. Bloos, A.J.H. Visschedijk, C.W.M. van der Maas and P.Y.J. Zasndveld, 1999: Sectoral emission inventories of greenhouse gases for 1990 on a per country basis as well as on 1×1. *Envir. Sci. Policy*, **2**, 241-263.

Oram, D.E., C.E. Reeves, S.A. Penkett and P.J. Fraser, 1995: Measurements of HCFC-142b and HCFC-141b in the Cape Grim air archive: 1978-1993. *Geophys. Res. Lett*., **22**, 2741-2744.

Oram, D.E., C.E. Reeves, W.T. Sturges, S.A. Penkett, P.J. Fraser and R.L. Langenfelds, 1996: Recent tropospheric growth rate and distribution of HFC-134a (CF_3CH_2F). *Geophys. Res. Lett*., **23**, 1949-1952.

Oram, D.E., W.T. Sturges, S.A. Penkett, J.M. Lee, P.J. Fraser, A. McCulloch and A. Engel, 1998: Atmospheric measurements and emissions of HFC-23 (CHF_3). *Geophys. Res. Lett*., **25**, 35-38.

Oram, D.E., W.T. Sturges, S.A. Penkett and P.J. Fraser, 1999: Tropospheric abundance and growth rates of radiatively-active halocarbon trace gases and estimates of global emissions. In *IUGG 99: abstracts, Birmingham*. [England]: International Union of Geodesy and Geophysics, 213 pp, abstract MI02/W/12-A4.

Orkin, V.L., E. Villenave, R.E. Huie and M.J. Kurylo, 1999: Atmospheric lifetimes and global warming potentials of hydrofluoroethers: Reactivity toward OH, UV spectra, and IR absorption cross sections. *J. Phys. Chem*., **103**, 9770-9779.

Oum, K.W., M.J. Lakin and B.J. Finlayson-Pitts, 1998: Bromine activation in the troposphere by the dark reaction of O-3 with seawater ice. *Geophys. Res. Lett*., **25**, 3923-3926.

Park, J.H., M.K.W. Ko, C.H. Jackman, R.A. Plumb, J.A. Kaye and K.H. Sage (eds.), 1999: M&M-2, NASA: Models and Measurements Intercomparison II. TM_1999_209554, September 1999, 502 pp.

Parrish, D.D., J.S. Holloway, M. Trainer, P.C. Murphy, G.L. Forbes and F.C. Fehsenfeld, 1993: Export of North-American ozone pollution to the North-Atlantic ocean. *Science*, **259**, 1436-1439.

Parton, W.J., M. Hartman, D. Ojima and D. Schimel, 1998: DAYCENT and its land surface submodel: description and testing. *Global Planet. Change*, **19**, 35-48.

Penkett, S.A., A. Volz-Thomas, D.D. Parrish, R.E. Honrath and F.C. Fehsenfeld, 1998: The North Atlantic Regional Experiment (NARE II), Preface. *J. Geophys. Res*., **103**, 13353-13356.

Penner, J.E., D.H. Lister, D.J. Griggs, D.J. Dokken and M. McFarland (eds.), 1999: Aviation and the Global Atmosphere. A Special Report of IPCC Working Groups I and III, Cambridge University Press, Cambridge, UK, 373 pp.

Petit, J.R., J. Jouzel, D. Raynaud, N.I. Barkov, J.M. Barnola, I. Basile, M. Bender, J. Chappellaz, Davis, G. Delaygue, M. Delmotte, V.M. Kotlyakov, M. Legrand, V.Y. Lipenkov, C. Lorius, L. Pepin, C. Ritz, E. Saltzman and M. Stievenard, 1999: Climate and atmospheric history of the past 420,000 years from the Vostok ice core, Antarctica. *Nature*, **399**, 429-436.

Pickering, K.E., A.M. Thompson, Y. Wang, W.-K Tao, D.P. McNamara, V.W.J.H. Kirchoff, B.G. Heikes, G.W. Sachse, J.D. Bradshaw, G.L. Gregory and D.R. Blake, 1996: Convective transport of biomass burning emissions over Brazil during TRACE a. *J. Geophys. Res*., **101**, 23993-24012.

Pickering, K.E., Y. Wang, W.-K. Tao, C. Price and J.-F. Müller, 1998: Vertical distribution of lightning NOx for use in regional and global chemical transport models. *J. Geophys. Res*., **103**, 31203-31216.

Pitari, G., B. Grassi and G. Visconti, 1997: Results of a chemical-transport model with interactive aerosol microphysics. Proc. XVIII Quadrennial Ozone Symposium, R. Bojkov and G. Visconti (eds.), pp 759-762.

Platt, U. and G.K. Moortgat, 1999: Heterogeneous and homogeneous chemistry of reactive halogen compounds in the lower troposphere - XXIII General Assembly of the EGS. *J. Atmos. Chem*., **34**, 1-8.

Prados, A.I., R.R. Dickerson, B.G. Doddridge, P.A. Milne, J.L. Moody and J.T. Merrill, 1999: Transport of ozone and pollutants from North America to the North Atlantic Ocean during the 1996 Atmosphere/Ocean Chemistry Experiment (AEROCE) intensive. *J. Geophys. Res*., **104**, 26219-26233.

Prather, M.J., 1996: Natural modes and time scales in atmospheric chemistry: theory, GWPs for CH_4 and CO, and runaway growth. *Geophys. Res. Lett*., **23**, 2597-2600.

Prather, M.J., 1998: Time scales in atmospheric chemistry: coupled perturbations to N_2O, NOy, and O_3. *Science*, **279**, 1339-1341.

Prather, M.J. and C.M. Spivakovsky, 1990: Tropospheric OH and the lifetimes of hydrochlorofluorocarbons (HCFCs). *J. Geophys. Res*., **95**, 18723-18729.

Prather, M.J. and D.J. Jacob, 1997: A persistent imbalance in HOx and NOx photochemistry of the upper troposphere driven by deep tropical convection. *Geophys. Res. Lett*., **24**, 3189-3192.

Prather, M. and R. Sausen, 1999: Chapter 6. Potential Climate Change from Aviation. In: Aviation and the Global Atmosphere, edited by J.E. Penner et al., Cambridge University Press, pp 185-215.

Prather, M., R. Derwent, D. Ehhalt, P. Fraser, E Sanhueza and X. Zhou, 1995: Other tracer gases and atmospheric chemistry. In: *Climate Change 1994*, [Houghton, J.T. , L.G. Meira Filho, J. Bruce, Hoesung lee, B.A. Callander, E. Haites, N. Harris and K. Maskell (eds.)], Cambridge University Press, Cambridge, UK, pp 73-126.

Price, C. and D. Rind, 1992: A simple lightning parameterization for calculating global lightning distributions. *J. Geophys. Res*., **97**, 9919-9933.

Price, C., J. Penner and M. Prather, 1997a: NOx from lightning 1. Global distribution based on lightning physics. *J. Geophys. Res*., **102**, 5929-5941.

Price, C., J. Penner and M. Prather, 1997b: NOx from lightning 2. Constraints from the global electric circuit. *J. Geophys. Res*., **102**, 5943-5951.

Prinn, R.G. and R. Zander, 1999: Chapter 1, Long-lived Ozone Related Compounds. In: Scientific Assessment of Ozone Depletion: 1998. Global Ozone Research and Monitoring Project - Report No. 44, World Meteorological Organization, Geneva, Switzerland, pp 1.1-54.

Prinn, R.G., D.M. Cunnold, R. Rasmussen, P.G. Simmonds, F.N. Alyea, A.J. Crawford, P.J. Fraser and R.D. Rosen, 1990: Atmospheric emissions and trends of nitrous oxide deduced from 10 years of ALE/GAGE data. *J. Geophys. Res*., **95**, 18369-18385.

Prinn, R.G., R.F. Weiss, B.R. Miller, J. Huang, F.N. Alyea, D.M. Cunnold, P.J. Fraser, D.E. Hartley and P.G. Simmonds, 1995:

Atmospheric trend and lifetime of CH_3CCl_3 and global OH concentrations. *Science*, **269**, 187-192.

Prinn, R.G., R.F. Weiss, P.J. Fraser, P.G. Simmonds, F.N. Alyea and D.M. Cunnold, 1998: The ALE/GAGE/AGAGE database. DOE-CDIAC World Data Center (e-mail to: cpd@ornl.gov), Dataset No. DB-1001.

Prinn, R., H. Jacoby, A. Sokolov, C. Wang, X. Xiao, Z. Yang, R. Eckhaus, P. Stone, D. Ellerman, J. Melillo, J. Fitzmaurice, D. Kicklighter, G. Holian and Y. Liu, 1999: Integrated global system model for climate policy assessment: Feedbacks and sensitivity studies. *Clim. Change*, **41**, 469-546.

Prinn, R.G., R.F. Weiss, P.J. Fraser, P.G. Simmonds, D.M. Cunnold, F.N. Alyea, S. O'Doherty, P. Salameh, B.R. Miller, J. Huang, R.H.J. Wang, D.E. Hartley, C. Harth, L.P. Steele, G. Sturrock, P.M. Midgley and A. McCulloch, 2000: A history of chemically and radiatively important gases in air deduced from ALE/GAGE/AGAGE. *J. Geophys. Res.*, **105**, 17751-17792.

Quay, P.D., S.L. King, J. Stutsman, D.O. Wilbur, L.P. Steele, I. Fung, R.H. Gammon, T.A. Brown, G.W. Farwell, P.M. Grootes and F.H. Schmidt, 1991: Carbon isotopic composition of atmospheric CH_4: Fossil and biomass burning source components. *Global Biogeochem. Cycles*, **5**, 25-47.

Quay, P., J. Stutsman, D. Wilbur, A. Stover, E. Dlugokencky and T. Brown, 1999: The isotopic composition of atmospheric methane. *Global Biogeochem. Cycles*, **13**, 445-461.

Rahn, T. and M. Whalen, 1997: Stable isotope enrichment in stratospheric nitrous oxide. *Science*, **278**, 1776-1778.

Rahn, T., H. Zhang, M. Whalen and G.A. Blake, 1998: Stable isotope fractionation during ultraviolet photolysis of N_2O. *Geophys. Res. Lett.*, **25**, 4489-4492.

Randel, W.J., R.S. Stolarski, D.M. Cunnold, J.A. Logan, M.J. Newchurch and J.M. Zawodny, 1999: Trends in the vertical distribution of ozone. *Science*, **285**, 1689-1692.

Ridgwell, A.J., S.J. Marshall and K. Gregson, 1999: Consumption of methane by soils: A process-based model. *Global Biogeochem. Cycles*, **13**, 59-70.

Rinsland, C.P., N.B. Jones, B.J. Connor, J.A. Logan, N.S. Pougatchev, A. Goldman, F.J. Murcray, T.M. Stephen, A.S. Pine, R. Zander, E. Mahieu and P. Demoulin, 1998: Northern and southern hemisphere ground-based infrared spectroscopic measurements of tropospheric carbon monoxide and ethane. *J. Geophys. Res.*, **103**, 28197-28217.

Roelofs, G.-J. and J.S. Lelieveld, 1997: Model study of cross-tropopause O_3 transports on tropospheric O_3 levels. *Tellus*, **49B**, 38-55.

Roelofs, G.-J., J.S. Lelieveld and R. van Dorland, 1997: A three dimensional chemistry/general circulation model simulation of anthropogenically derived ozone in the troposphere and its radiative climate forcing. *J. Geophys. Res.*, **102**, 23389-23401.

Rohrer, F., D. Brüning, E. Gobler, M. Weber, D. Ehhalt, R. Neubert, W. Schüβler, and I. Levine, 1998: Mixing ratios and photostationary state of NO and NO_2 observed during the POPCORN field campaign at a rural site in Germany. *J. Atmos. Chem.*, **31**, 119-137.

Rosenlof, K.H., A.F. Tuck , K.K. Kelly, Kelly, J.M. Russell and M.P. McCormick, 1997: Hemispheric asymmetries in water vapor and inferences about transport in the lower stratosphere. *J. Geophys. Res.*, **102**, 13213-13234.

Rudolph, J., 1995: The tropospheric distribution and budget of ethane. *J. Geophys. Res.*, **100**, 11369-11381.

Sander, S.P., R.R. Friedl, W.B. DeMore, A.R. Ravishankara, D.M. Golden, C.E. Kolb, M.J. Kurylo, R.F. Hampson, R.E. Huie, M.J. Molina and G.K. Moortgat, 2000: Chemical Kinetics and Photochemical Data for Use in Stratospheric Modeling. Supplement to Evaluation No. 12 - Update of Key Reactions and Evaluation No.13, JPL Publication 00-3, Jet Propulsion Laboratory, California Institute of Technology, Pasadena, CA.

SAR, see IPCC, 1996.

Sass, R.L., F.M. Fisher Jr., A. Ding and Y. Huang, 1999: Exchange of methane from rice fields: national, regional, and global budgets. *J. Geophys. Res.*, **104**, 26943-26951.

Schauffler, S.M. and J.S. Daniel, 1994: On the effects of stratospheric circulation changes on trace gas trends. *J. Geophys. Res.*, **99**, 25747-25754.

Schimel, D., D. Alves, I. Enting, M. Heimann, F. Joos, D. Raynaud, T. Wigley, M. Prather, R. Derwent, D. Ehhalt, P. Fraser, E. Sanhueza, X. Zhou, P. Jonas, R. Charlson, H. Rodhe, S. Sadasivan, K.P. Shine, Y. Fouquart, V. Ramaswamy, S. Solomon, J. Srivinasan, D. Albritton, R. Derwent, I. Isaksen, M. Lal and D. Wuebbles, 1996: Chapter 2, Radiative Forcing of Climate Change. In: Climate Change 1995: The Science of Climate Change. Contribution of Working Group I to the Second Assessment Report of the Intergovernmental Panel on Climate Change [Houghton, J.T., L.G. Meira Filho, B.A. Callander, N. Harris, A. Kattenberg, and K. Maskell (eds.)]. Cambridge University Press, pp 65-131.

Schultz, M.G., D.J. Jacob, Y.H. Wang, J.A. Logan, E.L. Atlas, D.R. Blake, N.J. Blake, J.D. Bradshaw, E.V. Browell, M.A. Fenn, F. Flocke, G.L. Gregory, B.G. Heikes, G.W. Sachse, S.T. Sandholm, R.E. Shetter, H.B. Singh and R.W. Talbot, 1999: On the origin of tropposheric ozone and NOx over the tropical South Pacific. *J. Geophys. Res.*, **104**, 5829-5843.

Shine, K.P., R.G. Derwent, D.J. Wuebbles and J.-J. Morcrette, 1990: Chapter 2. Radiative Forcing of Climate. In: Climate Change: The IPCC Scientific Assessment, edited by J.T. Houghton, G.J. Jenkins, J.J. Ephraums, Cambridge University Press, Cambridge, UK, pp 41-68.

Sillman, S., J.A. Logan and S.C. Wofsy, 1990: A regional scale-model for ozone in the united-states with subgrid representation of urban and power-plant plumes. *J. Geophys. Res.*, **95**, 5731-5748.

Simmonds, P.G., S. O'Doherty, J. Huang, R. Prinn, R.G. Derwent, D. Ryall, G. Nickless and D. Cunnold, 1998: Calculated trends and the atmospheric abundance of 1,1,1,2-tetrafluoroethane, 1,1-dichloro-1-fluoroethane, and 1-chloro-1,1-difluoroethane using automated in-situ gas chromatography mass spectrometry measurements recorded at Mace Head, Ireland, from October 1994 to March 1997. *J. Geophys. Res.*, **103**, 16029-16037.

Simmonds, P.G., R.G. Derwent, S. O'Doherty, D.B. Ryall, L.P. Steele, R.L. Langenfelds, P. Salameh, H.J. Wang, C.H. Dimmer and L.E. Hudson, 2000: Continuous high-frequency observations of hydrogen at the Mace Head baseline atmospheric monitoring station over the 1994-1998 period. *J. Geophys. Res.*, **105**, 12105-12121.

Simmons, A.J., A. Untch, C. Jakob, P. Kallberg and P. Unden, 1999: Stratospheric water vapour and tropical tropopause temperatures in ECMWF analyses and multi-year simulations. *Quart. J. R. Met. Soc.*, Part A, **125**, 353-386.

Singh, H.B., M. Kanakidou, P.J. Crutzen and D.J. Jacob, 1995: High concentrations and photochemical fate of oxygenated hydrocarbons in the global troposphere. *Nature*, **378**, 50-54.

Singh, H.B., A.N. Thakur, Y.E. Chen and M. Kanakidou, 1996: Tetrachloroethylene as an indicator of low Cl atom concentrations in the troposphere. *Geophys. Res. Lett.*, **23**, 1529-1532.

Spivakovsky, C.M., J.A. Logan, S.A. Montzka, Y.J. Balkanski, M. Foreman-Fowler, D.B.A. Jones, L.W. Horowitz, A.C. Fusco, C.A.M. Brenninkmeijer, M.J. Prather, S.C. Wofsy and M.B. McElroy, 2000: Three-dimensional climatological distribution of tropospheric OH: update and evaluation. *J. Geophys. Res.*, **105**, 8931-8980.

Staehelin, J., J. Thudium, R. Buehler, A. Volz-Thomas and W. Graber, 1994: Trends in surface ozone concentrations at Arosa (Switzerland). *Atmos. Env.*, **28**, 75-87.

Staehelin, J., R. Kegel and N.R.P. Harris, 1998: Trend analysis of the homogenized total ozone series of Arosa (Switzerland), 1926-1996. *J. Geophys. Res.*, **103**, 8389-8399.

Stauffer, B., G. Fischer, A. Neftel and H. Oeschger, 1985: Increase of atmospheric methane recorded in Antarctic ice core. *Science*, **229**,

1386-1388.

Steele, L.P., R.L. Langenfelds, M.P. Lucarelli, P.J. Fraser, L.N. Cooper, D.A. Spenser, S. Chea and K. Broadhurst, 1996: Atmospheric methane, carbon dioxide, carbon monoxide, hydrogen, and nitrous oxide from Cape Grim air samples analysed by gas chromatography. In: Baseline Atmospheric Program Australia, 1994-95, edited by R.J. Francey, A.L. Dick and N. Derek, pp 107-110.

Stevens, C.M. and A. Engelkemeir, 1988: Stable carbon isotopic composition of methane from some natural and anthropogenic sources. *J. Geophys. Res*., **93**, 725-733.

Stevenson, D.S., C.E. Johnson, W.J. Collins, R.G. Derwent and J.M. Edwards, 2000: Future tropospheric ozone radiative forcing and methane turnover - the impact of climate change. *Geophys. Res. Lett*., **27**, 2073-2076.

Sturges, W.T., T.J. Wallington, M.D. Hurley, K.P. Shine, K. Sihra, A. Engel, D.E. Oram, S.A. Penkett, R. Mulvaney and C.A.M. Brenninkmeijer, 2000: A potent greenhouse gas identified in the atmosphere: SF_5CF_3. *Science*, **289**, 611-613.

Sturrock, G.A., S. O'Doherty, P.G. Simmonds and P.J. Fraser, 1999: *In situ* GC-MS measurements of the CFC replacement chemicals and other halocarbon species: The AGAGE program at Cape Grim, Tasmania. Proceedings of the Australian Symposium on Analytical Science, Melbourne, July 1999, Royal Australian Chemical Institute, 45-48.

Suess, E., G. Bohrmann, J. Greinert and E. Lausch, 1999: Flammable ice. Scientific American, 52-59/76-83.

Sundet, J.K., 1997: Model Studies with a 3-D Global CTM using ECMWF data. Ph.D. thesis, Dept. of Geophysics, University of Oslo, Norway.

Talbot, R.W., J.E. Dibb, E.M. Scheuer, D.R. Blake, N.J. Blake, G.L. Gregory, G.W. Sachse, J.D. Bradshaw, S.T. Sandholm and H.B. Singh, 1999: Influence of biomass combustion emissions on the distribution of acidic trace gases over the southern Pacific basin during austral springtime. *J. Geophys. Res.*, **104**, 5623-5634,.

Thakur, A.N., H.B. Singh, P. Mariani, Y. Chen, Y. Wang, D.J. Jacob, G. Brasseur, J.-F. Müller and M. Lawrence, 1999: Distribution or reactive nitrogen species in the remote free troposphere: data and model comparisons. *Atmos. Env*., **33**, 1403-1422.

Thompson, T.M., J.W. Elkins, J.H. Butler, S.A. Montzka, R.C. Myers, T.H. Swanson, T.J. Baring, A.D. Clarke, G.S. Dutton, A.H. Hayden, J.M. Lobert, J.M. Gilligan and C.M. Volk, 1994: 5. Nitrous oxide and Halocarbons Division. In: Climate Monitoring and Diagnostics Laboratory - No. 22 Summary Report 1993, edited by J.T. Peterson and R.M. Rosson, US Department of Commerce, NOAA/ERL, Boulder, CO, pp 72-91.

Thompson, A.M., K.E. Pickering, D.P. McNamara, M.R. Schoeberl, R.D. Hudson, J.H. Kim, E.V. Browell, V.W.J.H. Kirchhoff and D. Nganga, 1996: Where did tropospheric ozone over southern Africa and the tropical Atlantic come from in October 1992? Insights from TOMS, GTE TRACE A and SAFARI 1992. *J. Geophys. Res*., **101**, 24251-24278.

Thompson, A.M., L.C. Sparling, Y. Kondo, B.E. Anderson, G.L. Gregory and G.W. Sachse, 1999: Perspectives on NO, NOy and fine aerosol sources and variability during SONEX. *Geophys. Res. Lett.*, **26**, 3073-3076.

van Aardenne, J.A., G.R. Carmichael, H. Levy, D. Streets and L. Hordijk, 1999: Anthropogenic NOx emissions in Asia in the period 1990-2020. Atmos. Env., 33, 633-646.

Van Dorland, R., F.J. Dentener and J. Lelieveld, 1997: Radiative forcing due to tropospheric ozone and sulfate aerosols. *J. Geophys. Res*., **102**, 28079-28100.

Vogt, R., R. Sander, R. Von Glasow and P.J. Crutzen, 1999: Iodine chemistry and its role in halogen activation and ozone loss in the marine boundary layer: A model study. *J. Atmos. Chem*., **32**, 375-395.

Volk, C.M., J.W. Elkins, D.W. Fahey, G.S. Dutton, J.M. Gilligan, M. Lowenstein, J.R. Podolske, K.R. Chan and M.R. Gunson, 1997: Evaluation of source gas lifetimes from stratospheric observations. *J. Geophys. Res*., **102**, 25543-25564.

Volz, A. and D. Kley, 1988: Evaluation of the Montsouris series of ozone measurements made in the nineteenth century. *Nature*, **332**, 240-242.

Wahlen, M., N. Tanaka, R. Henery, B. Deck, J. Zeglen, J.S. Vogel, J. Southon, A. Shemesh, R. Fairbanks and W. Broecker, 1989: Carbon-14 in methane sources and in atmospheric methane: The contribution of fossil carbon. *Science*, **245**, 286-290.

Wang, M.X. and X. Shangguan, 1996: CH_4 emission from various rice fields in P.R. China. *Theoretical and Applied Climatology*, **55**, 129-138.

Wang, Y.H. and D.J. Jacob, 1998: Anthropogenic forcing on tropospheric ozone and OH since preindustrial times. *J. Geophys. Res*., **103**, 31123-31135.

Wang, Y., J.A. Logan and D.J. Jacob, 1998a: Global simulation of tropospheric O_3-NOx-hydrocarbon chemistry. 2. Model evaluation and global ozone budget. *J. Geophys. Res*., **103**, 10727-10755.

Wang, Y., D.J. Jacob and J.A. Logan, 1998b: Global simulation of tropospheric O_3-NOx-hydrocarbon chemistry. 3. Origin of tropospheric ozone and effects of non-methane hydrocarbons. *J. Geophys. Res*., **103**, 10757-10767.

Wauben, W.M.F., J.P.F. Fortuin, P.F.J. van Velthoven and H. Kelder, 1998: Comparison of modelled ozone distributions with sonde and satellite observations. *J. Geophys. Res*., **103**, 3511-3530.

Wennberg, P.O., T.F. Hanisco, L. Jaegle, D.J. Jacob, E.J. Hintsa, E.J. Lanzendorf, J.G. Anderson, R.-S. Gao, E.R. Kein, S.G. Donnelly, L.A. Del Negro, D.W. Fahey, S.A. McKeen, R.J. Salawitch, C.R. Webster, R.D. May, R.L. Herman, M.H. Profitt, J.J. Margitan, E.L. Atlas, S.M. Schauffer, F. Flocke, C.T. McElroy and T.P. Bui, 1998: Hydrogen radicals, nitrogen radicals and the production of O_3 in the upper troposphere. *Science*, **279**, 49-53.

Wild, O. and M.J. Prather, 2000: Excitation of the primary tropospheric chemical mode in a global CTM. *J. Geophys. Res*., **105**, 24647-24660.

Wingen, L.M. and B.J. Finlayson-Pitts, 1998: An upper limit on the production of N_2O from the reaction of $O(^1D)$ with CO_2 in the presence of N_2. *Geophys. Res. Lett*., **25**, 517-520.

WMO, 1999: Scientific Assessment of Ozone Depletion: 1998. Global Ozone Research and Monitoring Project - Report No. 44, World Meteorological Organization, Geneva, Switzerland, 732 pp.

Yienger, J.J. and H. Levy II, 1995: Empirical model of global soil-biogenic NOx emissions. *J. Geophys. Res*., **100**, 11447-11464.

Yienger, J.J., A.A. Klonecki, H. Levy II, W.J. Moxim and G.R. Carmichael, 1999: An evaluation of chemistry's role in the winter-spring ozone maximum found in the northern midlatitude free troposphere. *J.Geophys. Res*., **104**, 3655-3667.

Yoshida, N. and S. Toyoda, 2000: Constraining the atmospheric N_2O budget from intramolecular site preference in N_2O isotopomers. *Nature*, **405**, 330-334.

Yung, Y.L. and C.E. Miller, 1997: Isotopic fractionation of stratospheric nitrous oxide. *Science*, **278**, 1778-1780.

Zander, R., P. Demoulin, D.H. Ehhalt, U. Schmidt and C.P. Rinsland, 1989: Secular increase of total vertical column abundance of carbon monoxide above central Europe since 1950. *J. Geophys., Res*., **94**, 11021-11028.

Zander, R., D.H. Ehhalt, C.P. Rinsland, U. Schmidt, E. Mahieu, J. Rudolph, P. Demoulin, G. Roland, L. Delbouille and A.J. Sauval, 1994: Secular trend and seasonal variability of the column abundance of N_2O above Jungfraujoch station determined from IR solar spectra. *J. Geophys. Res*., **99**, 16745-16756.

Ziemke, J.R., S. Chandra and P.K. Bhartia, 1998: Two new methods for deriving tropospheric column ozone from TOMS measurements: Assimilated UARS MLS/HALOE and convective-cloud differential techniques. *J. Geophys. Res*., **103**, 22115-22127.